Katrin Huber, Dipl.-Ing.

Precise Point Positioning with Ambiguity Resolution for real-time applications

Doctoral Thesis

to achieve the university degree of

Doktorin der technischen Wissenschaften

submitted to

Graz University of Technology

Supervisor:
Ao.Univ.-Prof. Dipl.-Ing. Dr.techn. Robert Weber
Vienna University of Technology
Department of Geodesy and Geoinformation

Co-Supervisor:
Univ.-Prof. Dipl.-Ing. Dr.h.c.mult. Dr.techn. Bernhard Hofmann-Wellenhof
Graz University of Technology
Institute of Geodesy, NAWI Graz

Graz, February 2015

Affidavit

I declare that I have authored this thesis independently, that I have not used other than the declared sources/resources, and that I have explicitly indicated all material which has been quoted either literally or by content from the sources used. The text document uploaded to TUGRAZonline is identical to the present doctoral dissertation.

Date	Signature

Acknowledgement

This thesis may not have been possible without the aid of several people, which is why I dedicate the following paragraphs to them:

First of all, I want to thank my co-supervisor Prof. Dr. Bernhard Hofmann-Wellenhof, who initially motivated me to start a thesis on the topic of Precise Point Positioning (PPP) and my supervisor Ao. Prof. Dr. Robert Weber from the Vienna University of Technology (TU Vienna), who supported me with his detailed knowledge on Global Navigation Satellite Systems (GNSS) and always found some time for scientific discussions. I also want to thank my colleague Fabian Hinterberger, who worked nearly simultaneously on his thesis on network corrections for PPP at the TU Vienna. As our two topics are strongly related, we could discuss many details to support each other.

Special thanks go to my colleagues at the former Institute of Navigation at the TU Graz (INAS), which is called Institute of Geodesy, Working Group Navigation from January 2015 on: First of all, I have to thank the head of the institute, Ao. Prof. Dr. Manfred Wieser, who gave me the opportunity to specialise on the topic of PPP within the last years. He further supported me by enabling flexible working times to catch enough time for the development of this thesis. I also want to thank Roman Lesjak who has been my office mate for the last years and, furthermore, always helped me to solve my problems implementing the PPP client software, when I was at my wits' end. Of course thanks goes to all of my nice colleagues at INAS, who gave me a comfortable working environment as well as a lot of funny and relaxing breaks to replenish my energy.

Beyond that I want to thank my family, especially my dad, who supported my diploma studies not only financially but also morally. He further motivated me to start and, even more important, to finish my Ph.D. studies. Therefore, this thesis would not have been possible without him.

At this point, I would also like to thank all my friends, who did listen to my problems patiently and contributed to funny, interesting and relaxing spare times which helped to sometimes even forget about work and refill my batteries.

Last but not least, I want to thank my boyfriend Martin Steinegger, who is not only my companion in life, but also my best friend. Without his calming nature and understanding I may never have finished this piece of work.

Thanks to all of you.

Abstract

In the last two decades Precise Point Positioning (PPP) has become a well-established technique for positioning by means of Global Navigation Satellite Systems (GNSS) for a wide range of post-processing applications. By using code and phase measurements of a single GNSS station or rover, and by utilising precise orbit and clock information derived from global GNSS networks, highly precise positions can be obtained. The influence of the atmosphere has to be treated, as it cannot be eliminated by building observation differences as it is performed in relative GNSS techniques such as Real-time kinematic (RTK). Usually 99 % of the ionospheric delay or advance can be eliminated by using the ionosphere-free linear combination of dual-frequency observations. The tropospheric influence can be divided into a hydrostatic or dry and a wet part. While the hydrostatic part can be modelled accurately, the remaining wet part is rather unpredictable and, therefore, should be estimated during the adjustment procedure to achieve utmost accuracies.

Nevertheless, within the last years also the demand for real-time PPP increased. Therefore, in 2012 the International GNSS Service (IGS) Real-Time Working Group started a pilot project to broadcast real-time precise orbits and clock correction streams. Though, real-time PPP is still in its starting phase and currently only a few applications make use of the technique. Recently, a new Radio Technical Commission for Maritime Services (RTCM) standard including the so-called State Space Representation (SSR) messages for orbit, clock and code bias corrections in real-time was developed (RTCM 3.1, Amendment 5). Unfortunately, these corrections are still not able to fix the problem of integer ambiguity resolution in PPP, which results from receiver- and satellite-based Uncalibrated Phase Delays (UPD) contaminating the estimated phase ambiguities. Therefore, common PPP approaches are based on estimating only one combined real-valued parameter for the ambiguities plus the UPDs, which leads to the long convergence times that occur together with PPP processing and a limited accuracy for real-time PPP compared to relative techniques such as RTK. Currently, the instantaneous integer ambiguity resolution at the zero-difference level is the major topic of many scientific investigations in the field of GNSS, since it may be the solution for the problem of the slow convergence in PPP.

In 2009 the author started researching in the field of GNSS algorithms at the Institute of Navigation at the TU Graz (INAS). This research was performed within the scope of a series of projects dealing with PPP. In order to test and verify several products and techniques related to PPP, a Matlab software package was started being developed that initially was only capable of simple code-based positioning using precise ephemerides. Later on it was extended to a tool for highly precise phase-based positioning using several GNSS product types, among others the new real-time SSR streams. Developing that software the idea of making a thesis on the topic of PPP came up for the first time, even though the exact direction of this thesis had not been clear at that time.

In 2012 the research project PPPserve was brought to life, that now had the intention to investigate algorithms and corrections necessary for PPP with Ambiguity Resolution and Fixing

(PPP-AR). The project consortium of that project consisted of the Vienna University of Technology (TU Vienna), the Graz University of Technology (TU Graz) and the GNSS service provider Wiener Netze GmbH operating the national station network Echtzeit Positionierung Austria (EPOSA). PPPserve was funded by the Austrian Research Promotion Agency (FFG) in the course of their 8^{th} call of their Austrian Space Applications Programme (ASAP) and had a lifetime of about two years. The project aimed at the development of appropriate algorithms for real-time PPP with special emphasis on the ambiguity resolution of zero-difference observations. During this research project a fully functional system was developed consisting of two major parts:

At the network-side a module was implemented, that calculates satellite-based Wide-Lane (WL) and Narrow-Lane (NL) UPDs from real-time observation data of about 85 European GNSS stations obtained from the IGS via Networked Transport of RTCM via Internet Protocol (Ntrip). The WL phase delays are quite stable over long periods, while the NL phase delays have to be re-established more often (every 15 minutes). Due to operational purposes they are calculated and transmitted to the user every 30 seconds.

The UPDs calculated at the network-side are submitted to the rover by means of a real-time module either in a proprietary file format or via an additional RTCM message. At the user-side the rover receives the correction data sets and applies them in a modified PPP algorithm to correct the phase observations and further to enable integer ambiguity resolution on the basis of WL and NL observables. In the course of PPPserve a user client software was implemented that encloses adequate algorithms for PPP with ambiguity resolution. This software was based on the aforementioned PPP tool developed by the author at INAS. By means of this PPP client software, called PPPsoft throughout this thesis, the phase biases from the network solution were evaluated and tested together with data from other organisations researching on the same topic. PPPsoft and especially the parts and algorithms developed for PPP-AR are simultaneously the central topic of this thesis.

The results of the PPP approach with ambiguity fixing were rather promising and could show that the phase bias corrections calculated within PPPserve are suitable to recover the integer nature of the WL and NL ambiguities. Also the bias application and the PPP positioning algorithms installed at rover-side work quite well. Nevertheless, there is still the potential to enhance the solution concerning convergence time and robustness. At the moment the PPP solution requires at least some minutes to fix the first set of ambiguities (WL and NL) to integers, which is strongly depending on the satellite geometry and the quality of the approximate receiver coordinates. Therefore, one topic of investigations was to find methods minimising this remaining convergence time. One option to solve this problem may be the introduction of regional information such as external values for the tropospheric delay to eliminate this parameter from the equation system. Concerning the robustness we are dealing with one major problem: Especially during the filter initialisation period ambiguities are sometimes fixed to wrong integers, which degrade the position solution significantly.

Within the last years several research groups developed methods for the estimation of UPDs to enable integer PPP, but only little research on the application of these biases and the problems involved was made or at least published. Therefore, this thesis will focus on the development of a user client and its algorithms required to enable a fixed PPP solution. Problems and actual results will be shown and discussed with respect to convergence times and other quality parameters.

This Ph.D. thesis deals with the development of adequate algorithms for phase-based PPP, as well as the products and methods that are required to enable integer ambiguity resolution within a PPP client. These investigations were accompanied by the development of the Matlab software PPPsoft, that is finally capable of PPP with ambiguity fixing in near real-time. The design of the user client and implemented algorithms for real-time PPP are presented together with results achieved by means of the implemented standard PPP solution that is based on estimating float ambiguities. In a further step, the development of the PPP-AR solution is presented. For this purpose also the UPD data used to compensate the satellite based hardware delays is described. Solutions using UPD corrections calculated by the Centre national d'études spatiales, Toulouse, France (CNES) as well as UPDs calculated at the Department of Geodesy and Geoinformation at the TU Vienna (GEO) during the project PPPserve are presented. Problems and deficiencies of PPP-AR are investigated on the basis of the most recent results produced by the user client. The coordinate convergence prior and after ambiguity fixing together with the dependence of the solution's quality on the satellite geometry is discussed. Further problems arising with integer ambiguity fixing such as the occurrence, detection and the treatment of wrong integer fixes are also treated in this document. Concluding, the profit of integer-fixed PPP compared to the standard PPP approach has been analysed.

Contents

List of Figures

List of Tables

List of Acronyms

APC	Antenna Phase Centre
ARP	Antenna Reference Point
APOS	Austrian Positioning Service
ASAP	Austrian Space Applications Programme
BEV	Bundesamt für Eich- und Vermessungswesen
BKG	Bundesamt für Kartographie und Geodäsie
BNC	Ntrip client and server software of the BKG
CNES	Centre national d'études spatiales, Toulouse, France
CODE	Center for Orbit Determination in Europe
DCB	Differential Code Bias
DGNSS	Differential GNSS
DOY	Day Of Year
ECEF	Earth Centered Earth Fixed
EPOSA	Echtzeit Positionierung Austria
FFG	Austrian Research Promotion Agency
FOC	Full Operational Capability
GEO	Department of Geodesy and Geoinformation at the TU Vienna
GLONASS	Globalnaja nawigazionnaja sputnikowaja sistema
GNSS	Global Navigation Satellite Systems
GPS	Global Positioning System
GUI	Graphical User Interface
IERS	International Earth Rotation and Reference Systems Service
IF	Ionosphere-free
IGS	International GNSS Service
INAS	Institute of Navigation at the TU Graz
IOD	Issue Of Data
ITRF	International Terrestrial Reference Frame
ITRS	International Terrestrial Reference System
JPL	Jet Propulsion Laboratory
LAMBDA	Least squares AMBiguity Decorrelation Adjustment
LOS	Line of Sight
MW	Melbourne-Wübbena
NEU	North, East and Up
NL	Narrow-Lane
NRCan	Natural Resources Canada
Ntrip	Networked Transport of RTCM via Internet Protocol
PCO	Phase Centre Offset
PCV	Phase Centre Variation
PPP	Precise Point Positioning

PPP-AR	PPP with Ambiguity Resolution and Fixing
RINEX	Receiver Independent Exchange Format
RTCM	Radio Technical Commission for Maritime Services
RTK	Real-time kinematic
RTPP	Real-time Pilot Project
SD	Single-difference
SPP	Single Point Positioning
SSR	State Space Representation
TEC	Total Electron Content
TU Vienna	Vienna University of Technology
TU Graz	Graz University of Technology
UPD	Uncalibrated Phase Delays
UTM	Universal Transverse Mercator
VTEC	Vertical Total Electron Content
WL	Wide-Lane
ZD	Zero-difference
ZHD	Zenith Hydrostatic Delay
ZTD	Zenith Total Delay
ZWD	Zenith Wet Delay

1 Introduction

The rapid development of Global Navigation Satellite Systems (GNSS) within the last two decades has led to a revolution in the field of geodesy. Among others, especially the disciplines of land surveying and the navigation of all kinds of vehicles have strongly profited from the practical and uncomplicated use of satellite-based navigation systems. Currently, there is a variety of different navigation and surveying systems, using standalone GNSS or GNSS integrated with other available sensors such as Inertial Measurement Units (IMU). GNSS-based systems can be found in everyday life in all imaginable pricing categories. Low-cost positioning and navigation equipment is for example installed in smartphones, while high end GNSS systems are used in space navigation or land surveying. The number of navigation satellites is growing, as meanwhile there are four different GNSS in space, some of them still in their installation phase. These systems are the well-known Global Positioning System (GPS) brought to life by the US military, its Russian pendant the Globalnaja nawigazionnaja sputnikowaja sistema (GLONASS), the Chinese system BeiDou as well as the European system Galileo. The latter two systems have not reached their Full Operational Capability (FOC) yet. All these developments have caused that positioning by means of GNSS is and will be a hot topic in scientific research now and in the future. There are various different satellite-based positioning techniques, some of them are known since the very beginning of GNSS and some of them are comparably new and still have a potential for enhancements. One of these upcoming techniques is Precise Point Positioning (PPP) which is the main topic of investigations in this thesis.

1.1 Satellite based positioning techniques

Generally, positioning techniques based on GNSS rely on measuring so-called pseudoranges between usually ground based static or moving receivers (rover) and the currently used GNSS satellites in space. Pseudoranges can have diverse accuracies depending on whether the measurement is based on code or phase observations.

Code-based pseudoranges rely on measuring the one-way travel time of a signal. Therefore, code modulations are applied to the carrier waves, that are broadcast by the satellites in the microwave band using frequencies between 1.2 and 1.6 GHz. Code-based measurements nowadays achieve maximum accuracies of a few decimetres corresponding to about 1 ns in signal travel time. In contrast, phase based pseudoranges achieve a much higher accuracy at the 1-2 mm level, which corresponds to about 0.5-1.0 % of the carriers' wavelength. Assuming that the precise position of the satellites is known and modelling further error sources, the remaining unknown parameters of the positioning process are the three-dimensional rover site coordinates and the rover receiver's clock correction. This receiver clock correction originates in the one-way communication between satellite and receiver, where both devices use different and un-synchronised oscillators. Due to this clock correction the term pseudorange is used in contrast to the unbiased range measurement in

case of synchronised satellite and rover clocks. The effect of oscillator errors on range measurements is illustrated in Figure 1.1.

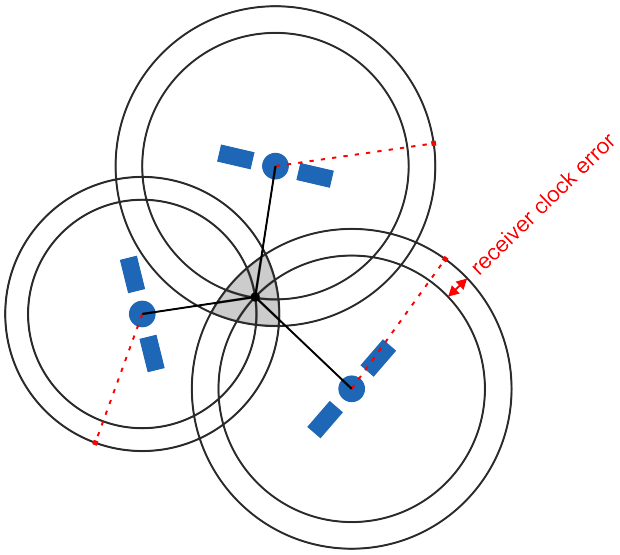

Figure 1.1: Effect of clock error on range measurements

The drawback of distance measurements, as they are used in GNSS-based positioning, is that they are affected by a number of error sources. An overview on main error sources influencing GNSS observations is given in Figure 1.2. Primarily, these error sources are global effects such as the imprecise knowledge of satellite orbits and satellite clocks in relation to the GNSS system time. Apart from that, signals are delayed or advanced while passing the atmosphere, which can be divided in a dispersive part called ionosphere and a non-dispersive part, the troposphere. The term dispersiveness means, that the signal delay in a medium depends on the frequency of the signal. The influences on the GNSS signal due to the ionosphere and troposphere can be described as regional effects, as these vary with regional and local conditions. Additionally, GNSS measurements are exposed to a number of local, respectively device-specific effects, which are difficult or even impossible to model accurately.

By using the precise phase measurements, an additional problem occurs. Phase measurements are ambiguous, meaning that the number of full carrier wave cycles between a satellite and the receiver measuring its signal is not known. When the receiver starts tracking a satellite, it measures the fractional phase plus an integer number of cycles that does not coincide with the real number of cycles, as this cannot be accessed any more. As soon as the satellite gets tracked the receiver recognises every full cycle reached and counts it continuously from now on. The difference to the true number of cycles, therefore, is also an integer value under ideal conditions and stays constant as long as the satellite is tracked. This remaining full number of cycles for every satellite-receiver pair is called phase ambiguity and is illustrated in Figure 1.3. During processing, these ambiguities have to be determined and ideally also fixed to their integer values in order to exploit the accuracy potential of phase measurements. Unfortunately, the ambiguity value is affected by additional device-specific errors in practice, which complicates the so-called ambiguity resolution process. An overview on measurement types used in GNSS-based positioning can be found in Hofmann-Wellenhof et al. (2007, p. 105ff).

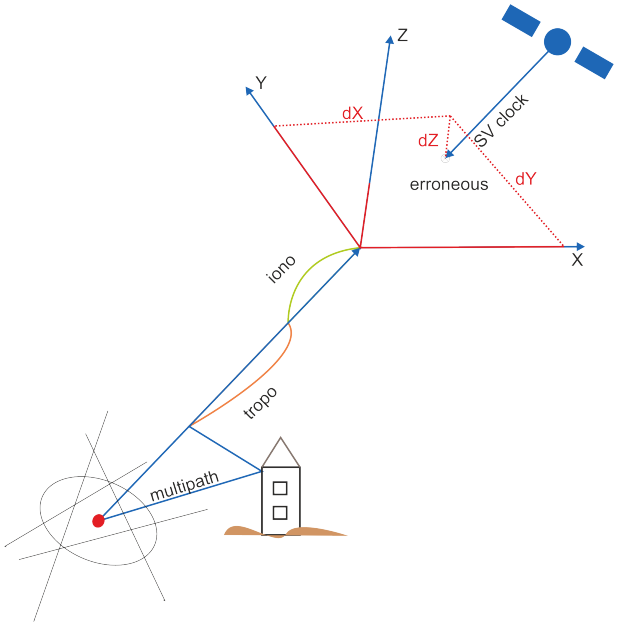

Figure 1.2: GNSS main errors in SPP

Apart from the measurement type, GNSS techniques are further distinguished by the observation model. There are zero-difference models such as Single Point Positioning (SPP), where code observations are used without building any differences and, therefore, only single receivers are needed. This zero-difference technique is independent from additional infrastructure, but results in only low accuracies of a few meters. In contrast, highly precise positioning resulting in accuracies at the millimetre to centimetre level is particularly possible by forming the difference between the phase observations of a rover at the user-side and observations of a reference station nearby, whose position is accurately known. This approach is also called relative positioning (see Hofmann-Wellenhof et al., 2007, p. 173ff) and allows to minimise or even to eliminate global, regional and time-dependent errors. The degree of mitigation of regional effects is depending on the baseline length denoting the distance between the receiver and the reference station.

As soon as differences between observations of different receivers and satellites are built, phase ambiguities can be assumed to be integer values, because most of the errors leading to a corruption of the ambiguities' integer nature cancel. This simplifies and accelerates the determination and fixing of integer ambiguities. This so-called difference-technique is a standard procedure in many present-day GNSS methods for point positioning. If this relative positioning technique is performed in real-time we refer to it as Real-time kinematic (RTK), which currently is the most popular precise GNSS method and is used for highly demanding applications by default. Therefore, nowadays for RTK the reference observations are not only available from a nearby station installed by the user himself, but also from GNSS correction data services offered by GNSS service providers. These providers generally operate a network of GNSS reference stations distributed over the service area. In Austria an example for such a data service is Echtzeit Positionierung Austria (EPOSA), operated by the companies Energie Burgenland AG, ÖBB Infrastruktur AG and Wiener Netze GmbH (http://www.eposa.at, 2014) or the Austrian Positioning Service (APOS) operated by the Bundesamt für Eich- und Vermessungswesen (BEV). Observation data from each reference

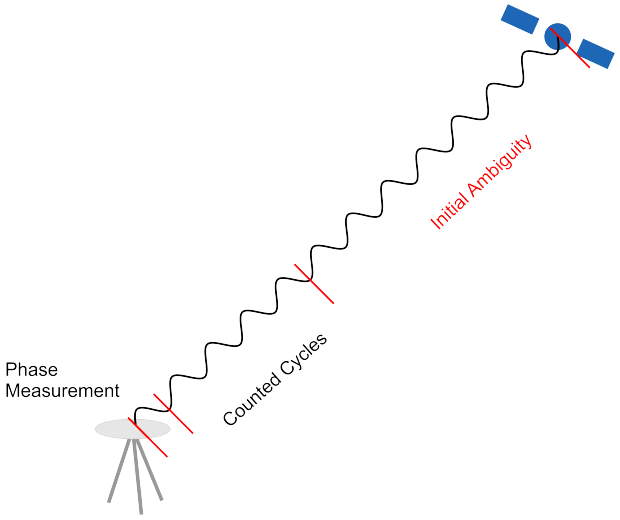

Figure 1.3: GNSS phase ambiguities

station in a network are sent to a service control facility in real-time, where they, on the one hand, are used to compute miscellaneous regional error models and, on the other hand, are delivered to users in standardised formats like Radio Technical Commission for Maritime Services (RTCM). Dependent on the data quality and further implemented information on the transformation of the established rover coordinates into certain reference systems, different service levels are offered.

For more detailed information on network-based RTK methods the reader is referred to Wübbena et al. (2001). A comparison of network-RTK and the PPP technique is given in Landau et al. (2009). For further details concerning positioning techniques by means of satellite navigation systems the reader is referred to Hofmann-Wellenhof et al. (2007) and the huge variety of other available literature on this topic.

1.2 Precise Point Positioning (PPP)

What is PPP?

One upcoming GNSS positioning technique is PPP, which is also the central topic of this doctoral thesis. PPP can be denoted as enhanced SPP, where code and carrier-phase measurements of a single GNSS receiver are used to calculate precise positions. Therefore, instead of the ephemerides broadcast by the satellites themselves, precise satellite orbit and clock data provided by GNSS analysis centres or station networks are used for the processing. Further error sources such as the ionospheric and tropospheric delay cannot be limited by building observation differences, as it is the case for relative positioning techniques such as RTK. PPP therefore is called a zero-difference technique, which implies that all additional error terms have to be modelled or estimated.

To compensate for the delay or advance a GNSS signal experiences while travelling through the ionosphere, a special observation model for dual-frequency data can be used. The error caused by the ionosphere is the largest error influence apart from satellite and receiver clock errors.

Therefore, the so-called ionosphere-free linear combination is used, which combines observations of two frequencies in a way that the first order term of the ionospheric effect is eliminated. This first order term makes up about 99.9 % of the ionospheric influence, which is sufficient for positioning techniques aiming at a maximum position accuracy of one or more centimetres, such as PPP. If only single-frequency data is available, the ionospheric influence has to be modelled instead; for example by using so-called ionospheric maps.

The signal delay due to the tropospheric refraction can either be modelled or estimated as an unknown parameter in the adjustment. As only the dry part of the tropospheric delay can be modelled accurately by analytical models it is a common procedure to estimate the remaining wet part of the tropospheric delay for highly precise applications.

Other minor error terms occurring in PPP are the receiver and satellite specific phase centre offsets and variations, tidal errors such as the solid earth tides or phase wind-up effects. All these error influences are treated in section 2.4.

PPP categories

The PPP technique can be subdivided by the following criteria:

The first criterion is the latency of the processing, meaning that PPP can be performed either in post-processing or in real-time. For post-processing there is no temporal limitation. This means that not only the best orbit and clock products can be awaited, but it is also possible to process several epochs together to reach a better accuracy. For static PPP in post-processing centimetre-level accuracies can be reached for observation periods of more than one or even two hours. The accuracy decreases with shortening observation length (see Anquela et al., 2013).

In real-time the PPP positions have to be calculated epoch-wise and the accuracy depends in a first place on the quality of the available precise orbit and especially clock products. Generally, there are two possibilities to achieve these ephemerides in real-time. Either so-called ultra-rapid orbits and clock corrections by the International GNSS Service (IGS) can be used, which can be downloaded from ftp-servers in intervals of 6 hours. Alternatively, continuous RTCM correction streams, the so-called State Space Representation (SSR) messages, can be used. These are defined in the RTCM 3.1 documentation (Radio Technical Commission for Maritime Services, 2011) and contain corrections to broadcast ephemerides to enable PPP in real-time. By applying ephemeris correction streams, it is also possible to achieve accuracies of a few centimetres for static PPP after approximately 30 to 90 minutes of observation depending on the quality of the ephemeris product.

Apart from the latency it can be further distinguished between static and kinematic PPP. While for static PPP the additional information that the receiver coordinates are time-independent can be used for smoothing, kinematic processing lacks this information. To increase the accuracy and smooth the trajectory dynamic models can be applied instead. Therefore, kinematic processing is not that accurate as static processing. Though, under good GNSS conditions decimetre-level accuracies can be reached after an initialisation time of 30 to 60 minutes (c.f. Abdallah and Schwieger, 2014), providing that no data gaps disturb the solution.

The last categorisation of the PPP processing can be made according to the number of GNSS frequencies used. Generally, we distinguish between single-frequency, dual-frequency or multiple-frequency processing, whereas dual- or multiple-frequency PPP mainly have the advantage that the ionospheric error can be compensated by using special linear combinations. Unfortunately, these linear combinations always have the side-effect, that the observation noise is increased.

A bit of history

The concept of Precise Point Positioning (PPP) was first introduced in the 1970's by R.R. Anderle (cf. Anderle, 1977 and Kouba and Héroux, 2001), and was characterised as single station positioning with fixed precise orbit solutions and Doppler satellite observations. Nevertheless, at that time precise ephemerides were not available in a quality as they are today. PPP needed another 20 years to awaken the interest of research institutes and scientists. First investigations using dual-frequency data from a single GPS receiver have been published in 1997 by the Jet Propulsion Laboratory (JPL) (c.f. Zumberge et al., 1997). In this publication positioning accuracies of a few centimetres in post-processing mode were reported. Since then a lot of online PPP services for post-processing analysis have been offered like JPLs Auto Gipsy, or CSRS-PPP by Natural Resources Canada (NRCan).

In the beginning, PPP has only been used for post-processing analysis, while nowadays the focus has changed. Today, research mainly deals with the preparation of PPP methods for real-time applications. Therefore, in 2007 the IGS started its Real-time Pilot Project (RTPP) (see http://www.rtigs.net, 2014) with the goal to offer real-time product streams for PPP to the GNSS community. The SSR messages for their transmission used at that time, were not standardised until 2011, when they were adopted in the official RTCM 3.1 format. Thanks to the RTPP today's real-time products or strictly speaking corrections for clocks and orbits have strongly increased in quality, from decimetres to a few centimetres, which enables a number of new areas of application for PPP.

Strengths and opportunities

PPP has become a valuable alternative to other GNSS techniques like RTK or Differential GNSS (DGNSS), as it has several advantages compared to them. One major strength of PPP is its cost-efficiency, arising from the fact that the technique does not need more than one individual GNSS receiver. No nearby reference station or dense regional station network is directly needed as it would be the case for differencing methods like RTK. Available corrections are globally valid and therefore there are no spatial limitations in the application of PPP. Station or rover data can be processed in a standalone solution, which avoids common effects occurring with network processing. The coordinate solution is calculated directly in the reference frame of the ephemeris set. PPP is also a common technique to access clock parameters or troposphere delays as well as site movements due to earthquakes or plate tectonics.

Though, the GNSS community is still working on solving the well-known problems of this technique. First, there is the problem, that the noise is significantly increased by using the ionosphere-free linear combination, while Total Electron Content (TEC) models for single-frequency PPP are available only at a level of a few decimetres. Further, the use of PPP for real-time applications is

limited by the quality and availability of orbit and clock products. For scientific use there are several real-time products offered by research institutions and analysis centres, but there are hardly any standalone product services for commercial use by now, even though some receiver manufacturers offer all-in-one PPP packages. These usually include receivers modified to use proprietary PPP corrections that are transmitted via e.g. a satellite link. One example for such a service is the RTX service by Trimble (see http://www.trimble.com/positioning-services, 2014).

Apart from the precise ephemerides for PPP several additional model corrections are needed to achieve the highest possible accuracies, which complicate and decelerate the positioning procedure. Last but not least, PPP suffers from the problem that integer ambiguities cannot be fixed for zero-difference processing without using external corrections from a reference station network. This problem arises due to the existence of hardware specific biases distorting the integer nature of ambiguity estimates. Therefore, PPP ambiguities are usually estimated as float values, which is mainly responsible for the long PPP convergence times (see Table 1.1). These hardware specific delays do not only occur for phase observables, they rather adulterate also the code observables. Code-specific biases can be treated either by using correction values from Differential Code Bias (DCB) tables published by e.g. the Center for Orbit Determination in Europe (CODE) (http://www.aiub.unibe.ch/content/research/satellitengeodaesie, 2014), or by applying the bias corrections offered in real-time SSR messages, while phase specific corrections are not publicly available by now. These phase biases are denoted as Uncalibrated Phase Delays (UPD) throughout this thesis and are treated in Chapter 4 in detail.

Convergence Time	Accuracy
15 to 30 min	<dm
30 to 90 min	a few cm
after 2 to 4 h	almost no improvement

Table 1.1: Common static position accuracies and convergence times for dual-frequency data

In Table 1.1 common static position accuracies of dual-frequency PPP are listed together with their accompanying convergence times. Of course the overall accuracy naturally depends on the quality of the introduced satellite orbits and clock corrections. In Section 2.2 a detailed overview on orbits and clock products available for PPP will be given. The reader is also referred to Weber and Hinterberger (2013) for general fundamentals on the topic of PPP and related real-time products.

1.3 Project PPPserve

In the following section a short overview on the research project PPPserve (Network based GNSS Phase Biases to enhance PPP Applications – A new Service Level of GNSS Reference Station Provider) is given, since the work performed in this project stands in close relation to the work presented in this thesis. PPPserve was a national research project financed by the Federal Ministry for

Transport, Innovation and Technology (BMVIT), represented by the Austrian Research Promotion Agency (FFG) in the course of their 8th Austrian Space Applications Programme (ASAP). The project started in January 2012 and ended in November 2013 after a project runtime of 18 + 2 months. The project consortium consisted of the Institute of Navigation at the TU Graz (INAS), the Department of Geodesy and Geoinformation at the TU Vienna (GEO) and the company Wiener Netze GmbH operating the nationwide GNSS reference site network and service EPOSA. The project's goal was the development and realisation of adequate algorithms to enhance fast GNSS based point positioning providing accuracies at the few-centimetre-level by establishing a service for PPP with Ambiguity Resolution and Fixing (PPP-AR).

The idea of launching the project PPPserve came up due to several reasons. The commonly used RTK technique is based on building and processing observation differences, while the required observation corrections are forwarded to the user community in the standardised RTCM format. In contrast to this differencing technique, the PPP model is based on code and phase single point positioning, which requires a limited amount of correction data just transferring model parameters instead of observation corrections. In PPP therefore spatially and temporally correlated error sources have to be modelled properly as they are not eliminated or minimised due to differencing. Leading receiver manufacturers have already agreed on a new RTCM standard (RTCM 3.1, Amendment 5, State Space Representation = SSR) supporting PPP corrections (c.f. Radio Technical Commission for Maritime Services, 2011). New receiver hard- and software issued in the near future will be capable to process this standard. Therefore, GNSS service providers have to adapt to this situation by offering new service levels. Nevertheless, the inability to access integer ambiguities without external aid, as it is common for differencing techniques, remains. This still is the main problem occurring with PPP processing. Unfortunately, RTCM 3.1 provides solely global SSR information like satellite orbit and clock correction models. This information is still not sufficient to allow for phase ambiguity resolution in real-time and positioning therefore suffers from long convergence times compared to RTK. This convergence period can make up about 10 to 30 minutes to reach position accuracies of only one decimetre as it was already stated in Table 1.1. Nevertheless, the advantage of PPP compared to the RTK technique is a dramatically reduced requirement of bandwidth for data transmission between the service provider and the user.

For this reason PPPserve aimed at the calculation and further provision of so-called satellite phase biases which are the missing link at user side to allow for PPP-based phase ambiguity resolution. Applying relevant satellite phase biases allows for fixing ambiguities to integers in PPP mode, which further reduces the convergence time significantly in the ideal case. In the start-up phase of the project two techniques for establishing these phase biases (UPDs) were investigated. Software to determine these parameters from the observation data of the regional GNSS service provider EPOSA was established by the project lead, Vienna University of Technology (TU Vienna). These parameters were forwarded to the user community in a proprietary format as a new service level to allow for a fast ambiguity resolution. At the user-side, which was developed by the INAS, the transmitted UPDs can be applied to the observations or rather linear combinations of observations to re-establish the integer characteristics of ambiguities and allow for ambiguity fixing in the course of a modified PPP algorithm. As soon as the ambiguities are treated as known quantities, the computational burden is strongly reduced and the phase observables can be considered as highly precise and unambiguous phase ranges. The processing scheme of the system developed in PPPserve is visualised in Figure 1.4.

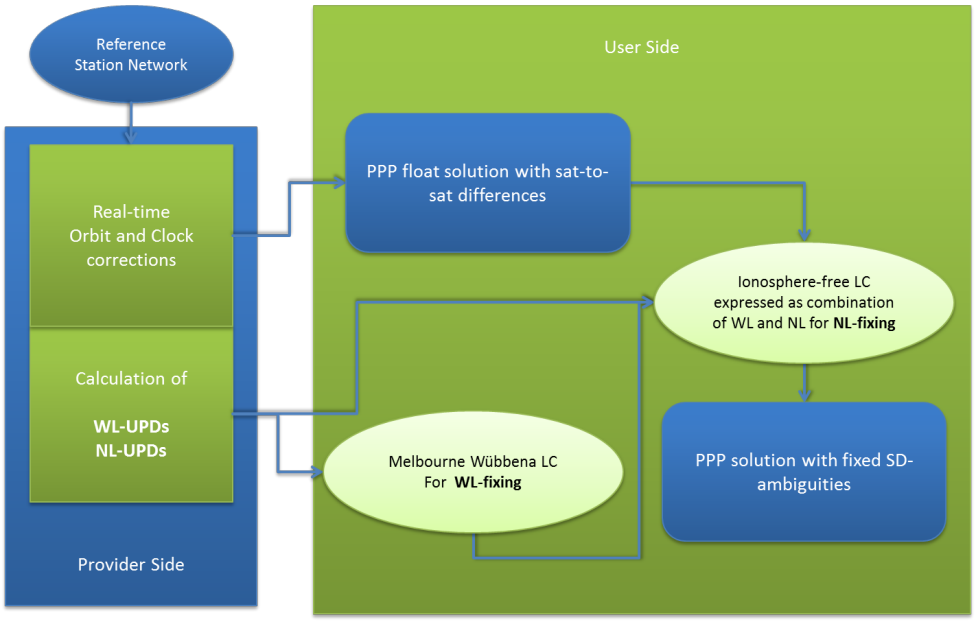

Figure 1.4: PPPserve processing scheme

The project's work flow consisted of a design and evaluation phase covering the processing of real GNSS observation data in order to identify the adequate method for the determination of phase biases. Subsequently, by means of simulated observation phase bias data, the potential of the chosen approach to re-establish UPDs was investigated and the quality and accuracy of the calculated parameters was evaluated. Further on, observation data of at least one month was used to establish time series of the UPDs and check their temporal stability. Introducing the UPDs to rover observation data for PPP completed the design and evaluation phase.

Based on the attained knowledge, a real-time service shall be set up that estimates Wide-Lane (WL) and Narrow-Lane (NL) UPDs from the reference sites' observation data at the EPOSA central computing facility and forwards these parameters to the user client in a proprietary format. The calculation of the UPDs has to take place at least every 10 to 30 minutes, which originates in the temporal instability of especially the NL biases. In parallel, also global corrections respectively satellite orbits and clocks are established. The processing of these global corrections in PPPserve was performed at the TU Vienna by means of knowledge and software already established in previous projects investigating the topic of PPP.

At the user-side a PPP client called PPPsoft was developed able to receive and apply the UPDs calculated at the network-side. The development of this user client is based on a standard PPP software developed by the author at INAS during earlier research on algorithms used for PPP. The implementation of the client software as well as its modification and expansion for features enabling ambiguity resolution is a main topic of this Ph.D. thesis. Further, PPPsoft served as a platform to test several approaches for PPP-AR and to evaluate the phase bias data from different sources such as the TU Vienna or Centre national d'études spatiales, Toulouse, France (CNES). Further details on the research project PPPserve are given in Weber et al. (2013).

In the frame of PPPserve also another Ph.D. thesis is being developed by my colleague Fabian

Hinterberger at TU Vienna, that is strongly linked to this thesis. Mr. Hinterberger worked on the network-part of PPPserve and was developing the algorithms and software for the calculation of satellite phase biases from a station network. Many of the results presented in this thesis are calculated with UPDs and other data produced by him. For detailed information on algorithms for the calculation of satellite phase biases at TU Vienna the reader is referred to the thesis of Fabian Hinterberger (Hinterberger, 2015).

1.4 Goals of the thesis

The main goal of this thesis with the title *'Precise Point Positioning with Ambiguity Resolution for real-time applications'* was the development of algorithms and methods for PPP to enable highly precise positioning with optional ambiguity resolution in near real-time. All the investigations were made on the basis of a PPP client named PPPsoft, that is implemented from the scratch in Matlab, a programming environment for numerical computing. The client-software is being developed since 2010 at the Institute of Navigation at the TU Graz (INAS), with the initial intention to create a playground for GNSS single point processing. On the one hand the implementation of PPPsoft contributed to a better understanding of certain parts of the PPP processing and on the other hand the software could be used to test and evaluate specific algorithms.

The temporal developments of the thesis and the user client can be divided into the following steps:

At first the general environment for PPP had to be set up. This included input functions for observation data, different types of ephemerides, and other necessary and optional input data. Further, models to compensate for major error influences and adjustment functions were developed. The first milestone of the thesis was the completion of a PPP software being able to process phase and code observations using standard PPP observation models, such as the ionosphere-free linear combination. The first versions of the software were only able to operate in post-processing mode, but the algorithms were implemented already in preparation for a real-time mode. Though, during this phase of the thesis a lot of knowledge on GNSS processing and products was collected, which was the basis for the further steps.

The second goal in the course of this Ph.D. work was the investigation of real-time products for PPP as well as their usage. At that time analysis centres like the IGS already had started their RTPP, and offered the new PPP SSR messages for orbit, clock and code bias corrections at least to the research community. Therefore, the PPP client was modified to work also in near real-time with the aid of correction streams calculated by several analysis centres and broadcast by the e.g. IGS. Also the TU Vienna is one of the organisations contributing to the IGS service by producing orbit and clock streams.

The final and most complicated part of this thesis was the research on the topic of PPP-AR. The investigation started with a literature research on already existing work on this topic published by other research institutions. In a second step, already existing phase bias products by these institutes were searched for the purpose of testing and evaluation of the PPP-AR algorithms.

Finally, two different phase bias products were used for the investigations in this thesis. On the one hand CNES offered a test environment called PPP-wizard (see http://www.ppp-wizard.net, 2014) including a test software and bias products. On the other hand the products established by

the TU Vienna in the course of the PPPserve project were used for testing and developing the PPP ambiguity resolution techniques and algorithms.

1.5 Outline of the thesis

Based on the aforementioned goals as well as on the development steps of PPPsoft this document is composed of the following chapters:

Chapter 1 is called *'Introduction'* and gives a short motivation and introduction to GNSS, PPP and this Ph.D. thesis.

Afterwards, the principles of the GNSS technique PPP are summarised in Chapter 2 *'Principles of PPP'*. This chapter includes information on the standard observation model used by most of the commercial software packages, as well as the products available for PPP such as satellite orbits and clock corrections and their usage. The fundamentals of the atmosphere from a geodesist's point of view are given together with possibilities to deal with the influences of the atmosphere on GNSS signals. This chapter further treats the nature of other error influences, such as the phase wind-up effect, phase centre offsets in the satellites' and the receiver's antennas or tidal effects together with options to account for them. Finally, a short summary of the adjustment model used in PPPsoft concludes this chapter.

Chapter 3 is called *'Software for standard PPP'* and deals with the implemented PPP client software in general and algorithms for standard PPP established in the course of this thesis. The organisation of the software is shown together with relevant input and output data to perform PPP with float ambiguity estimation. Finally, some aspects and considerations that came up already in the early phase of the thesis are discussed together with first results of the implemented PPP float solution and problems of PPP processing in general.

The content of Chapter 4 is the topic of *'PPP with Ambiguity Resolution'* or shortly PPP-AR. At this point of the thesis the general problems preventing ambiguity resolution with PPP are treated. Further, this chapter presents approaches to make PPP-AR possible in a user client and presents UPD corrections established by the research institutions CNES and TU Vienna. It is shown, how these data are applied in the user client, and how the fixing procedures are realised in order to obtain an integer-fixed PPP solution.

Chapter 5 *'Results and problems'* presents and compares several results calculated by means of fixed and float PPP solutions using example datasets. Problems and phenomena occurring with PPP-AR are shown on the basis of several case studies.

Finally, in Chapter 6 named *'Conclusions and potential future developments'* conclusions concerning the work of this thesis are drawn and the reader gets a short prospect on possible future developments on the topic of PPP-AR.

2 Principles of PPP

The principle of GNSS PPP using code and phase measurements of isolated receivers, as it is used in some commercial processing packages, is described in this chapter in order to give a basis for the further considerations in this thesis. These basics include the standard observation model, ephemeris data and error handling. For this thesis only signals of the GPS system were used, even though the processing software PPPsoft (presented in Chapter 3.1) is able to process also data from other satellite systems, such as GLONASS, in a standard solution estimating only float ambiguities. The PPP-AR solution is only available for GPS measurements. Therefore, key values of GPS signals only are given in Table 2.1.

Carrier	Frequency	Wavelength	Modulated Codes
L1	1575.42 MHz	0.1903 m	C/A, L1C*, P1(Y), M-Code
L2	1227.60 MHz	0.2442 m	L2C, P2(Y)
L5	1176.45 MHz	0.2544 m	L5I and L5Q

Table 2.1: GPS signals – source: Hofmann-Wellenhof et al. (2007) and http://www.navipedia.net (2014), * signal will be provided on GPS III satellites

2.1 Observation model

Basically, within PPP code and phase measurements of single static or kinematic receivers are used to estimate an independent solution of three-dimensional position coordinates, receiver clock estimates and tropospheric parameters with the aid of externally provided precise orbit and clock information instead of using the imprecise navigation data broadcast by the satellites themselves. The geodetic datum of the estimated parameters is solely given by the datum of the satellite ephemerides. Therefore, they are consistent with the global reference system at the epoch of observation. Relative techniques do not allow the estimation of independent, unbiased clock or troposphere solutions, which is possible by means of PPP processing.

As an introduction to the considerations on the processing by means of PPP, which follow later on in this document, the observation equations for undifferenced observations are described subsequently.

After widely eliminating satellite orbit and clock errors by using external ephemerides products, which can be obtained by several analysis centres contributing to the IGS for free, the functional

model for the zero-difference code pseudoranges P_i and phase pseudoranges $\lambda_i\Phi_i$ for the carrier i with the wavelength λ_i reads

$$P_i = \rho - cdt_r + \Delta_{trp} + \Delta_{ion} + \Delta_{other} \tag{2.1}$$
$$\lambda_i\Phi_i = \rho - cdt_r + \Delta_{trp} - \Delta_{ion} + \lambda_i b_i + \lambda_i w + \Delta_{other}. \tag{2.2}$$

The term ρ denotes the geometric distance between the satellite and the receiver antenna containing their three-dimensional coordinates. dt_r is the receiver clock error with respect to GPS time, while c stands for the speed of light. For the sake of completeness the satellite specific clock errors would be denoted as dt^s, but here already are eliminated by using precise clock corrections. Δ_{trp} stands for the tropospheric and Δ_{ion} for the ionospheric delay. The ionosphere is a dispersive medium, which means that the delay is frequency-dependent. It further has an opposite sign for code and carrier observations due to different group and phase velocities (c.f. Hofmann-Wellenhof et al., 2007, p116ff).

The phase measurement in (2.2) contains additional terms compared to the code equation, the ambiguity parameter b_i and the phase windup effect w. The ambiguity term b_i can be interpreted as the sum of real-valued initial phase biases originating in the receiver's and the satellite's hardware $\Delta\Phi_i^s$ and $\Delta\Phi_{i,r}$ plus the integer ambiguities N_i representing the full number of cycles not recorded by the receiver:

$$b_i = \Delta\Phi_i^s + \Delta\Phi_{i,r} + N_i. \tag{2.3}$$

Other corrections described by the term Δ_{other} contain relativity corrections, tidal corrections or antenna phase centre offsets and variations. These have to be accounted for by means of appropriate models.

For the dual-frequency case the influence of the ionosphere is strongly reduced by building the so-called Ionosphere-free (IF) linear combination of code P_{IF} and phase pseudoranges $\lambda_{IF}\Phi_{IF}$ resulting in

$$P_{IF} = \frac{f_1^2}{f_1^2 - f_2^2}P_1 - \frac{f_2^2}{f_1^2 - f_2^2}P_2 = \rho - cdt_r + \Delta_{trp} + \Delta_{other} \tag{2.4}$$
$$\lambda_{IF}\Phi_{IF} = \frac{f_1^2}{f_1^2 - f_2^2}\lambda_1\Phi_1 - \frac{f_2^2}{f_1^2 - f_2^2}\lambda_2\Phi_2 = \rho - cdt_r + \Delta_{trp} + \lambda_{IF}w + \lambda_{IF}b_{IF} + \Delta_{other}, \tag{2.5}$$

where λ_{IF} is the corresponding wavelength for the linear combination of the GPS carriers L1 and L2, that is very small and has no practical application.

Unfortunately, the IF linear combination is not only eliminating the first order term of the ionosphere, but is also increasing the observation noise by a factor of approximately three compared to the isolated L1 signal. Another side effect is that real-valued coefficients have to be used for this linear combination, since they have to be composed of the frequencies f_i of the single carriers i in order to eliminate the influence of the frequency dependent ionospheric delay as reported in Hofmann-Wellenhof et al. (2007, p126ff). This causes that the IF ambiguities do not possess integer nature any more, even if there were no hardware specific phase biases in the single-frequency ambiguities left.

2.2 Satellite orbits and clocks

For PPP it is necessary to use the most precise satellite orbits and clock corrections available, as the satellites' ephemerides are treated as known quantities. This means that the PPP model does not envisage to get rid of errors in these precise ephemerides, therefore they remain in the solution and further affect and limit the accuracy level of the coordinates and other parameters. Such precise orbits and clocks can be accessed in several ways. The simplest way is to download them from the ftp-servers of the IGS and contributing analysis centres. Meanwhile, also the possibility to receive real-time PPP correction streams came up, transmitted via a new RTCM standard – the so-called SSR messages. All these correction products for satellite orbits and clocks as well as their usage will be described in the following paragraphs.

2.2.1 The International GNSS Service (IGS)

The IGS produces and offers precise ephemerides since 1994 – additional products are models for the ionospheric and tropospheric delay, satellite antenna offsets and variations, or differential code bias information. This voluntary collaboration of more than 200 organisations collects, archives, and distributes GPS and GLONASS observation data sets from more than 300 GNSS stations all over the world to meet the objectives of a wide range of scientific and engineering applications and studies. These data are analysed and combined to form the IGS products, which are freely available for the scientific community. IGS products further support scientific activities such as improving and extending the International Terrestrial Reference Frame (ITRF) maintained by the International Earth Rotation and Reference Systems Service (IERS), monitoring deformations of the solid earth and variations in the liquid earth (sea level, ice sheets, etc.) and in earth rotation, determining orbits of scientific satellites, and monitoring the troposphere and ionosphere (c.f. http://www.igs.org, 2014 and Kouba, 2009).

2.2.2 Ephemerides for post-processing

Traditionally, the precise ephemeris products provided by the IGS and other analysis centres always have been essential for PPP processing. The IGS produces and offers orbits and clock corrections in three different accuracy levels and with a different latency. An overview on IGS' precise ephemerides is given in Table 2.2.

- The **final**,
- the **rapid** and
- the **ultra-rapid** ephemerides

are available in the .sp3 and the .clk format. The .sp3 format is used to store satellite positions and clock information with an arbitrary update rate. Nevertheless, most ephemerides stored in .sp3 files have a data rate of 15 min. The clock RINEX format (.clk) is used for high-rate satellite clock corrections with an update rate of up to 5 seconds. To provide highest position accuracies it is necessary to use the high-rate satellite clocks and to interpolate orbits and clocks to the time of transmission of the individual satellites (c.f. Kouba, 2009) e.g. by means of the Lagrange interpolation method as recommended in Hofmann-Wellenhof et al. (2007, p. 52f). Format descriptions for the .sp3 or .clk format can be found in http://igscb.jpl.nasa.gov (2014).

	Type	Accuracy	Latency	Sample Interval
Broadcast	orbits	100 cm	real-time	daily
	clocks	5 ns RMS, 2.5 ns SDev		
Ultra-Rapid	orbits	5 cm	real-time	15 min
(predicted)	clocks	3 ns RMS, 1.5 ns SDev		
Ultra-Rapid	orbits	3 cm	3 - 9 hours	15 min
(observed)	clocks	150 ps RMS, 50 ps SDev		
Rapid	orbits	2.5 cm	17 - 41 hours	15 min
	clocks	75 ps RMS, 25 ps SDev		5 min
Final	orbits	2.5 cm	12 - 18 days	15 min
	clocks	75 ps RMS, 20 ps SDev		Sat.: 30 s, Stn.: 5 min

Table 2.2: IGS ephemeris products table – source: http://www.igs.org (2014)

The most accurate GPS ephemerides are the IGS final orbits and clock products. These are available with a latency of 12-18 days and therefore can be used only for post-processing for non-critical applications concerning time. The final orbits have a nominal precision of at least 2.5 cm, while clock corrections have an RMS of about 75 ps corresponding to about 2.25 cm in range. If the processing has to take place closer to the time of observation, IGS rapid products can be used. These are available only 1 day after the observation and nominally have precisions of at least 2.5 cm for orbits and again 75 ps for clocks. Hence, nowadays the final and the rapid products do not differ much and produce comparable results for most applications. Nevertheless, both have the disadvantage of being not available at the time of observation.

The reference frame of GNSS orbits usually corresponds to the latest version of the ITRF at epoch of date. Currently, the satellite orbits are calculated in the ITRF2008 frame (see http://itrf.ensg.ign.fr/ITRF_solutions/2008, 2015) defining also the frame of position coordinates produced by the PPP solution.

Further, it should be mentioned that precise orbits often are referred to the satellites' centre of mass (COM), while the code and phase measurements are referred to the antenna's phase centre (APC) of the respective frequency. Therefore, corrections to compensate for the resulting difference in range have to be applied as described in Section 2.4.4.

2.2.3 Ephemerides for real-time processing

IGS ultra-rapid products

When it comes to real-time processing, the need for predicted orbit and clock products arises. For this purpose the so-called ultra-rapid products are offered by the IGS since 2000 and were originally designed to serve meteorological applications and Low Earth Orbiters missions (c.f. Kouba, 2009). Ultra-rapid ephemerides are available also in the .sp3 format and contain 24 hours of observed and 24 hours of predicted orbits and clock corrections. As the accuracy of especially the satellite clocks becomes significantly worse after some hours of prediction, these ultra-rapid products are calculated and provided 4 times a day. The nominal accuracies of the calculated ultra-rapid products are 3 cm for orbits and an RMS of about 150 ps (corresponds to 4.5 cm in range) for clock corrections, while the predicted part still offers 5 cm accuracies for orbits but only 3 ns (corresponds to 90 cm in range) for clocks. When using the clock corrections only shortly after their prediction, better accuracies can be reached. Unfortunately, for most standard GPS equipment it is not possible to download ephemerides from an ftp-server. Therefore, there is a need for other realisations to forward real-time ephemerides to PPP users.

RTCM State Space Representation SSR

Message Type	Message Name
1057	SSR GPS Orbit Correction
1058	SSR GPS Clock Correction
1059	GPS Code Bias
1060	SSR GPS Combined Orbit and Clock Corrections
1062	SSR GPS High Rate Clock Correction
1063	SSR GLONASS Orbit Correction
1064	SSR GLONASS Clock Correction
1065	SSR GLONASS Code Bias
1066	SSR GLONASS Combined Orbit and Clock Correction
1068	SSR GLONASS High Rate Clock Correction

Table 2.3: RTCM 3.1 SSR messages

Recently in 2011 the Radio Technical Commission for Maritime Services (RTCM) committee has released a new version of the RTCM standard exchange format for real-time GNSS data streams (RTCM 3.1 Amendment 5). This format covers a number of so-called State Space Representation (SSR) messages allowing the exchange of orbit corrections and clock corrections to broadcast ephemerides as well as code bias information for both the GPS and the GLONASS

system. These messages are transferred via internet in a binary format using the Networked Transport of RTCM via Internet Protocol (Ntrip) protocol. This binary format has to be decoded by an RTCM client software prior to use. Many commercial receivers do already have an RTCM functionality, which has always been required to use RTK or DGNSS services. Though, the receiver manufacturers do have to prepare also for using the new SSR messages for PPP processing.

These new messages designated for PPP are listed in Table 2.3. Further information on SSR messages and the actual RTCM standard can be found in the RTCM documentation (Radio Technical Commission for Maritime Services, 2011).

Networked Transport of RTCM via Internet Protocol (Ntrip)

According to http://igs.bkg.bund.de/ntrip (2014) Ntrip is an application-level protocol for streaming GNSS data over the internet. The protocol is based on the Hypertext Transfer Protocol HTTP/1.1 enhanced to support GNSS data streams.

Ntrip is an RTCM standard specifically designed for the dissemination of GNSS data over the internet. Mainly differential correction data (e.g in the RTCM-104 format), but also other kinds of GNSS data streaming to stationary or mobile users is addressed by this standard, whereby it allows simultaneous PC, Laptop, PDA, or receiver connections to a broadcasting host. Further, Ntrip supports wireless internet access through mobile IP networks like GSM, GPRS, EDGE, or UMTS.

Figure 2.1 shows an overview on the whole communication between its three system software components – NtripClients, NtripServers and NtripCasters. The NtripCaster is the actual HTTP server program, whereas NtripClient and NtripServer are acting as HTTP clients.

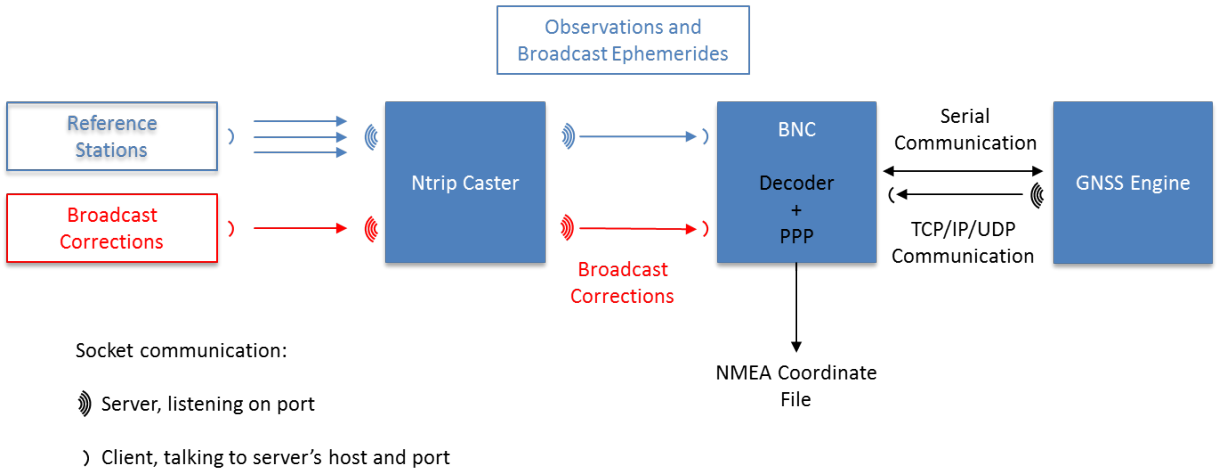

Figure 2.1: Ntrip scheme for broadcasting PPP corrections by **BNC** – source: http://software.rtcm-ntrip.org/svn/trunk/BNC/src/bnchelp.html (2015)

Ntrip is designed as an open non-proprietary protocol, which is comparatively easy to implement, when having limited client and server platform resources available. Its application is not meant

to be limited to one particular plain or coded stream content, rather it is able to distribute any kind of GNSS data. Further, Ntrip was designed for mass usage, meaning that it can disseminate hundreds of streams simultaneously for up to thousand users.

Orbit corrections to broadcast ephemerides

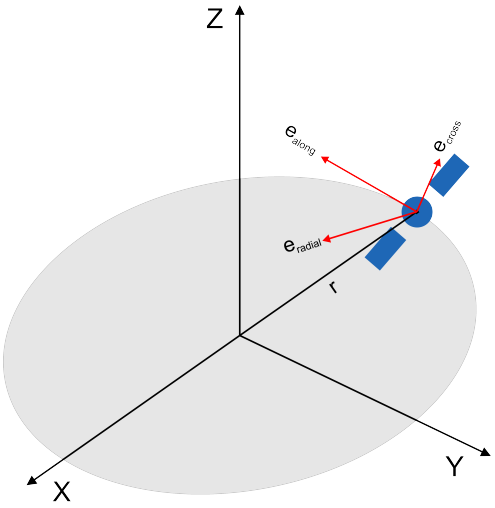

Figure 2.2: Orbit correction to broadcast ephemerides

Subsequently, the SSR corrections for PPP as well as their usage are further described. The real-time corrections for broadcast ephemerides are given as along-track, across-track and radial component in the orbital system (Figure 2.2). Every set of corrections is linked to a certain set of broadcast ephemerides by an Issue Of Data (IOD) number. The correction components have to be transformed into the Earth Centered Earth Fixed (ECEF) system in order to be consistent with the satellite positions calculated from the broadcast ephemerides.

The axes of the orbital system defined in the ECEF system are given by equations (2.6), (2.7) and (2.8), where the position of the satellite $\vec{x}_{sat}$ as well as the corresponding velocity vector $\vec{v}_{sat}$ must be known in the ECEF system:

$$\vec{e}_{along} = \frac{\vec{v}_{sat}}{\left|\vec{v}_{sat}\right|} \tag{2.6}$$

$$\vec{e}_{across} = \frac{\vec{x}_{sat} \times \vec{v}_{sat}}{\left|\vec{x}_{sat} \times \vec{v}_{sat}\right|} \tag{2.7}$$

$$\vec{e}_{radial} = \vec{e}_{along} \times \vec{e}_{across} \,. \tag{2.8}$$

With these axes a rotation matrix for the rotation of a vector from the orbital system into the ECEF system can be built by

$$R = \left[\vec{e}_{radial}, \vec{e}_{along}, \vec{e}_{across}\right]. \tag{2.9}$$

With this rotation matrix the rotation of the correction vector from the orbital system $\vec{r}_{ORB}$ to the ECEF system $\vec{r}_{ECEF}$ is performed by

$$\vec{r}_{ECEF} = R \cdot \vec{r}_{ORB}\ . \tag{2.10}$$

Finally, the corrections are subtracted from the orbits calculated from the broadcast ephemerides to get the more precise satellite positions. For further information on SSR corrections for orbits the reader is referred to the RTCM 3.1 documentation (Radio Technical Commission for Maritime Services, 2011).

Clock Corrections to broadcast ephemerides

The clock corrections included in the SSR messages are also linked to a special set of broadcast clock corrections by an IOD. The corrections for the broadcast clock corrections are given by means of the coefficients c_0, c_1 and c_2 for a polynomial of 2$^{\text{nd}}$ degree. dt is the time difference between the time of transmission and the reference epoch of the SSR clock correction. From these parameters the clock correction term dt_{clock} in meters can be calculated by

$$dt_{clock} = c_0 + c_1 \cdot dt + c_2 \cdot dt^2. \tag{2.11}$$

Therefore, the coefficients closest to the satellite's time of transmission are chosen from the subset of messages fitting to the broadcast ephemeris set. Note, that the coefficients are given in meters instead of units of time. If the time difference dt becomes too large, inaccuracies in the calculated correction may occur. For example the c_0 term can change a few centimetres within only 5 seconds. Therefore, if no correction set is fitting to the satellite's time of transmission, the corresponding satellite should be excluded from the processing or at least its weight should be reduced. Thereby, the threshold for the acceptable time difference dt is depending on the accuracy requirement of the specific application.

The clock correction value from the navigation message is corrected simply by adding the correction from the real-time clock stream dt_{clock} converted to units of time. A detailed description of SSR clock corrections can be found in the RTCM 3.1 documentation (Radio Technical Commission for Maritime Services, 2011).

The IGS Real-time Pilot Project (RTPP)

In 2007 the IGS released a call for participation for their RTPP. Since that time several agencies have been participating in the network management and monitoring of the IGS RTPP. These agencies are making available information to the real-time analysis centres, as well as real-time users.

The main goals of the RTPP defined by the IGS include

- to manage and maintain a global IGS real-time GNSS tracking network,
- to generate combined real-time IGS analysis products,
- to develop standards and formats for real-time data collection and distribution and
- to develop standards and formats for the generation and distribution of real-time analysis products.

To access RTPP's real-time ephemeris streams, researchers can freely register for the IGS Ntrip broadcaster. Further information on the RTPP is given on their homepage (http://www.rtigs.net, 2014).

2.3 The atmosphere

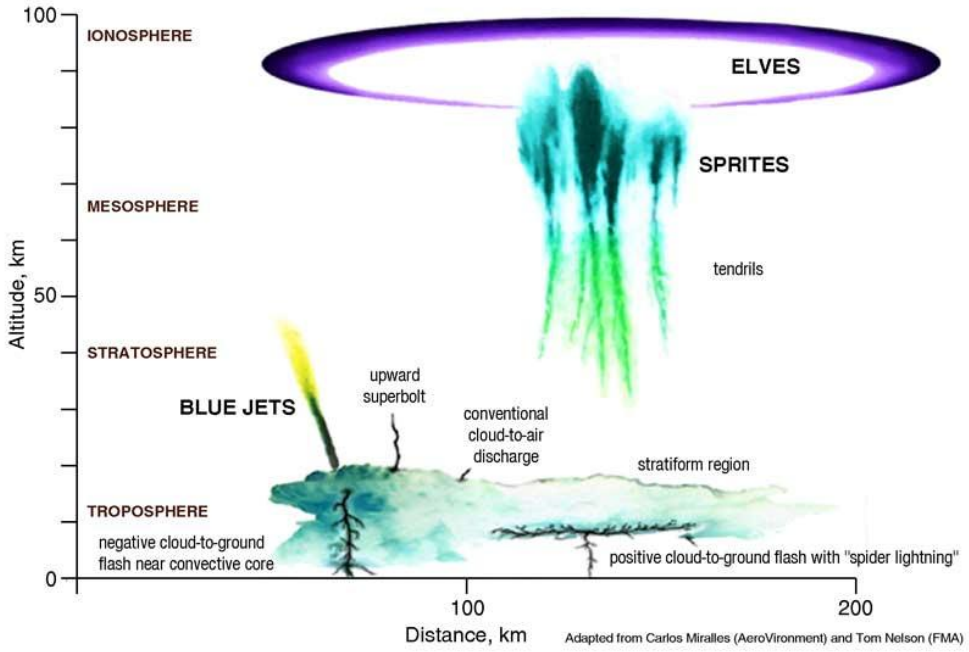

Figure 2.3: Structure of the atmosphere – source: http://de.wikipedia.org (2014)

The atmosphere can be categorised according to many different characteristics, but for geodetic purposes its electromagnetic structure is the most interesting feature. Therefore, we distinguish a lower, for radio waves up to 15 GHz non-dispersive neutral part, namely the troposphere, and a dispersive higher part that is electrically charged, the ionosphere. The troposphere starts at the earth's surface and reaches up to approximately 50 km. It actually contains the troposphere and stratosphere, but is simply called the troposphere in the geodetic community. The ionosphere comprises the mesosphere, which starts in a height of approximately 50 km, the thermosphere and the exosphere and reaches up to approximately 1000 km. Figure 2.3 shows the layer structure of the atmosphere for a better imagination. More details on the layers of the atmosphere as well as their characteristics can be found in Hofmann-Wellenhof and Legat (2003, page 67ff).

The propagation errors occurring while the signal is passing the atmosphere are the largest error terms influencing the PPP solution and together can reach tens of meters for single observations of satellites with a low elevation. Within the coordinate solution mainly the height component is affected by unmodelled tropospheric errors, while ionospheric errors influence the horizontal and the height component of the position solution. Therefore, it is essential to compensate for atmospheric effects carefully, when desiring a highly precise position solution.

2.3.1 Tropospheric propagation error

The tropospheric propagation error is caused by the refractivity of gas molecules in the air. This refractivity varies with temperature T, pressure p and the partial pressure of the water vapour e. All these measures are functions of height, while, as mentioned earlier, the frequency does not influence the delay. Therefore, we do not need to distinguish between signals on different carriers in the L-band. The drawback of this non-dispersiveness is that the tropospheric delay cannot be eliminated by observing dual-frequency data, as it can be done for the ionospheric effect.

There are two ways to mitigate the effect of the troposphere – it can be modelled by analytical models, strongly reduced by using external troposphere files from analysis centres, or directly estimated from the observation data. The tropospheric delay can be divided into a dry (or hydrostatic) and a wet part. The dry part of the troposphere makes up about 90 % of the delay and is easily predictable, as it varies only slowly with time. The dry part of the tropospheric error makes up about 2 meters in zenith direction, but can reach up to 10 m for satellites with low elevation angles. The wet part of the tropospheric delay makes up only a few decimetres (1-3 dm), but is difficult to model, as it varies faster than the dry part in a rather unpredictable way. Further it depends on the water vapour in the atmosphere (e.g. clouds) and therefore on local weather conditions.

Hopfield model

Empirically developed and widely used models are the Hopfield model (c.f. Hopfield, 1969) and the Saastamoinen model (c.f. Saastamoinen, 1972). In the course of this thesis mainly the Hopfield model was used and, therefore, is described subsequently.

The Hopfield model is based on meteorological data and produces rather accurate troposphere delays. The Zenith Total Delay (ZTD) is composed of the Zenith Wet Delay (ZWD) and the Zenith Hydrostatic Delay (ZHD), as described by

$$ZTD = ZHD + ZWD \tag{2.12}$$

and

$$\Delta_{trp} = ZHD \cdot m_d(E) + ZWD \cdot m_w(E)\,[\mathrm{m}]\,, \tag{2.13}$$

with

$$ZHD = \frac{10^{-6}}{5} \cdot 77.64 \cdot \frac{p}{T + 273.16} \cdot (40136 + 148.72T) \tag{2.14}$$

and

$$ZWD = \frac{10^{-6}}{5}(-12.96 \cdot (T + 273.16) + 3.718 \cdot 10^5) \cdot \frac{e}{(T + 273.16)^2} \cdot 11000. \tag{2.15}$$

To calculate the ZHD and the ZWD the temperature T is inserted in degree Celsius (C) and the atmospheric pressure p and the partial pressure of the water vapour e in units of millibar (mb). $m_d(E)$ and $m_w(E)$ are the so-called mapping functions for the dry part and the wet part of the tropospheric delay and can be calculated by

$$m_d(E) = \frac{1}{sin\sqrt{E^2 + 6.25}} \tag{2.16}$$

and

$$m_w(E) = \frac{1}{sin\sqrt{E^2 + 2.25}}. \tag{2.17}$$

These mapping functions can be understood as a scale factor to map the delay in zenith direction onto the line of sight between satellite and receiver by using the elevation angle E of the respective satellite (expressed in degrees) in the observation site. The Hopfield model and mapping functions are valid for satellites with an elevation angle of $E > 5°$ up to $E \approx 90°$. For satellites in or near the zenith the values for m_d and m_w are approximately 1, as in these models the Line of Sight (LOS) is simplified as straight line.

Troposphere estimation

As the wet part of the troposphere is very dependent on local weather conditions, it is not possible to yield centimetre or even millimetre position accuracies just with the aid of analytical models. Therefore, for highly precise point positioning it is common to estimate the wet part of the troposphere during the adjustment procedure. As mentioned earlier, this remaining part can still make up about two decimetres in zenith direction.

The details on parameter estimation in PPP processing are treated later on in Section 2.5.

2.3.2 Ionospheric propagation error

The ionosphere is the electrically charged, higher part of the atmosphere and can be characterised by the free, charged and neutral particles it contains. Its ionisation varies during one day and is dependent on the solar radiation. Generally the lowest ionisation occurs before sunrise. A detailed description of ionospheric layers and their ionisation can be found in Hofmann-Wellenhof et al. (2007, page 65f).

The refraction in the ionosphere is described by the Total Electron Content (TEC), that varies as a function of the solar activity, seasonal and diurnal variations and the earth's magnetic field.

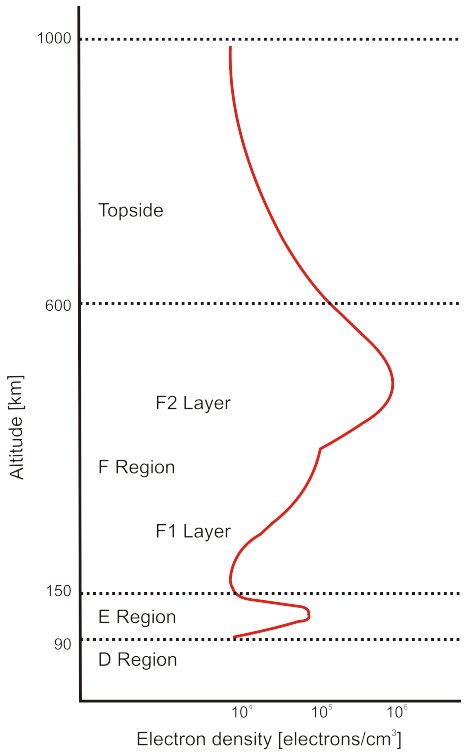

Figure 2.4: Electron density in the atmosphere – source: http://de.wikipedia.org (2014)

Following the formulas in Hofmann-Wellenhof et al. (2007, page 118f), the ionospheric delay for pseudoranges (group delay) or advance for phases (phase delay) can be described simplified as

$$\Delta_{ph}^{Iono} = \int \frac{c_2}{f^2}\, ds_0 \qquad\qquad \Delta_{gr}^{Iono} = -\int \frac{c_2}{f^2}\, ds_0. \tag{2.18}$$

As the coefficient c_2 is a function of the electron density N_e along the signal path (given in Hz) with

$$c_2 = -40.3\, N_e, \tag{2.19}$$

the ionospheric advance/delay can be alternatively described as

$$\Delta_{ph}^{Iono} = -\frac{40.3}{f^2} \int N_e\, ds_0 \qquad\qquad \Delta_{gr}^{Iono} = \frac{40.3}{f^2} \int N_e\, ds_0, \tag{2.20}$$

where s_0 is the geometric range between satellite and receiver. Figure 2.4 shows the electron density in electrons/cm^3 in the atmosphere as a function of height.

At this place the TEC is defined as

$$TEC = \int N_e\, ds_0. \tag{2.21}$$

The TEC is usually given in TEC units whereby 1 TECU = 10^{16} electrons per m^2. Further, the TEC is usually given as Vertical Total Electron Content (VTEC) which is valid only for the LOS to satellites in the zenith. To calculate the delay for satellites in arbitrary elevation, the delay has to be mapped to the respective elevation angle. Most commonly, TEC models are single-layer models, where the free electrons are assumed to concentrate in a thin layer in a height between typically 300 to 400 km. Meanwhile, there exist also three-dimensional ionospheric model approaches, which do not ignore the fact that the free electrons are spread over a broader spectrum of height than only a single layer. One example for such a three-dimensional TEC model is the tomographic model based on the electron density function as described in Zhang et al. (2013).

Mitigation of the ionospheric delay

The ionospheric propagation error is one of the largest residual error terms in PPP processing, but, thanks to its frequency dependence, it can be almost eliminated by using the IF linear combination of dual-frequency observations as described in (2.5).

After simplifying the observation equation (2.2) for a signal on carrier L1 and L2 by dividing the right hand terms into a geometric part a (containing all the non-frequency dependent terms) and an ionospheric part b we get

$$L_1 = a + \frac{1}{f_1^2} \cdot b \qquad\qquad L_2 = a + \frac{1}{f_2^2} \cdot b. \tag{2.22}$$

These equations can be combined to eliminate the ionospheric part b by

$$\frac{f_1^2}{f_1^2 - f_2^2} L_1 - \frac{f_2^2}{f_1^2 - f_2^2} L_2 = a, \tag{2.23}$$

which is also called the Ionosphere-free (IF) linear combination of observation equations. Note, that for (2.22) the opposite signs for code and phase delays are not relevant, as they are eliminated anyway. These have to be considered only when modelling the ionosphere. Further note, that the IF linear combination is based on the simplification that only the first order term of the ionosphere is considered. Therefore the higher order terms remain in the observation, which, under normal ionospheric conditions, has no influence on a solution at the accuracy level of PPP processing.

If only single-frequency observation data is available, another method to mitigate the influence of the ionosphere has to be used. Possible methods are the usage of the broadcast Klobuchar model (see Klobuchar, 1987), that eliminates only about 50 % of the ionospheric influence, or rather global TEC models made available by the IGS. Anyway, as single-frequency processing is not treated in this thesis, no further information on this topic is given here. The reader is referred to the manifold literature on single-frequency processing and ionosphere mitigation methods instead.

2.4 Other corrections

The PPP technique is usually based on observations of single stations or rovers, therefore no differences between measurements of different receivers are built. This keeps the positioning results independent from other stations or networks, but implicates other problems such as the necessity to correct for various errors that would have cancelled in difference-mode. In the following the main error sources beside the aforementioned ones are listed and shortly explained.

2.4.1 Differential Code Biases (DCBs)

Code observables are subject to instrumental biases that are individual for each type of code measurement as well as each receiver and satellite. Therefore, for GPS these biases occur between the C1, P1 and P2 measurements (and all other code observables not used in this thesis). Unfortunately, these biases are not accessible in the absolute sense, which is why they are called Differential Code Bias (DCB). Between these three observables the following differences shall be considered:

$$B_{P1P2} = B_{P1} - B_{P2} \tag{2.24}$$

$$B_{P1C1} = B_{P1} - B_{C1}. \tag{2.25}$$

Values for DCBs are calculated by CODE on a monthly basis. They can be accessed by means of ASCII files from the ftp-server ftp://ftp.unibe.ch/aiub/CODE . The magnitude of B_{P1P2} biases is rather large and can make up to some meters, while according to Dach et al. (2007) values for the B_{P1C1} are three times smaller. Note, that by using IGS clock corrections the IF linear combination of B_{P1} and B_{P2} code biases is already contained and does not have to be treated any more. Anyway, if C1 measurements are used instead of P1, the B_{P1C1} correction still has to be applied.

LC	P1/P2	C1/X2=C1+(P2−P1)	C1/P2
L1	$+1.546 \cdot B_{P1P2}$	$+1.546 \cdot B_{P1P2} + B_{P1C1}$	$+1.546 \cdot B_{P1P2} + B_{P1C1}$
L2	$+2.546 \cdot B_{P1P2}$	$+2.546 \cdot B_{P1P2} + B_{P1C1}$	$+2.546 \cdot B_{P1P2}$
L3	0	$+B_{P1C1}$	$+2.546 \cdot B_{P1C1}$
L4	$-B_{P1P2}$	$-B_{P1P2}$	$-B_{P1P2} + B_{P1C1}$
L5	$-1.984 \cdot B_{P1P2}$	$-1.984 \cdot B_{P1P2} + B_{P1C1}$	$-1.984 \cdot B_{P1P2} + 4.529 \cdot B_{P1C1}$
L6	0	$-B_{P1C1}$	$-0.562 \cdot B_{P1C1}$

Table 2.4: Application of DCBs with respect to different observable types – source: Dach et al. (2007, page 283)

Table 2.4 shows how the DCBs are applied to the different observable types considering the following linear combinations: L1 and L2 stand for the uncombined measurements on the respective GPS frequencies. L3 stands for the Ionosphere-free (IF) linear combination. L4 is the Geometry-free

combination, L5 is the Wide-Lane (WL) combination and L6 is the Melbourne-Wübbena (MW) combination.

The coefficients occurring in Table 2.4 are calculated from the respective combinations of the GPS frequencies:

$$f_2^2/(f_1^2 - f_2^2) = 1.546 \qquad f_1^2/(f_1^2 - f_2^2) = 2.546 \tag{2.26}$$

$$f_1 f_2/(f_1^2 - f_2^2) = 1.984 \qquad f_1/(f_1 - f_2) = 4.529 \qquad f_1/(f_1 + f_2) = 0.562 \tag{2.27}$$

For further details on code biases and their application the reader is referred to the manual of the Bernese software version 5.0 (Dach et al., 2007, page 279ff).

2.4.2 Phase wind-up effect

The so-called phase wind-up effect occurs due to the changing relative orientation of satellite and receiver antennas (see Figure 2.5). Satellites move along their orbital paths and have to change their orientation permanently to ensure that the plane containing the solar panels is directed perpendicular to the sun to obtain the maximum energy from solar radiation. Meanwhile, the satellites' antennas keep pointing to the centre of the earth, but are rotated as a result of the whole satellites' rotation. These rotations lead to phase variations that can be seen in the phase observables as a variation in range. Usually, these rotations are slow. Only during so called noon and midnight turns, where the satellite orbits intersect the line between sun and earth, also rapid rotations can occur. Phase data from satellites during such eclipsing seasons can be eliminated from the observations. For precise positioning such as PPP also the permanent small rotations have to be considered, as the range error for phases can make up half of the wavelength. Code ranges are not affected by the phase wind-up effect.

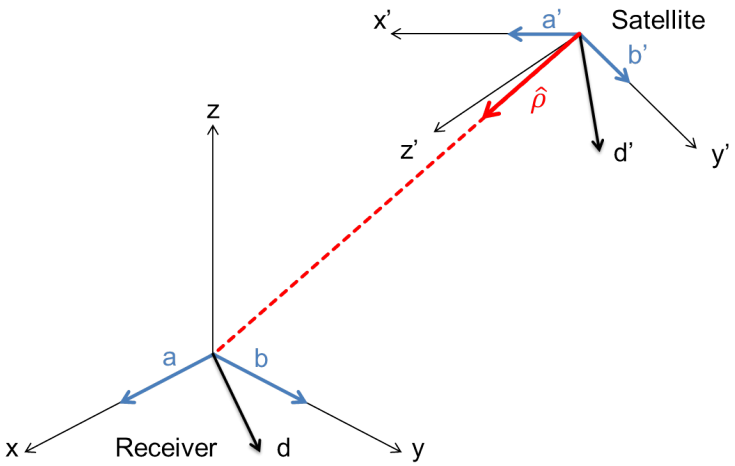

Figure 2.5: Layout of the antennas' orientation – source: http://www.navipedia.net (2014)

Receiver antennas can also rotate in the case of kinematic positioning. However, these rotations are absorbed by the receiver clock solution in case of a vertically mounted static receiver.

According to Wu et al. (1993) the correction $w \equiv \Delta\Phi$ to compensate for the effect of phase wind-up for the motion of a satellite can be calculated by

$$\Delta\Phi = \delta\varphi + 2N\pi \tag{2.28}$$

with $\delta\varphi$ being the fractional part of one cycle, while N is the number of full cycles. $\delta\varphi$ is calculated by

$$\delta\varphi = \text{sign } \zeta \ \arccos\left(\frac{d' \cdot d}{\|d'\| \cdot \|d\|}\right) \tag{2.29}$$

with

$$\zeta = \hat{\rho}\left(d' \times d\right). \tag{2.30}$$

The integer number of full cycles N can be derived by

$$N = \text{round}\left[\frac{\Delta\Phi_{prev} - \delta\varphi}{2\pi}\right], \tag{2.31}$$

where $\Delta\Phi_{prev}$ is the phase correction from the previous epoch. d and d' are the dipoles for the receiver and the transmitter. N can be initialised as zero in the beginning of the processing.

The terms d and d' are calculated by

$$d = \hat{a} - \hat{\rho}(\hat{\rho} \cdot \hat{a}) + \hat{\rho} \times \hat{b} \tag{2.32}$$

$$d' = \hat{a}' - \hat{\rho}(\hat{\rho} \cdot \hat{a}') - \hat{\rho} \times \hat{b}', \tag{2.33}$$

where $\hat{\rho}$ is the unit vector pointing from the satellite to the receiver along the LOS. The unit vectors $\hat{a}$ and $\hat{b}$ point to the east and the north direction of the receiver coordinate system denoted as x and y in Figure 2.5. $\hat{a}'$ and $\hat{b}'$ are also unit vectors and point towards the x' and the y' direction of the satellite's reference system as shown in Figure 2.5, while z' points towards the earth's centre, x' is perpendicular to z' in the plane sun-satellite-earth and y' is completing the system along the solar panels.

2.4.3 Tidal effects

A station experiences periodic movements due to the tidal deformation of the earth. These movements are rather similar for large areas. Therefore, these effects do not have to be considered in relative positioning techniques for baselines up to 100 km. Anyway, in PPP processing these site displacement effects are mirrored in the position solution if not corrected by models. In the following only the largest site displacement effects consisting of

- solid tides,
- ocean loading and
- pole tides

are treated, since all errors smaller than 1 cm are negligible for PPP processing anyway.

Solid tides

The largest tidal site displacement effect for GNSS positioning is the displacement of the earth's crust or solid earth tide. If not considered, this effect can result in periodic positioning errors of up to 30 cm in height and up to 5 cm in horizontal direction (c.f. Kouba, 2009).

The solid earth tides are caused by the same gravitational forces as the ocean tides, mainly from the sun and the moon, and can be described by spherical harmonics of degree n and order m characterised by the Love number h_{mn} and the Shida number l_{nm}. For an accuracy of a few mm it is sufficient to use only the second degree of these numbers. Kouba (2009) recommends to correct the Cartesian receiver coordinates by

$$\Delta\overrightarrow{r} = \sum_{j=2}^{3} \frac{GM_j}{GM}\frac{r^4}{R_j^3} \cdot \left\{ \left[3\ l_2(\widehat{R}_j \cdot \widehat{r})\right] \widehat{R}_j + \left[3\ (\frac{h_2}{2} - l_2)(\widehat{R}_j \cdot \widehat{r})^2 - \frac{h_2}{2}\right] \widehat{r} \right\}$$
$$+ \left[-0.025\ m \cdot \sin\varphi \cdot \cos\varphi \cdot \sin\left(\theta_G + \lambda\right)\right] \cdot \widehat{r}, \quad (2.34)$$

where GM and GM_j are the gravitational parameters of the earth, the moon (for $j = 2$) and the sun (for $j = 3$). r and R_j are the geocentric state vectors of earth, moon and sun, while $\widehat{r}$ and $\widehat{R}_j$ are the corresponding unit vectors. h_2 and l_2 are the second degree Love and Shida numbers, φ and λ are the receiver coordinates and θ_G is the Greenwich Mean Sidereal Time.

Ocean loading

Ocean loading is a secondary tidal effect that occurs due to the elastic response of the earth's crust to ocean tides. Ocean loading results in the deformation of the sea floor and adjacent land. According to Kouba (2009) the resulting site displacements are nearly an order of magnitude smaller than those caused by to the solid tides. Further, the displacements due to ocean loading are more local. Therefore the effect can be neglected in the following cases:

- For single epoch positioning at the 5 cm level or worse,
- for mm-level static positioning over a 24 h period and
- for mm-level positioning of static receivers far away from coastal regions.

Under other circumstances and also for troposphere and clock solutions the effect has to be taken into account. In the positioning tool PPPsoft no correction for the effect of site displacements due to ocean loading has been implemented.

Polar tides

The polar tides are crustal deformations of the earth due to the polar motion. According to Kouba (2009) these are also very small values that have to be taken into account only for long term observations of some months.

2.4.4 Antenna reference points and phase centre offsets

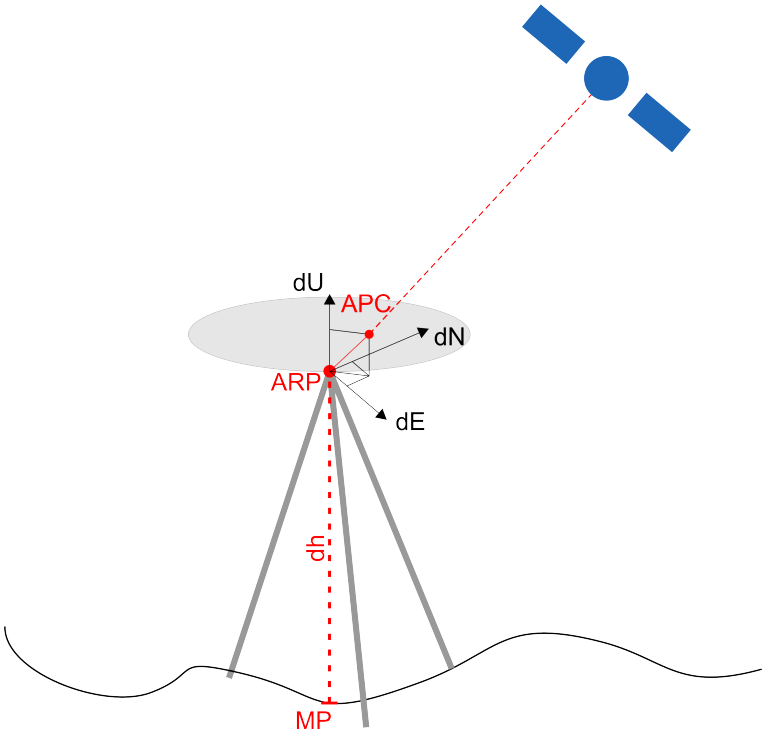

Figure 2.6: Reference points of receiver antenna

Measurements usually are referred to the receiver's Antenna Phase Centre (APC) as it is shown in Figure 2.6. The APC is frequency and also elevation dependent and is usually located inside the antenna which is rather uncomfortable for e.g. measuring the antenna height, hence a point at the bottom of the antenna is chosen as the Antenna Reference Point (ARP). Therefore, the position coordinates have to be corrected from the APC to the ARP by means of phase center corrections. Alternatively, it is possible to project the difference between the APC and the ARP onto the line of sight and directly correct the range measurements. This is quite comfortable as the calculated position then is directly referred to the ARP.

Recent values for Phase Centre Offset (PCO) and the elevation dependent Phase Centre Variation (PCV) for L1 and L2 frequencies for common receivers are given in the IGS Antex format .atx and can be downloaded via ftp-link from the IGS web site http://igscb.jpl.nasa.gov (2014).

It is rarely possible that the ARP and the unknown point where the coordinates have to be estimated – here it is called monument point (MP) – coincide. Therefore, another coordinate correction, the so-called Antenna Reference Point (ARP) correction, is necessary. Usually, only the up-direction which stands for the antenna height has to be corrected. Nevertheless it is possible that also an offset in north- or east-direction occurs.

The .atx files by the IGS also contain corrections between the GNSS satellites' phase (PC) and mass centres (MC). These corrections are needed especially when using IGS final, rapid or predicted orbits, as they are referenced to the satellites' mass centres. For highly precise position

solutions also an antenna phase centre variation can be applied, which describes additional azimuth dependent changes in the phase centres. More information on this topic can be found in Kouba (2009).

2.5 Adjustment in PPP

For GNSS processing two general strategies can be distinguished: For the post-processing mode it is possible to process all epochs in one least squares adjustment with iterations. This procedure is called batch adjustment and has the advantage, that no filtering or smoothing of the parameters is necessary. The drawback is that the computational burden of a batch adjustment is extremely high, as huge matrices have to be inverted. Especially in the case of undifferenced observations, a lot of parameters have to be estimated (c.f. Kouba, 2009).

Nevertheless, this strategy is not practicable to real-time processing, as regularly new observations are added to the adjustment. In this thesis PPP algorithms suitable for calculations in real-time or near real-time were implemented, even though many tests were performed in post-processing. Therefore, another strategy for the adjustment had to be found.

A sequential least squares adjustment approach or rather a Kalman filter seemed to be a suitable alternative for real-time PPP processing, since the computational burden is lower. This arises from the fact that the new observations of the actual epoch do only update the state vector, which is why not all epochs have to be processed again. The Kalman filter even supports the dynamic modelling of the states with respect to time, and therefore it is suitable for non-static processes. The stochastic behaviour of the parameters from epoch to epoch can be modelled and used as additional constraints on the parameters. An example therefore is the estimation of the ZWD of the troposphere, that according to Kouba (2009) can be modelled as a random walk process, that varies only slowly with time (2-5 mm/$\sqrt{\text{hour}}$).

Note that, since the observation models for PPP contain non-linear dependencies between parameters, an Extended Kalman filter is used, that is based on the initial linearisation of the equation system.

2.5.1 Kalman filter

The Kalman filter is an algorithm for the estimation of time-dependent and varying parameters named after R. E. Kalman, one of the developers of the underlying theory (c.f. Kalman, 1960). It is widely applied for navigation, guidance and control of vehicles. Its principle, as it is used in this thesis, is visualised in Figure 2.7 and shortly described by means of the following equations:

A priori values for the parameters x_0 as well as the respective initial variances and covariances in P_0 have to be defined in the beginning of the processing. The functional relation between the observations z_j and the parameters x_j is described by the design matrix H_j.

1. In a first step the gain computation takes place, where the so called gain matrix K_j is calculated from the variance/covariance matrix $\tilde{P}_j$ of the predicted parameter vector $\tilde{x}_j$, that has been calculated in the previous epoch $j-1$. A further input for the gain computation is the variance/covariance matrix R_j of the actual observations z_j. The gain matrix can be

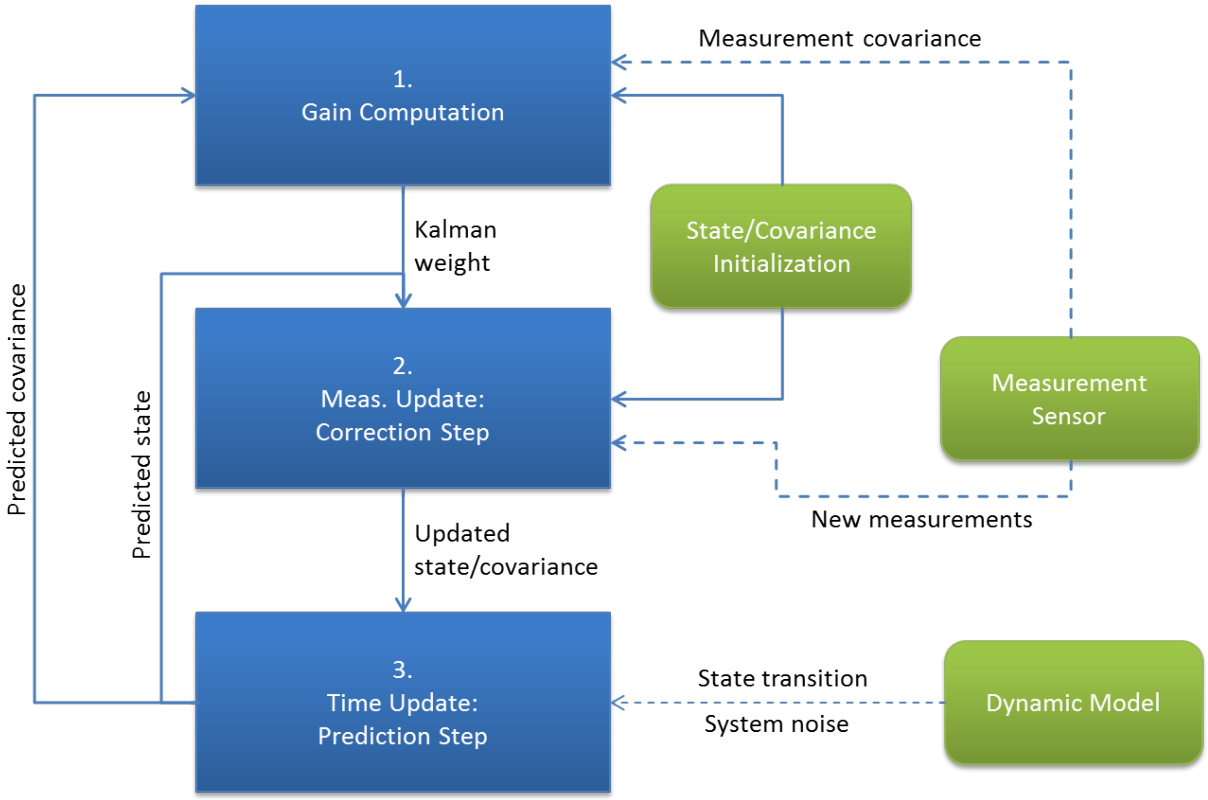

Figure 2.7: Scheme of steps in a Kalman filter (inspired by Hofmann-Wellenhof et al., 2007, page 248)

interpreted as a measure for the gain achieved by the new measurements compared to the prediction of the parameters derived in the previous epoch (c.f. Hofmann-Wellenhof and Legat, 2003 page 52ff) and can be calculated by

$$K_j = \tilde{P}_j H_j^T \left(H_j \tilde{P}_j H_j^T + R_j \right)^{-1}. \tag{2.35}$$

2. In a second step the so-called measurement update takes place. Here the predictions of the parameters get corrected by means of the new measurements of the epoch. The resulting estimated parameter vector $\hat{x}_j$ together with the respective variance/covariance matrix P_j read

$$\hat{x}_j = \tilde{x}_j + K_j \left(z_j - H_j \tilde{x}_j \right), \tag{2.36}$$
$$P_j = \left(I - K_j H_j \right) \tilde{P}_j. \tag{2.37}$$

3. In a last step the prediction of the parameters $\tilde{x}_{j+1}$ and the covariances $\tilde{P}_{j+1}$ for the next epoch have to be calculated by

$$\tilde{x}_{j+1} = \Phi_j \hat{x}_j \tag{2.38}$$
$$\tilde{P}_{j+1} = \Phi_j P_j \Phi_j^T + C_j. \tag{2.39}$$

Φ_j is called transition matrix describing the dynamical behaviour of the parameters from one epoch to the next. Uncertainties of this dynamical model are expressed in terms of the system or process noise matrix C_j.

More detailed information on Kalman filtering and other adjustment approaches can be found in Hofmann-Wellenhof and Legat (2003). The foundation of the Kalman filter is given in Kalman (1960), while Landau (1988) describes its application in the context of GNSS processing.

2.5.2 Parameters and observables

After applying precise orbits and clock products and eliminating the ionospheric influence by using the Ionosphere-free (IF) linear combination as described in (2.5) the unknown parameters x to be estimated in the Kalman filter and the observations z for the $i = 1...n$ satellites look as follows:

$$x = \begin{bmatrix} X \\ Y \\ Z \\ dt_r \\ zwd \\ N_1 \\ \vdots \\ N_n, \end{bmatrix} \quad \text{and} \quad z = \begin{bmatrix} P_{IF,1} \\ \lambda_{IF}\Phi_{IF,1} \\ \vdots \\ P_{IF,n} \\ \lambda_{IF}\Phi_{IF,n} \end{bmatrix}, \tag{2.40}$$

where $P_{IF,i}$ are the IF code pseudoranges, while $\lambda_{IF}\Phi_{IF,i}$ are the respective phase measurements in units of length.

Since the observation equations used for GNSS positioning and therefore also PPP are non-linear equations, the functional dependence as described in equations (2.4) and (2.5) has to be linearised by building partial derivatives of the observation equations with respect to each parameter. The design matrix H describes the linearised functional dependence between the parameters and the observations and contains the following terms: X_i, Y_i and Z_i are the precise ECEF coordinates of the satellites i, ρ is the geometric distance between the receiver and the satellites and wmf_i is the value for the mapping function of the wet troposphere calculated for the elevation angle of each satellite. The design matrix H reads

$$H = \begin{bmatrix} \frac{\partial P_1}{\partial X} & \frac{\partial P_1}{\partial Y} & \frac{\partial P_1}{\partial Z} & \frac{\partial P_1}{\partial dt_r} & \frac{\partial P_1}{\partial \Delta_{tro}} & \frac{\partial P_1}{\partial N_1} & \cdots & \frac{\partial P_1}{\partial N_n} \\ \frac{\partial \lambda\Phi_1}{\partial X} & \frac{\partial \lambda\Phi_1}{\partial Y} & \frac{\partial \lambda\Phi_1}{\partial Z} & \frac{\partial \lambda\Phi_1}{\partial dt_r} & \frac{\partial \lambda\Phi_1}{\partial \Delta_{tro}} & \frac{\partial \lambda\Phi_1}{\partial N_1} & \cdots & \frac{\partial \lambda\Phi_1}{\partial N_n} \\ \vdots & \vdots & \vdots & \vdots & \vdots & \vdots & \ddots & \vdots \\ \frac{\partial P_n}{\partial X} & \frac{\partial P_n}{\partial Y} & \frac{\partial P_n}{\partial Z} & \frac{\partial P_n}{\partial dt_r} & \frac{\partial P_n}{\partial \Delta_{tro}} & \frac{\partial P_n}{\partial N_1} & \cdots & \frac{\partial P_n}{\partial N_n} \\ \frac{\partial \lambda\Phi_n}{\partial X} & \frac{\partial \lambda\Phi_n}{\partial Y} & \frac{\partial \lambda\Phi_n}{\partial Z} & \frac{\partial \lambda\Phi_n}{\partial dt_r} & \frac{\partial \lambda\Phi_n}{\partial \Delta_{tro}} & \frac{\partial \lambda\Phi_n}{\partial N_1} & \cdots & \frac{\partial \lambda\Phi_n}{\partial N_n} \end{bmatrix}$$

$$= \begin{bmatrix} -\frac{X_1-X}{\rho} & -\frac{Y_1-Y}{\rho} & -\frac{Z_1-Z}{\rho} & 1 & wmf_1 & 0 & \dots & 0 \\ -\frac{X_1-X}{\rho} & -\frac{Y_1-Y}{\rho} & -\frac{Z_1-Z}{\rho} & 1 & wmf_1 & 1 & \dots & 0 \\ \vdots & \vdots & \vdots & \vdots & \vdots & \vdots & \ddots & \vdots \\ -\frac{X_n-X}{\rho} & -\frac{Y_n-Y}{\rho} & -\frac{Z_n-Z}{\rho} & 1 & wmf_n & 0 & \dots & 0 \\ -\frac{X_n-X}{\rho} & -\frac{Y_n-Y}{\rho} & -\frac{Z_n-Z}{\rho} & 1 & wmf_n & 0 & \dots & 1 \end{bmatrix}. \tag{2.41}$$

The linearisation further implies that only additions to approximate start values for the parameters are calculated in the adjustment. The single parameters contained in x and estimated in this PPP user client approach are described in the following.

The three-dimensional receiver position coordinates represented by X, Y and Z can either be treated as static, meaning that the receiver is not moving during the whole observation period, or as kinematic with changing velocity and acceleration. In the static case only one set of coordinates has to be estimated for all epochs, while in kinematic mode the positions may vary with time. For example, in the static case the estimated coordinates directly serve as prediction for the following epoch with a system noise of zero, as ideally there should be no variation in the coordinates over time. Comparatively, in the kinematic mode the system noise can be set to a large value, to simulate that the coordinates in subsequent epochs are not linked at all. If the dynamic behaviour in the kinematic mode is known, it can be approximated and modelled in the transition matrix.

Also the estimated phase ambiguities N_i have to be constrained to exploit the potential of the precise phase observations. Ambiguities physically have the characteristic that they do not vary with time, as long as no cycle slip occurs. Therefore, they are treated as constants like the static coordinates with a system noise equal to zero.

As PPP is a single point positioning technique, the receiver's clock offset dt_r is still present in the observations and has to be estimated every epoch. The receiver clock parameter may vary strongly with time depending on the receiver type. Many receiver manufacturers use unstable oscillators that show a clear drift behaviour. In that case it is common, that the clock offset is reset, when exceeding a defined threshold. This results in a sawtooth shaped time series of the clock parameter. Further, many unmodelled errors map into the estimated receiver clock offset. Therefore, this parameter is usually estimated without any relation between the epochs. This dynamic behaviour is also denoted as white noise. Note, that while within PPPsoft only the offset between the oscillator's time and the true time (with respect to the GNSS time scale) is estimated, it is also possible to estimate the drift of the oscillator, which denotes the time derivative of the clock offset.

To yield highly precise positioning results it is necessary to estimate the remaining Zenith Wet Delay (ZWD) zwd of the troposphere. General fundamentals of the tropospheric delay were already desribed in Section 2.3. The ZWD is changing only slowly with time. Linked by the respective mapping function the ZWD of the troposphere can be estimated as a common measure for all satellites. A random walk process noise like 2-5 mm/$\sqrt{\text{h}}$ can be assigned to the ZWD (see Kouba, 2009).

2.5.3 Correlations

One problematic issue of the Kalman Filter is, that the variances of the parameters become inevitably small with time, as the previous state of coordinates and ambiguities is treated as correct as long as the process noise is kept low or even zero. Therefore, the correlations especially between ambiguity estimates become very high with advanced observation time, irrespective of the geometric correlation of the satellites. When it comes to ambiguity fixing, it can be assumed that one wrong ambiguity fix also leads to wrong fixes of related ambiguities. If and how this behaviour influences PPP-AR is treated later on in Section 3.2.

3 Software for standard PPP

In 2009, when the author's research on PPP related topics at INAS started, there were not many software packages available, that allowed any insight to algorithms and models used for PPP processing. Therefore, after one year of research, the decision was made to develop a tool containing all the algorithms needed for SPP and PPP processing. From that time on the PPP client software PPPsoft was developed to create a playground for testing and evaluating different algorithms, data products and strategies related to positioning by means of PPP. This software became the basis for the investigations made in this thesis and therefore, also for the PPP solution with ambiguity fixing, which is the most recent development in PPPsoft and the central topic of this thesis.

In the beginning of the developments a standard SPP solution was used as a basis, which was step by step enriched and extended by several functions, in order to allow for the calculation of a first code-based PPP solution. Some of the very first functions for model corrections as well as some input and output functions could be taken from a former colleague at INAS and reused for PPPsoft. These basic PPP processing functions had been implemented for a former research project. Further, some input functions were exploited from the GPS Easy Suite (see http://kom.aau.dk/borre/easy, 2014), which contains Matlab code for basic GNSS related operations (c.f. Borre, 2009 and Borre et al., 2007).

Later on, the multifunctional positioning tool PPPsoft was extended and redesigned in order to enable code- and phase-based positioning using different products to compensate for satellite orbit and clock errors, as well as for atmospheric and other effects. By means of these modifications positioning with accuracies at the cm-level became possible. Real-time as well as post-processing static and kinematic data could be processed and visualised in different ways. The drawback of the solution was, that the whole processing was still based on the estimation of real-valued ambiguities, which lead to long convergence times typical for PPP.

In the beginning of 2012, the project PPPserve (described in Section 1.3) came up. This project aimed at solving the well-known problem of PPP with Ambiguity Resolution and Fixing (PPP-AR). Therefore, the project team started the research on solving integer ambiguities within PPP. This also led to the implementation of functions enabling ambiguity resolution in the user client PPPsoft, which denotes the biggest and also the most innovative part of this thesis. Therefore, Chapter 4 is dedicated solely to the ambiguity resolution method implemented in the user client.

Nevertheless, this current chapter introduces the basic software PPPsoft for standard PPP, as well as some aspects of PPP in general. This serves as a preparation for the ambiguity resolution procedure treated in the subsequent chapters.

Before presenting the software PPPsoft, the two terms RTCM and Ntrip are shortly defined, as these two play a major role in the presented realisation of real-time PPP and therefore, do occur several times throughout this thesis.

RTCM

The Radio Technical Commission for Maritime Services (RTCM) is an international standards organisation, initially aiming at the development of standards for marine telecommunications. RTCM started in 1947 as a U.S. government advisory committee. Today it is consisting of and supported by private and also governmental organisations all over the world. Information on the organisation and its products can be found on http://www.rtcm.org (2015).

Within RTCM several Special Committees (SC) work on standardisation in specific fields of application. The SC 104 is working on Differential GNSS (DGNSS) and provides standards for all kinds of DGNSS and RTK operations.

Recently, in 2011, the RTCM 3.1 Amendment 5 was released (see Radio Technical Commission for Maritime Services, 2011), that for the first time contains standards for PPP corrections. These so-called State Space Representation (SSR) messages enable transmitting orbit corrections, clock corrections and code bias information for both, the GPS and the GLONASS system, to the user in real-time. A detailed description of SSR corrections for GPS and GLONASS was given in Section 2.2.

The document also includes a prospect on upcoming developments of SSR messages in the RTCM standard. In addition to the orbit and clock corrections for GPS and GLONASS there are plans to develop SSR messages for the Vertical Total Electron Content (VTEC) and the Slant Total Electron Content (STEC), as well as tropospheric messages and satellite phase bias messages. In 2013 a new RTCM standard (RTCM 3.2) was released, focusing now on Multi-Signal Message (MSM) support, which is designed to handle all constellations, signals, and observation types so as to ensure full compatibility with the information content of Receiver Independent Exchange Format (RINEX) observation files (c.f. Montenbruck et al., 2014).

Ntrip

According to http://igs.bkg.bund.de/ntrip (2014) Ntrip is an application level protocol that supports the streaming of GNSS data in the RTCM format via the internet. Ntrip is a generic and stateless protocol based on the Hypertext Transfer Protocol HTTP/1.1 that was designed to disseminate differential corrections or other kinds of GNSS data to stationary or mobile users over the internet (c.f. Radio Technical Commission for Maritime Services, 2011). Ntrip allows the simultaneous connection of several devices such as PCs, laptops, PDAs or receivers to a broadcasting host via mobile IP networks like GSM, GPRS, EDGE or UMTS.

3.1 PPPsoft

The central tool underlying this thesis is the PPP client application PPPsoft, consisting of a Graphical User Interface (GUI) and the PPP library containing all the functions required for

- the handling of input and output,
- the conversion of all data files to the internal format,
- the model calculation,
- the processing and filtering and the

- final visualisation of results.

The GUI as well as all other functions of PPPsoft were written in Matlab (the Language for Technical Computing, see http://www.mathworks.de/products/matlab, 2014). The latest version of the software is tested with Matlab 2013a. PPPsoft was written step by step for the purpose of research and investigations, which is why the focus is not set on portability or processing speed.

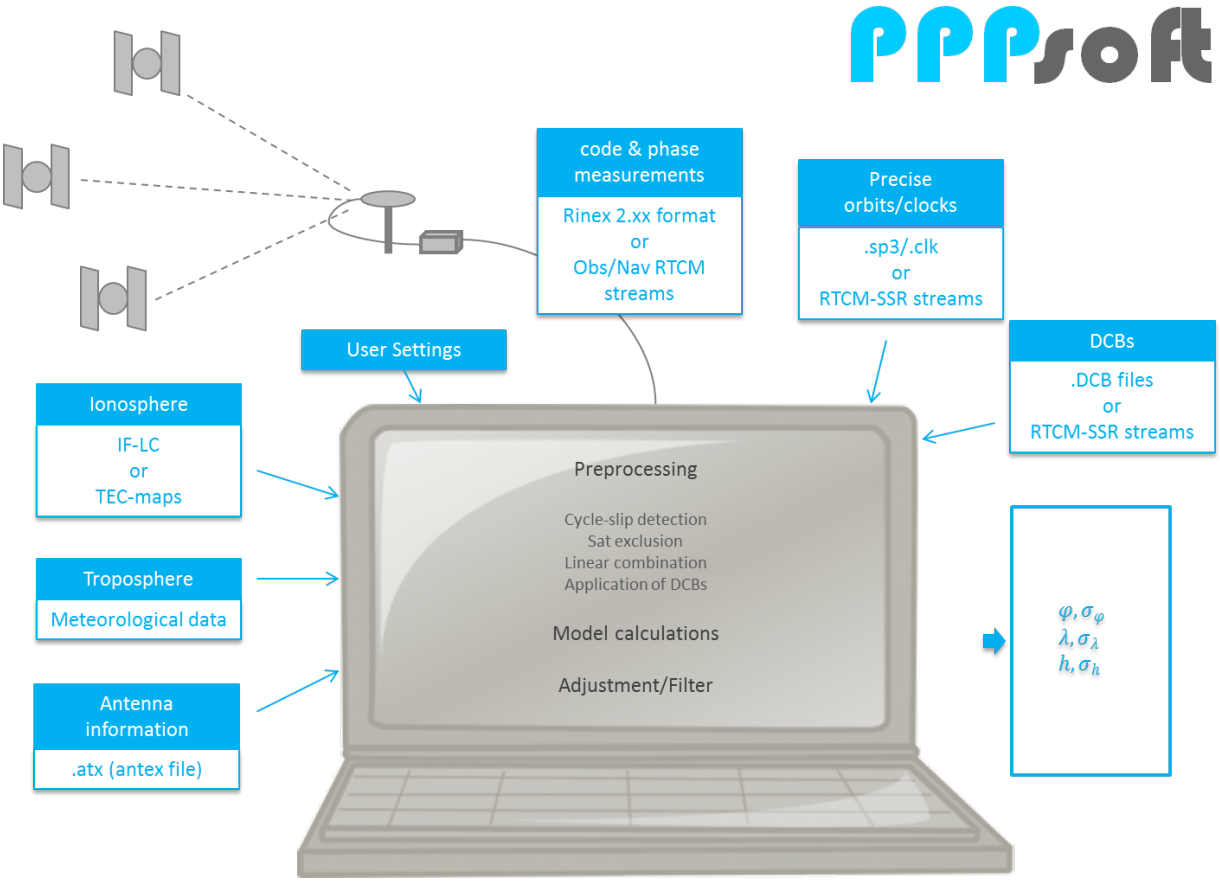

Figure 3.1: Processing scheme of PPPsoft

The paths for input and output files as well as the user's settings can be defined in the GUI that is shown in Figure 3.2. Many algorithms and models described in Chapter 2 were implemented in the development phase of PPPsoft. The key features of the software are shortly presented in the following sections according to the processing scheme visualised in Figure 3.1.

3.1.1 GNSS observation input

The most general way to store and exchange GNSS observation data for post-processing is to use the Receiver Independent Exchange Format (RINEX). While usually receiver manufacturers use their proprietary raw format to store the observation and broadcast ephemeris data in the receiver, every raw format can be converted to different versions of RINEX. Therefore in PPPsoft RINEX observation and navigation files can be read and processed in post-processing. At the

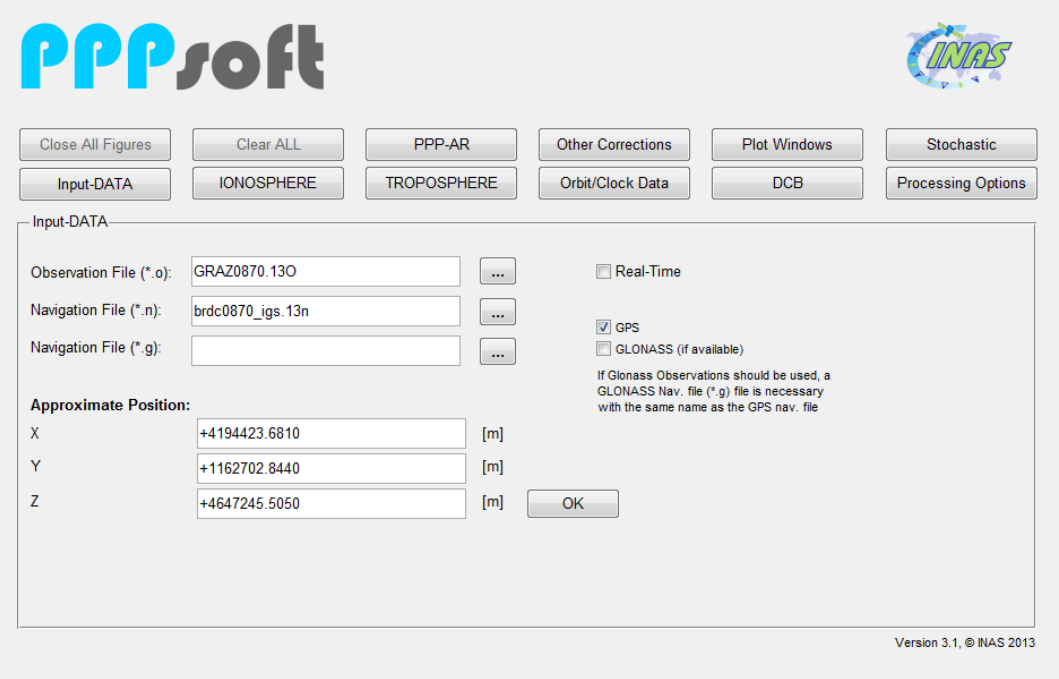

Figure 3.2: GUI of the PPP user client PPPsoft - observation input

moment the use of RINEX 2.xx is supported. Nevertheless, also the input functions for reading RINEX version 3.xx files are envisaged in the near future. The format descriptions for the different RINEX versions can be found in http://igscb.jpl.nasa.gov (2014).

For real-time applications real-time GNSS observation streams encoded in the standardised RTCM format can be used. In general, these binary observation and navigation streams can be produced by GNSS receivers, that are capable of RTCM coding and transmission. In PPPsoft there is no proprietary RTCM client implemented to decode these RTCM messages. For this purpose the external RTCM decoder BNC developed by the Bundesamt für Kartographie und Geodäsie (BKG) is used, which is an open-source software and offered for Microsoft Windows and Linux based platforms (available at http://igs.bkg.bund.de/ntrip, 2014). BNC enables to receive and decode RTCM streams from sources such as the IGS Ntrip caster www.igs-ip.net , which offers observation streams from several IGS stations. After reception the data can either be forwarded via TCP-IP port or logged in a file by the Ntrip client and server software of the BKG (BNC). When logged in a file, the observation and navigation data is stored again in a RINEX format file. For reasons of repeatability for PPPsoft these files are always stored, and can either be read immediately in near real-time or later on in post-processing in order to repeat the test scenario.

The rover's or station's approximate position coordinates, which are used as initial position for the adjustment procedure or rather Kalman filter, can either be read from the observation file header or entered manually. For unknown rovers only a coarse approximation of the initial coordinates is sufficient for the processing. Nevertheless, if accurate a priori position coordinates for the receiver are available, as it is the case for stations in a GNSS reference network, constraints on these coordinates can be defined. These initial coordinate constraints can be used to accelerate

the convergence dramatically. Further, to test the functionality of the PPP solution or different methods and products, well-known station coordinates can serve as a reference to evaluate the coordinates' accuracy. These are also used for the visualisation of offsets in the resulting position. In order to avoid displacements due to plate tectonics and to be consistent with the satellites' orbits the reference positions should ideally be available in the latest version of the ITRF (currently ITRF08 is used) and at the time of the observation.

For detailed information on the different realisations of the International Terrestrial Reference System (ITRS) the reader is referred to http://www.iers.org (2014).

It has to be mentioned that PPPsoft is able to process also multi-GNSS data (currently GLONASS, Galileo in progress), but as PPP with Ambiguity Resolution and Fixing (PPP-AR) is not implemented for the use with multiple GNSS in PPPsoft, this topic is not further treated in the course of this thesis.

3.1.2 Orbit and clock input

As PPP relies on the use of precise ephemeris products, several formats containing satellite orbits and clock corrections are implemented in PPPsoft. Apart from broadcast ephemerides transmitted by the satellites by means of their navigation message, also the more precise .sp3 and RINEX clock files can be chosen for post-processing. For real-time processing the use of RTCM SSR streams for example available from the IGS caster for GNSS products products.igs-ip.net is possible. These SSR streams contain orbit and clock corrections to correct the broadcast ephemerides. A theoretical description of these types of ephemerides was already given in Section 2.2.

Similar to the observation and navigation streams, the SSR streams containing ephemeris corrections are transmitted in the binary RTCM format and have to be decoded by BNC or any other RTCM client software.

```
! Orbits/Clocks: 29 GPS 0 Glonass
1060 0 1685 120605.0 G01   13   -0.450   0.484  -0.609  -0.131   0.00000   0.00003  -0.00023   0.00000   0.00000
1060 0 1685 120605.0 G02  102   -1.052   0.676   0.253  -0.332   0.00000   0.00001   0.00012   0.00000   0.00000
1060 0 1685 120605.0 G03  112   -2.557   1.957   0.255  -0.244   0.00000   0.00000  -0.00016  -0.00016   0.00000
1060 0 1685 120605.0 G04  158   -2.585   1.495  -0.261  -0.527   0.00000   0.00002  -0.00041  -0.00018   0.00000
1060 0 1685 120605.0 G05   69   -1.060   0.904   0.166  -0.054   0.00000  -0.00000  -0.00042   0.00006   0.00000
```

SSR message | GPS week | Sec. of week | Sat. PRN number | Eph.IOD | C0 clockterm [m] | Radial component [m] | Along-track comp. [m] | Cross-track comp [m] | C1 clockterm [m/s] | Velocity of rad. Comp. [m/s] | Velocity of along-track comp [m/s] | Velocity of cross-track comp. [m/s] | C2 clockterm [m/s²]

Figure 3.3: SSR messages after decoding by BNC – orbits and clocks

After their decryption these messages are recorded by BNC in an ASCII format, which is shortly described in Figure 3.3. The example dataset uses the RTCM message number 1060, which contains combined orbit and clock corrections for GPS and GLONASS data. The clock corrections to the corrections contained in the broadcast ephemerides are transmitted in form of coefficients of a second degree polynomial c0, c1 and c2 given in m, m/s and m/s^2, while the orbit corrections

consist of along-track, across-track and radial orbit and velocity corrections given in m and m/s. All these corrections are linked to a certain set of broadcast ephemerides, which is indicated by the IOD field.

3.1.3 Code biases

Additional to the orbit and clock corrections, the SSR streams contain corrections to compensate hardware-specific code biases for the individual satellites and signals, the so-called DCBs. Contrary to the DCB files available from CODE (see Section 2.4) the code corrections from the SSR messages are meant to be added directly to the uncombined signals. Therefore, no multiplication factor is needed. Figure 3.4 shows how these messages appear after decoding by BNC.

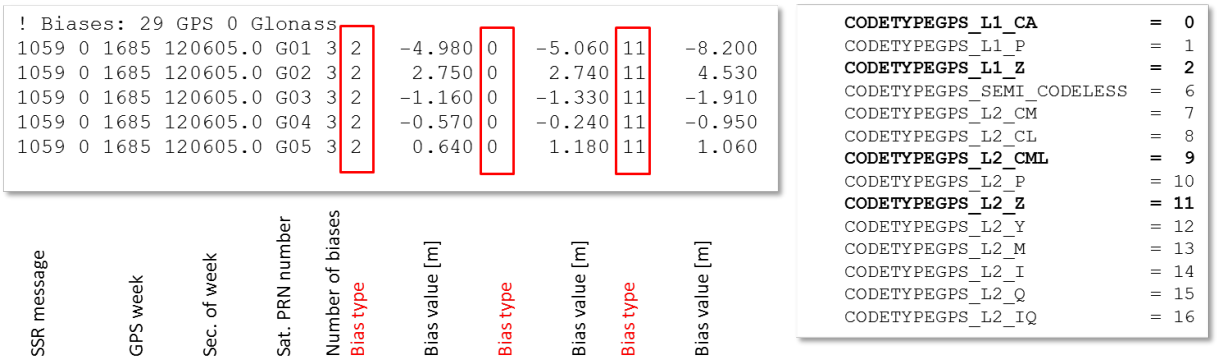

Figure 3.4: SSR messages after decoding by BNC – DCBs

In one message line several bias types can occur, as for example bias type 0 is the correction for the C/A-code on the GPS carrier L1, while bias type 2 is the correction for the P-code on the same carrier. A full list of bias types as given in BNC can also be seen in Figure 3.4 on the right hand side. All code bias corrections are given in meters. Despite their diverse representation, these biases are fully consistent with the monthly bias files published by CODE. Both representation types can be used within PPPsoft, but the SSR streams are more preferable for real-time applications, since the SSR corrections for orbits and clocks are used anyway.

3.1.4 Ionosphere & troposphere

As already described in Section 2.3 in the single-frequency case the ionospheric delay can be modelled by the Klobuchar model, which is broadcast by the satellites themselves in the navigation message. For a higher accuracy several regional and global TEC models and grids are available for download by GNSS analysis centres. Nevertheless, the ambiguity resolution approach in PPPsoft is only implemented for the dual-frequency case where the Ionosphere-free (IF) observation equation as described in equations (2.4) and (2.5) is used by default, therefore only the IF case is treated in this thesis in detail.

The tropospheric models available in PPPsoft are the Saastamoinen and the Hopfield model. These analytical models are dependent on temperature, pressure and humidity. Therefore, either

standard values or meteorology data files can be used (see Section 2.3). Although these analytical models are able to describe the whole tropospheric delay (hydrostatic + wet part), only the hydrostatic part can be modelled accurately. The residual usually wet part of the tropospheric delay is estimated as described in Section 2.5 to achieve the highest reachable accuracies for the solution. For GNSS stations it is also possible to read external troposphere solution files, which can reduce the convergence time especially for the height component. Though, this is only useful for testing purposes, as for arbitrary rover positions no such files from e.g. nearby GNSS stations may be available.

Test calculations, where external troposphere data is introduced in the PPP solution, are shown later on in Chapter 5.

3.1.5 Other settings

Apart from the main settings described above, a lot of other model corrections can be selected and calculated within PPPsoft. Their theoretical fundamentals have been already described in Section 2.4 in detail, and therefore are only listed in this chapter. These models include

- PCO corrections for the receiver's and the satellites' antenna,
- ARP corrections,
- tidal effects and
- phase wind-up corrections.

Several settings for the pre-processing, which are implemented in PPPsoft can be defined in the GUI. Available pre-processing functions include different methods for the detection of cycle slips or code smoothing by phases, which however is not used for PPP with Ambiguity Resolution and Fixing (PPP-AR) and is mentioned here only for the sake of completeness.

Figure 3.5 gives and overview on the stochastic settings, that are available in PPPsoft. The first decision by the user is whether the solution should be filtered or not. Thereby, it has to be mentioned that for epoch-wise processing an unfiltered code-plus-phase solution is no more accurate than a code-only solution, as the ambiguities cannot be constrained to constant values and vary in the range of the code noise.

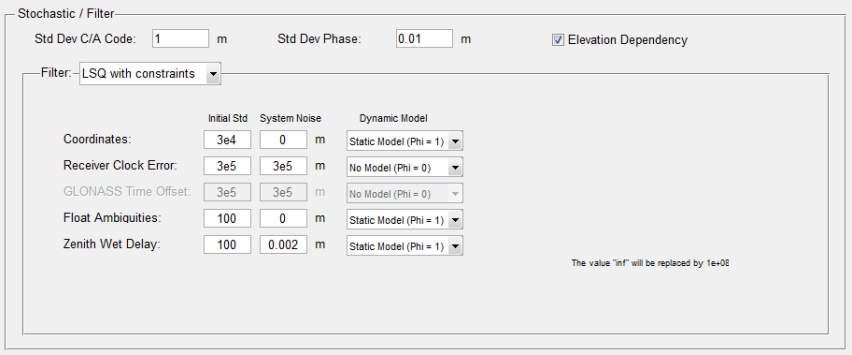

Figure 3.5: Stochastic settings PPPsoft

Further, settings for the quality of observables as well as for the quality of the initial coordinates for the filtered solution can be made. The observation weights are usually multiplied by the elevation dependent factor $factor = \sin^2(elevation)$ to minimise the effect of unmodeled errors occuring especially with satellites in a low elevation. For the Kalman filter the dynamical behaviour of the unknown parameters can be defined together with the system noise. The theoretical details on the Kalman filter can be found in Section 2.5. As for this thesis mainly static data was processed, it was abstained from any sophisticated dynamical models that make use of the velocity or acceleration of the rover so far. Instead, only the system noise of the single parameters can be varied.

3.1.6 Output

The output of the software can be defined by the user in several ways. By default a position file containing the geographic positions, which are defined by the geographic latitude φ, the geographic longitude λ and the ellipsoidal height h, referenced to the current realisation of the ITRF is produced. Alternatively, also three-dimensional Cartesian coordinates or plane coordinates in the Universal Transverse Mercator (UTM) system can be produced. Further an NMEA file or a .kml file, that can be read by Google Earth, can be exported.

To visualise the results of the solution different kinds of figures can be produced. These contain, among others, time series of the estimated positions, clock estimates, troposphere estimates, post-fit residuals of code and phase observations, satellite positions or ambiguities.

3.2 Some aspects

3.2.1 Sat-to-sat Single-difference (SD) solution

Generally, the observation model of standard PPP solutions is a Zero-difference (ZD) model. As described in Section 2.1, in a ZD model no differences are built between receivers or satellites, whereby the receiver-specific errors and effects like the receiver clock offsets or UPDs always remain in the observations. Therefore, they have to be estimated or compensated by modelling, even though these informations are not interesting for the user in the first place. Therefore, in PPPsoft not only a ZD solution was implemented but also a modified PPP observation model using satellite-to-satellite SDs. This SD model has been originally used for the PPP-AR solution, which generally is based on SD ambiguities (c.f. Section 4.2.3).

Design SD solution

As PPP in the broadest sense only denotes the processing of isolated stations, we could also switch to a slightly different model, where satellite-to-satellite Single-difference (SD) observations are built. This concept is visualised in Figure 3.6. By doing so, all receiver-specific errors (also receiver-specific UPDs) cancel and the parameters to be estimated are reduced by the receiver clock error. The remaining parameters x are the receiver's three-dimensional static or kinematic coordinates X, Y and Z, the wet part of the tropospheric zenith delay zwd and the ambiguities

N_{Ref-i}, which are now estimated not in an absolute sense, but with respect to a predefined reference satellite Ref. This reference satellite has to be chosen carefully, as the errors in the observation of the reference satellite are also contained in all SD observations. The observation vector z contains the SD code and phase observations $P_{IF,Ref-i}$ and $L_{IF,Ref-i}$, which are again only differences to the observations of the reference satellite. The observation vector z and the parameter vector x read

$$x = \begin{bmatrix} X \\ Y \\ Z \\ zwd \\ N_{Ref-1} \\ \vdots \\ N_{Ref-n} \end{bmatrix} \quad \text{and} \quad z = \begin{bmatrix} P_{IF,Ref-1} \\ L_{IF,Ref-1} \\ \vdots \\ P_{IF,Ref-n} \\ L_{IF,Ref-n} \end{bmatrix} \tag{3.1}$$

with

$$L_{IF,Ref-i} = \lambda_{IF}\Phi_{IF,Ref-i}. \tag{3.2}$$

In compliance with the partial derivatives of the ZD solution in equation (2.41), the design matrix H for the SD solution is built from the partial derivatives of the reference satellite minus the actual satellite resulting in

$$H = \begin{bmatrix} -\frac{X_{Ref}-X}{\rho_{Ref}} + \frac{X_1-X}{\rho_1} & -\frac{Y_{Ref}-Y}{\rho_{Ref}} + \frac{Y_1-Y}{\rho_1} & -\frac{Z_{Ref}-Z}{\rho_{Ref}} + \frac{Z_1-Z}{\rho_1} & wmf_{Ref-1} & 0 & \dots & 0 \\ -\frac{X_{Ref}-X}{\rho_{Ref}} + \frac{X_1-X}{\rho_1} & -\frac{Y_{Ref}-Y}{\rho_{Ref}} + \frac{Y_1-Y}{\rho_1} & -\frac{Z_{Ref}-Z}{\rho_{Ref}} + \frac{Z_1-Z}{\rho_1} & wmf_{Ref-1} & -1 & \dots & 0 \\ \vdots & \vdots & \vdots & \vdots & \vdots & \ddots & \vdots \\ -\frac{X_{Ref}-X}{\rho_{Ref}} + \frac{X_n-X}{\rho_n} & -\frac{Y_{Ref}-Y}{\rho_{Ref}} + \frac{Y_n-Y}{\rho_n} & -\frac{Z_{Ref}-Z}{\rho_{Ref}} + \frac{Z_n-Z}{\rho_n} & wmf_{Ref-n} & 0 & \dots & 0 \\ -\frac{X_{Ref}-X}{\rho_{Ref}} + \frac{X_n-X}{\rho_n} & -\frac{Y_{Ref}-Y}{\rho_{Ref}} + \frac{Y_n-Y}{\rho_n} & -\frac{Z_{Ref}-Z}{\rho_{Ref}} + \frac{Z_n-Z}{\rho_n} & wmf_{Ref-n} & 0 & \dots & -1 \end{bmatrix}. \tag{3.3}$$

Note, that compared to the design matrix of the ZD solution (2.41), here the column for the receiver clock is not used any more as the receiver clock parameter is eliminated by building the sat-to-sat SDs. Technically, the derivative for the ambiguity of the reference satellite N_{Ref} would be the IF wavelength λ_{IF} and the derivative for the actual satellite would be $-\lambda_{IF}$. To avoid a rank deficiency, N_{Ref} is treated as known quantity with the value 0 and therefore is eliminated from the equation system. Again the difference between the reference satellite's and the actual satellite's ambiguity N_{Ref-i} is estimated in meters instead of cycles, which is why the wavelength λ_{IF} is replaced by 1.

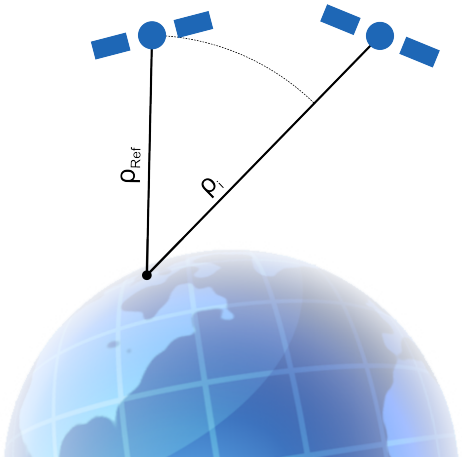

Figure 3.6: SD PPP principle

Regarding the functional dependency described in H in (2.41), it becomes obvious that the receiver's position still remains in the equation system. Therefore, mathematically there should be no difference between the coordinate solution of a ZD and a sat-to-sat SD solution (see Petovello, 2011).

The reference satellite and its dangers

The main disadvantage of the SD PPP solution is, that a reference satellite has to be chosen not only for the fixing procedure but also for the PPP float solution, which is calculated before. This leads to the loss of one set of observations already in the float solution. As all observations are subtracted from the ones of the reference satellite, the SD observations inevitably contain the errors of the reference satellite. Therefore, it is important to use the most reliable satellite as a reference, which in PPPsoft is assumed to be the one rising satellite with the highest elevation. Highly elevated satellites usually have the lowest noise and the least remaining error effects from unmodelled atmospheric influences and they rarely do suffer from cycle slips. These characteristics are mandatory for the chosen reference satellite, but unfortunately cannot be guaranteed. It may also happen that the chosen satellite has e.g. erroneous ephemeris data or other problems, which is naturally not dependent on the elevation. Nevertheless, as PPPsoft is only an experimental piece of software, the unlikely eventuality of a failure in the chosen reference satellite is not treated extensively, but should be further investigated in the future.

Visibility and change of reference Satellite

Initially, the highest rising satellite is chosen and taken as the actual reference satellite, as long as no obvious ephemeris errors occur. Unfortunately, a satellite is not visible for more than a few hours depending on how it is traversing the sky. Therefore, after some time it is likely that the reference satellite has to be changed. If this happens, also the estimated ambiguities have to be recalculated to be consistent with the new reference satellite. Therefore, the old reference satellite (PRN 4 in example (3.4)) has to be inserted in the vector of ambiguities again. Afterwards

the estimated ambiguity value of the new reference satellite (PRN 6 in example (3.4)) can be subtracted from the old values as descibed by

$$\begin{bmatrix} N_{4-1} \\ N_{4-2} \\ N_{4-3} \\ N_{4-4} \\ N_{4-5} \\ N_{4-6} \end{bmatrix} - N_{4-6} = \begin{bmatrix} N_{6-1} \\ N_{6-2} \\ N_{6-3} \\ N_{6-4} \\ N_{6-5} \\ N_{6-6} \end{bmatrix}. \tag{3.4}$$

Now all ambiguities are referenced to the new reference satellite. This new reference satellite has the ambiguity value zero after the subtraction, as the old reference satellite had before. Finally, the new reference satellite again is eliminated from the equation system.

Comparison with ZD solution

Several tests verified that the coordinate solutions of the undifferenced and the single-differenced version show comparable results; of course only under the assumption of error-free reference observations. Figure 3.7 shows an example calculation of station Graz Lustbühel on DOY 087 in 2013 using both observation models, the ZD and the SD model. The figures show the North, East and Up (NEU) coordinate differences of the solution with respect to the known station coordinates over the observation time.

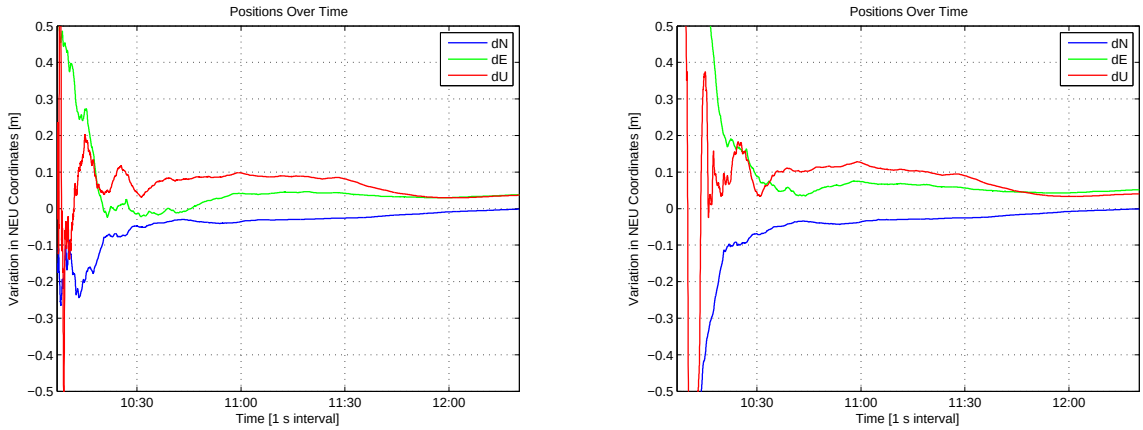

(a): ZD solution

(b): SD solution

Figure 3.7: Comparison of ZD and SD solution of Graz Lustbühel DOY 087 2013 using final IGS orbits and clocks

As one can see the solutions resemble each other within the range of a few centimetres. This difference occurs, since the inaccuracies of the reference satellite propagate within the whole solution, which is obviously the biggest problem of the SD observation model.

PPPsoft is capable of using both observation models the ZD and the SD model for the PPP float solution. Initially, the PPP-AR solution was implemented for the SD model only, but later on the software was re-designed for PPP-AR possible also with the ZD observation model. Nevertheless,

the ambiguity fixing itself still is based on single-differences of the float ambiguities. For this reason, the problems and aspects of choosing and changing the reference satellite are still present and therefore explained in this thesis.

3.2.2 Correlations in PPP

In the following paragraphs a phenomenon, that occurs together with PPP processing with coordinate constraints, is shortly described on the basis of one of the datasets used for the tests of the PPPserve client application. In the dataset of the station Graz Lustbühel on DOY 088 in 2013 a special satellite geometry can be found. The observation interval of this dataset is 1 s.

Figure 3.8 shows the respective skyplot and the elevation plot of the satellites. The skyplot in (a) contains the observed satellites from the user's point of view with the elevation of the satellites in degrees visualised as concentric circles and the azimuth in degrees running clockwise with the origin in the north direction. The elevation plot in (b) contains the satellites' elevation angles in degrees over the processing epochs. The values of the elevation angles are represented by the colours in the colourbar on the right hand side of the figure. The satellites are represented by their PRN numbers on the Y-axis.

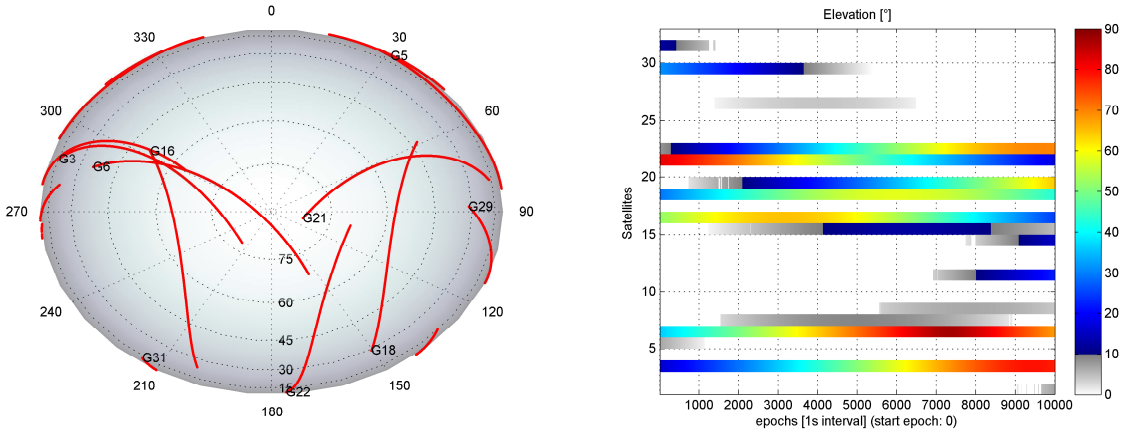

(a): Skyplot (b): Elevation

Figure 3.8: Satellite constellation of Graz Lustbühel DOY 088 2013

Figure 3.9 shows the visualisation of the respective correlation matrices of the estimated parameters at different times of the processing. These correlation matrices contain the following parameters: the 3D-coordinate components dX, dY, dZ, the estimated wet troposphere delay $dTro$ and afterwards the ambiguity estimates of the satellites in view. The colors represent the correlation of the matrix elements, where the dark red colour stands for a high positive correlation and the dark blue colour stands for a high negative correlation. The paler the colour looks, the weaker is also the correlation of the matrix components.

In the beginning of the processing the satellites PRN 3, PRN 6 and PRN 16 have quite a similar elevation and azimuth. That is why the ambiguities are also strongly correlated in epoch 10 as it is shown in Figure 3.9 (a). After some time, in epoch 420 (Figure 3.9 (b)) this correlation has reached

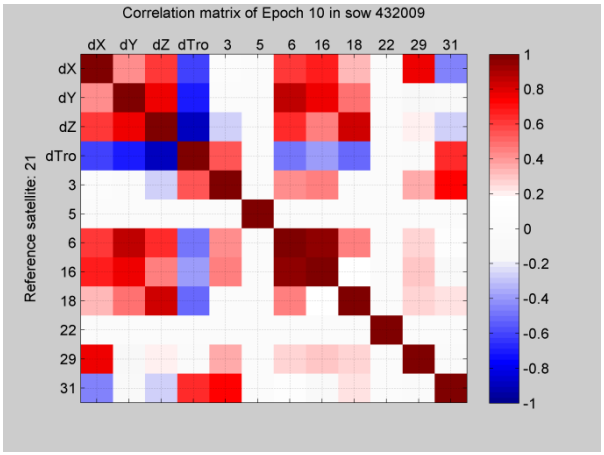

(a): Epoch 10

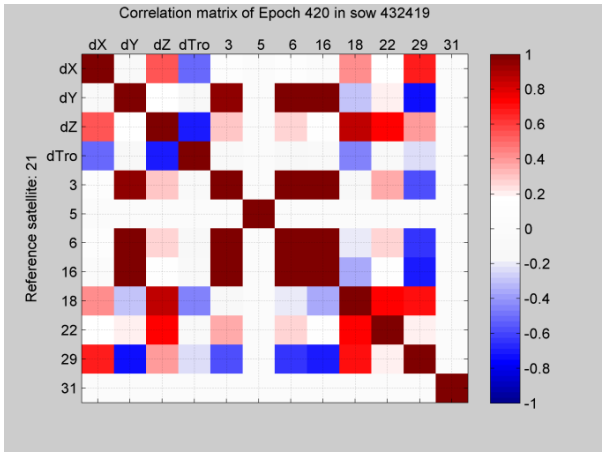

(b): Epoch 420

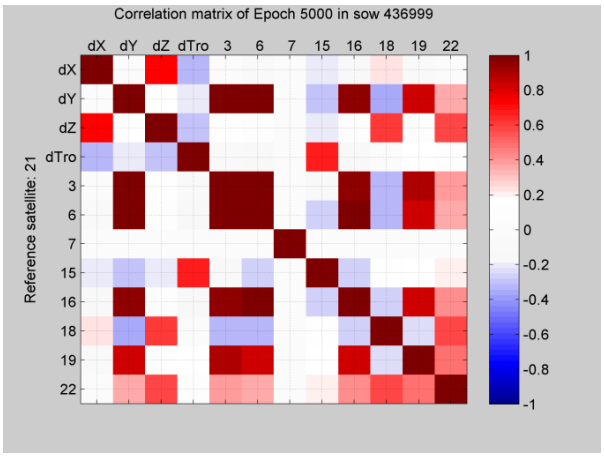

(c): Epoch 5000

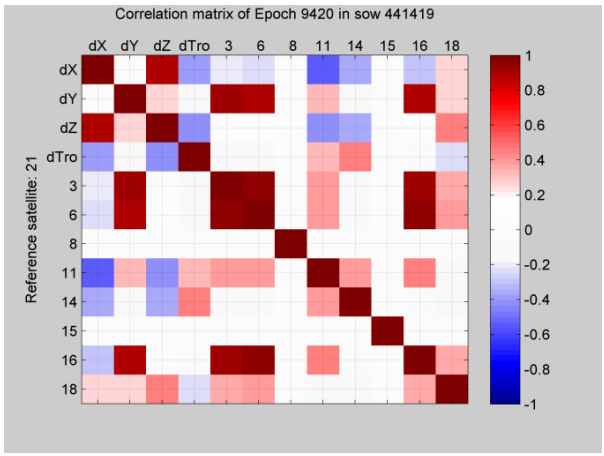

(d): Epoch 9420

Figure 3.9: Correlation plots of Graz Lustbühel DOY 088 2013

the maximum. The ambiguities are correlated with a factor of nearly 1 and also the correlation between these ambiguities and the Y-component of the coordinates is at its maximum. At that time the strong correlation between the satellites still is reasonable due to the satellites' geometry. Nevertheless, in Figure 3.9 (c) corresponding to epoch 5000 and Figure 3.9 (d) corresponding to epoch 9420 this high correlation of parameters can still be observed, even though physically the satellites now have drifted apart and one could assume, that also the correlation should fade. Several tests showed that such a correlation maximum remains present, until one of the satellites drops out for some reason, which may be either due to the absence of ephemeris corrections or a temporary obstruction of this satellite. Obviously, this effect is caused by the settings of the processing filter: In static PPP usually the process noise of the coordinates as well as the ambiguities is set to zero, which means that these parameters do not change over time. This is a necessary constraint to exploit the full potential of static PPP. Nevertheless, this may result in further problems when it comes to ambiguity fixing, as the parameters do influence each other to a high amount. For example, if one ambiguity is fixed to a wrong integer value, the other highly correlated ambiguities may also be fixed to a wrong value. Because the correlations are stuck at

their maximum values the solution may not get better with time and therefore changing satellite geometry, as it would be the expectable behaviour.

After localisation of this correlation behaviour further investigations on correlations within PPP were made in the course of this thesis. Some further samples on this topic are extensively described and analysed later on in Chapter 5.

3.3 Results for standard PPP

Type	Format	File	Information
Observations	RINEX 2.11	GRAZ0880.13O	interval of 1s
Epochs	1 Epoch is 1s	10000 – 30000	–
Obs. Time	GPS time	2:46:40 – 8:20:00	–
ORBIT/CLOCK	IGS final orbits and clocks	igs17335.sp3 igs17335.clk_30s	– –
	or		
	SSR correction by CNES	CLK9B0880.13C	recorded by PPP-wizard
DCBs	SSR correction by CNES	CLK9B0880.13C	recorded by PPP-wizard

Table 3.1: Test data used in PPP float solution

In the following some representative example results from the standard PPP solution with float ambiguities calculated with PPPsoft are shown. Therefore, station data from the IGS station Graz Lustbühel was used together with final IGS precise ephemerides, as well as together with real-time SSR streams containing orbit and clock corrections to broadcast ephemerides (details listed in Table 3.1). The reference position of the station is known precisely (mm-level) and given in ITRF08, the reference frame of the precise ephemerides, which further defines the geodetic datum of the PPP solution. The DCBs in the SSR messages are completely consistent with the DCB tables from e.g. CODE, which is why the recorded DCB corrections were used for the sake of simplicity.

3.3.1 Post-processing results

The results of the PPP float solution calculated with IGS precise orbits and clocks are visualised in Figure 3.10. Figure 3.10 (a) shows the differences of the NEU components of the static PPP solution compared to their reference coordinates over time. The solution shows a typical convergence behaviour, where after about 20-30 minutes the accuracy of the position components reaches the dm-level, after 1 hour the accuracy has increased to a few centimetres and the full convergence is reached after approximately 2 hours, meaning that no significant improvement can be detected after that time.

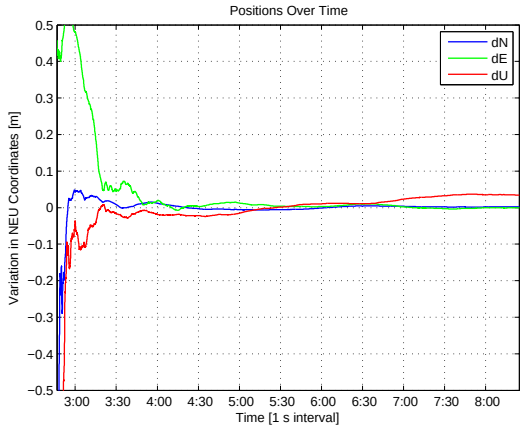

(a): NEU coordinate plot

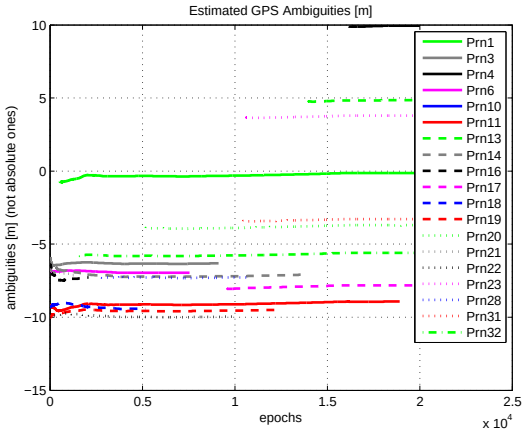

(b): Estimated ambiguities

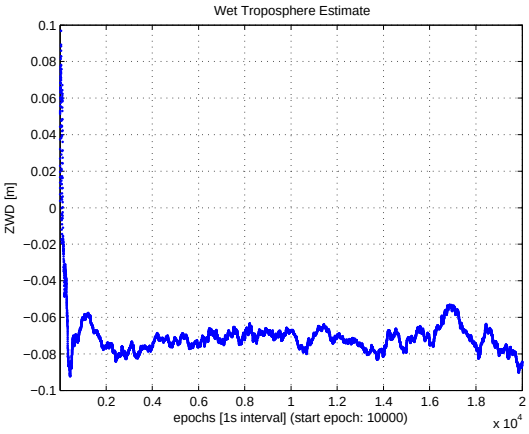

(c): Estimated ZWD

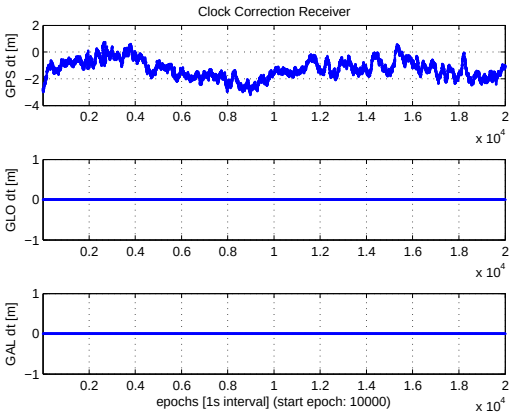

(d): Receiver clock correction

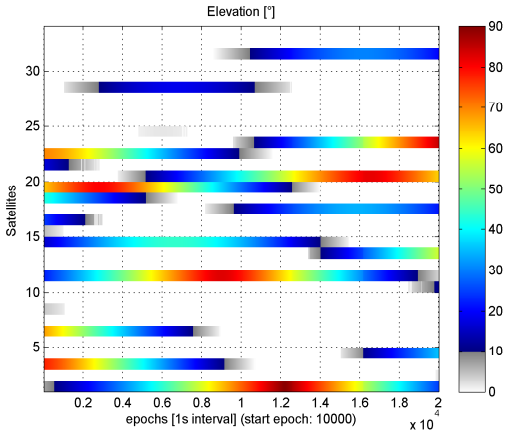

(e): Satellite Visibility

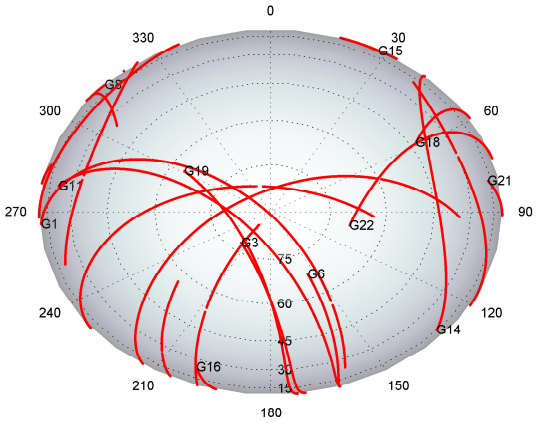

(f): Skyplot

Figure 3.10: PPP float solution of Graz Lustbühel DOY 088 2013 using IGS final products

The estimated float ambiguities in Figure 3.10 (b) also stay rather constant after the convergence time, which corresponds to the coordinate convergence. Note, that an initial integer value was subtracted from the ambiguities prior to their estimation for numerical reasons. This initial value for each frequency is calculated by converting the C/A-code measurement of a satellite to units of cycles, subtracting the actually measured phase and rounding the resulting value to the next integer.

Figure 3.10 (c) shows the respective solution for the ZWD, which is the wet delay of the troposphere that remains after applying e.g. the Hopfield model for the hydrostatic part of the delay. The estimated ZWD looks rather stable over the observation time of 5.5 hours. At a first glance, it seems strange that the remaining ZWD is negative. After further investigations it turned out that the Hopfield model used for the modelling of the ZHD of the troposphere, does overcompensate compared to troposphere solutions from analysis centres for the same station. Therefore, the remaining estimated ZWD part becomes negative to enable an appropriate PPP solution. Nevertheless, the resulting ZTD fits together rather well with other solutions, as it is also shown in Figure 5.15 in Chapter 5.

Figure 3.10 (d) contains the receiver clock error with respect to GPS time, that is estimated with a processing noise assumed as white noise. The clock used at the current station is a rather stable clock, while there are also GNSS stations using oscillators that have to be reset after a certain threshold for the offset is reached. This would appear as a sawtooth shaped graph.

Figures 3.10 (e) and (f) show the satellites' elevation angles as well as a skyplot visualising the satellite constellation from the user's point of view.

3.3.2 Real-time results

To demonstrate the functionality of PPPsoft in real-time mode, some further results were produced from the same GNSS dataset. This time real-time SSR orbit and clock corrections by CNES were used instead of the final products by the IGS in order to correct the inaccurate broadcast ephemerides (see Section 2.2). The SSR corrections were collected in real-time and recorded by PPP-wizard to be able to reconstruct the real-time situation. PPP-wizard virtually is a slightly modified BNC client by CNES. Therefore, the recorded files resemble the decoded files described in Section 3.1.

The real-time position results shown in Figure 3.11 (a) are impressive, especially, when thinking of the poor position quality of several decimetres to metres when using only broadcast ephemerides. By using the SSR orbit and clock correction messages the real-time PPP accuracy increases from meters to a few centimetres. Of course, the quality of the real-time streams cannot always be guaranteed compared to the IGS final products, as the latter ones are combined products from orbit calculations of several analysis centres in post-processing. The SSR message streams available so far are produced by single organisations. Nevertheless, the results lie within the range of the reference values at the centimetre-level, as long as the correction streams do not contain outliers.

Figure 3.11 (b) shows the respective ZWD estimates, that are also comparable to the calculation from the final products as shown in Figure 3.10 (c).

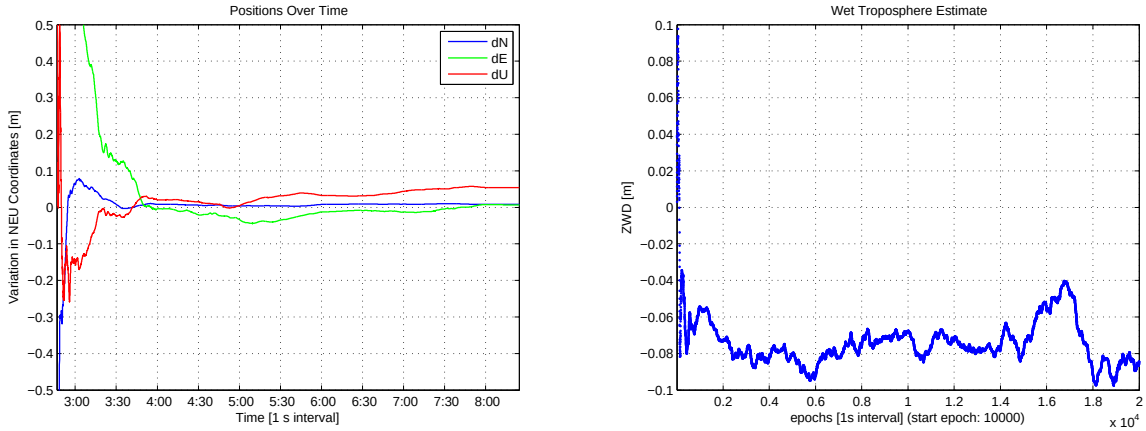

(a): NEU coordinate plot

(b): Remaining estimated ZWD

Figure 3.11: PPP float solution of Graz Lustbühel DOY 088 2013 using real-time orbit and clock data

Although the presented results were calculated in post-processing, either with data from ftp-servers or with recorded real-time data, PPPsoft is designed to process PPP solutions in near real-time. The operation in true real-time mode was successfully tested with observation update rates of up to 1 Hz.

4 PPP with Ambiguity Resolution

Many current investigations on the topic of PPP deal with the calculation and application of the instrumental biases affecting Zero-difference (ZD) phase measurements. These so called phase biases or Uncalibrated Phase Delays (UPD) are the key to re-establish the integer nature of phase ambiguities in PPP and constitute a main part of this doctoral thesis. Therefore, the following chapter will deal with the theoretical fundamentals of ambiguity fixing in combination with the PPP technique and presents types of UPD products that can be used for PPP with Ambiguity Resolution and Fixing (PPP-AR) in PPPsoft.

4.1 Problems preventing ambiguity fixing with PPP

To explain the problems preventing ambiguity fixing within PPP, which is a GNSS processing technique based on ZD measurements, let us resume the observation equations for undifferenced GNSS observables. The following equations, that constitute the Ionosphere-free (IF) observables after widely eliminating satellite orbit and clock errors by using external ephemeris products, were already shown in Section 2.1 (equations (2.3) - (2.5)), but are repeated at this point for a better understanding:

$$P_{IF} = \frac{f_1^2}{f_1^2 - f_2^2} P_1 - \frac{f_2^2}{f_1^2 - f_2^2} P_2 = \rho - cdt_r + \Delta_{trp} \tag{4.1}$$

$$\lambda_{IF}\Phi_{IF} = \frac{f_1^2}{f_1^2 - f_2^2} \lambda_1\Phi_1 - \frac{f_2^2}{f_1^2 - f_2^2} \lambda_2\Phi_2 = \rho - cdt_r + \Delta_{trp} + \lambda_{IF} b_{IF}. \tag{4.2}$$

Equations (4.1) and (4.2) describe the IF code and phase pseudoranges P_{IF} and $\lambda_{IF}\Phi_{IF}$, where λ_{IF} is the respective IF wavelength. The term ρ denotes the geometric distance between the satellite and the receiver antenna containing their three-dimensional coordinates. c stands for the speed of light while dt_r is the receiver-specific clock error with respect to GPS time. The term Δ_{trp} stands for the tropospheric signal delay. Note, that additional correction terms such as phase wind-up, phase centre offsets and tidal corrections are neglected here as they are not important for the following considerations.

The ambiguities on the single carriers (L1 and L2 for GPS) are integer values per definition, and can usually be fixed to these values in difference-approaches such as RTK. Only after the fixing of ambiguities the full potential of the highly precise phase observations can be exploited. Then they can be treated as highly precise and unambiguous pseudoranges. For PPP approaches this procedure is not common, as the following problems occur by using this ZD technique:

1st Problem - real-valued coefficients

As already mentioned in previous chapters, the linear combination eliminating the first order term of the ionosphere, unfortunately utilises real-valued coefficients. These coefficients have to be composed of the frequencies f_i of the single carriers i, since the ionospheric delay or advance has a frequency-dependent character. Therefore, also the combined bias term in the IF phase pseudorange $\lambda_{IF} b_{IF}$ results in

$$\lambda_{IF} b_{IF} = \frac{f_1^2}{f_1^2 - f_2^2} \lambda_1 b_1 - \frac{f_2^2}{f_1^2 - f_2^2} \lambda_2 b_2, \tag{4.3}$$

which yields a float value, while the integer ambiguities of the single frequencies $\lambda_i b_i$ are not accessible independently any more.

2nd Problem - UPDs

Even if the 1st problem of using real-valued coefficients for the linear combination would not exist, another error influence is contaminating the integer ambiguities.

The ambiguity term b_i, as estimated e.g. in a PPP float solution, cannot be directly treated as the pure integer ambiguity term, rather as the sum of real-valued initial phase biases originating in the receiver's and the satellite's hardware $\Delta\Phi_i^s$ and $\Delta\Phi_{i,r}$ plus the integer ambiguities N_i representing the full number of cycles not recorded by the receiver:

$$b_i = \Delta\Phi_i^s + \Delta\Phi_{i,r} + N_i. \tag{4.4}$$

In difference techniques these UPDs cancel and therefore are not relevant for fixing ambiguities, but for PPP the problem has to be treated or circumvented somehow.

4.1.1 Linear combinations

For the sake of completeness and to facilitate the understanding of the later consideration the Wide-Lane (WL) and the Melbourne-Wübbena (MW) linear combinations are shortly described in the following:

Wide-Lane (WL) linear combination

The WL linear combination is a combination between the GPS observables L1 and L2, leading to a huge wavelength of approximately of $\lambda \approx 0.86$ m compared to the single carriers. The WL observable L_{WL} is built by

$$L_{WL} = \frac{1}{f_1 - f_2}(f_1 L_1 - f_2 L_2), \tag{4.5}$$

while the respective combined WL phase ambiguity b_{WL} reads

$$b_{WL} = b_1 - b_2, \tag{4.6}$$

where f_i is the GPS frequency of the carrier i and L_i is the respective observation in units of length. In this linear combination the tropospheric and ionospheric delay is still present and has to be modelled. The wavelength of the combination can be calculated by

$$\lambda_{WL} = c/(f_1 - f_2). \tag{4.7}$$

Melbourne-Wübbena (MW) linear combination

To calculate integer WL ambiguities another linear combination, the so-called Melbourne-Wübbena (MW) combination of four observables (phase pseudoranges on L1 and L2, code measurements on L1 and L2) is more appropriate, since it eliminates the effect of ionosphere, troposphere, geometry and clocks. After applying the MW combination only ambiguities and noise remain in the observations. Due to its large wavelength of $\lambda \approx 0.86$ m, from this linear combination the ambiguities can be determined directly by averaging the combined observables. The MW observable L_{MW} is built by

$$L_{MW} = 1/((f_1 - f_2))(f_1 L_1 - f_2 L_2) - 1/(f_1 + f_2)(f_1 P_1 + f_2 P_2). \tag{4.8}$$

Here, the additional term P_i denotes the pseudorange observations on the frequency i. As this combination is using also code and phase measurements, the observation noise is strongly dependent on the quality of the code measurements. The remaining ambiguities have the same wavelength as the ambiguities of a pure WL combination with phases. Therefore, the ambiguities calculated from the MW linear combination can be directly used as WL ambiguities. The MW combination was originally described by Melbourne (1985) and Wübbena (1985).

4.1.2 General reformulation of the standard PPP model

To circumvent the aforementioned 1$^{\text{st}}$ problem, it is possible to reformulate the IF ambiguity described in (4.3), which is also the ambiguity term as estimated in the standard PPP float solution of dual-frequency measurements:

$$\lambda_{IF} b_{IF} = \frac{1}{f_1^2 - f_2^2}(f_1^2 \lambda_1 b_1 - f_2^2 \lambda_2 b_2). \tag{4.9}$$

At this point the WL linear combination of observations is introduced as described in (4.5) and (4.6). By using the WL representation of the ambiguity terms b_1 and b_2 we can express b_2 by

$$b_2 = b_1 - b_{WL} \tag{4.10}$$

and substitute b_2 in equation (4.9) to get

$$\lambda_{IF} b_{IF} = \frac{1}{f_1^2 - f_2^2}(f_1^2 \lambda_1 b_1 - f_2^2 \lambda_2 (b_1 - b_{WL})). \tag{4.11}$$

Further reformulations lead to the representation of the IF linear combination of ambiguities expressed by using the WL and the b_1 ambiguity term. b_1 is sometimes also denoted as NL ambiguity term b_{NL} due to its short wavelength compared to the WL combination.

To avoid confusion with the single-frequency ambiguity term, which has a different wavelength in the context of the standard IF linear combination (4.9), we call b_1 only b_{NL} in the subsequent section of this thesis. The NL wavelength λ_{NL} is calculated by

$$\lambda_{NL} = \frac{c}{f_1 + f_2} \tag{4.12}$$

and results in approximately 10.7 cm. The new representation of the IF ambiguity expressed by using the WL and the NL ambiguity is

$$b_c = \frac{f_1}{f_1 + f_2} b_{NL} + \frac{f_1 f_2}{f_1^2 - f_2^2} b_{WL} \tag{4.13}$$

with

$$\lambda_{IF} b_{IF} = \lambda_1 b_c. \tag{4.14}$$

The advantage of the IF ambiguity representation in (4.13) compared to the one in (4.9) is that not both, the WL and the NL term, have to be addressed in one processing step simultaneously. Rather the WL ambiguity can be calculated in the pre-processing step without any need for modelling errors, only by using the MW linear combination of observables (see (4.8)). The detailed process of WL-fixing is presented later on in Section 4.3.

After the successful fixing of WL ambiguities to integer values the only integer ambiguity term left in (4.13) is the NL ambiguity contained in b_{NL}. An estimate for b_{NL} can be calculated from the IF ambiguity estimated in the course of the float solution. The procedure of NL-fixing is also treated later on in Section 4.3.

4.1.3 Uncalibrated Phase Delays (UPD)

As already mentioned the 2$^{\text{nd}}$ and also more severe problem occurring with PPP is the presence of biases in the phase measurements as already described in (4.4). These so-called UPDs have their origin in the satellites' and the receiver's hardware and are usually contained in the estimated ambiguity parameter from the PPP float solution together with the "true" ambiguity. Unfortunately, the integer ambiguity and the UPDs cannot be separated in the rover without external help from station networks. The receiver-specific UPD is naturally different for every

GNSS receiver/antenna combination, while the biases for each navigation satellite can be calculated in a network solution and transmitted to the PPP user.

The concept to calculate and transmit satellite dependent UPDs, is already being investigated by a handful of organisations with the final goal to enable PPP with Ambiguity Resolution and Fixing (PPP-AR). Nevertheless, there are no standards for the production and transmission of UPDs by now. Further on, no official UPD products are available and only few publications touch the subject of applying UPDs and fixing ambiguities in a PPP user client so far. For example Shi (2012) describes a method for partial ambiguity fixing in PPP at the client-side.

In order to contribute to the newest developments of the PPP technique the project PPPserve described in Section 1.3 was brought to life to investigate the UPDs as well as their application and stability. In parallel, also this thesis is concentrating on the general algorithms and approaches enabling highly accurate positioning by means of PPP with and without ambiguity fixing.

4.2 Existing approaches for PPP-AR

In the course of this thesis a detailed literature research on the topic of PPP-AR was conducted. As a result, in the following section some promising approaches to recover the integer nature of ZD phase ambiguities to perform PPP-AR are presented. Building on that knowledge a service to provide phase bias information to PPP users in order to enable integer PPP was designed and developed in the course of the research project PPPserve. The user client software PPPsoft as already described in Section 3.1 was extended to make use of this bias information to perform integer PPP. This step is described in more detail in Section 4.3.

Generally, we can distinguish between two approaches, presented in recent studies, to enable integer resolution on ZD level by applying improved satellite-specific correction products, where phase biases have been separated from the integer ambiguities in different ways. A comparison of these methods can be found in Geng et al. (2010).

4.2.1 Phase recovery from fractional parts

The first approach is called phase recovery from fractional parts and was originally developed by Ge et al. (2008), who decomposed Ionosphere-free (IF) ambiguities into Wide-Lane (WL) and Narrow-Lane (NL) parts as it was demonstrated in the previous section (see equation (4.13)). Thereby an epoch-specific satellite-to-satellite Single-difference (SD) was used to eliminate the receiver-dependent calibration biases. Within a network of reference stations the WL phase biases were determined from averaging the fractional parts of all WL estimates using the Melbourne-Wübbena (MW) combination of the raw code and phase observables (see (4.8)). These WL phase biases are reported to be very stable over several days.

The NL phase biases are determined similarly by averaging the fractional parts of all NL ambiguity estimates derived from the WL ambiguities and the IF observables. Due to their short wavelength, the NL phase biases do not have such a high temporal stability as the WL parts. Further, they are dependent on the estimated float ambiguities and, therefore, also on the accuracy of ephemerides and models used for the processing. That is why they are proposed to be estimated in intervals of 15 minutes. The estimated WL and NL phase biases can then be applied to single-receiver

measurements to recover the integer nature of the respective ambiguities during the coordinate estimation process.

The process of the calculation of biases or rather UPDs in a network solution, similar to the approach proposed by Ge et al. (2008), is the main topic of the Ph.D. thesis of the author's colleague Fabian Hinterberger, who currently also is finishing his work at the Department of Geodesy and Geoinformation at the TU Vienna (GEO). To avoid an overlapping of the contents of both theses, the reader is referred to Hinterberger (2015) for a more detailed description of the process of calculating UPDs from a network solution, while this thesis concentrates on the description of the application of biases at the rover-side.

4.2.2 The decoupled clock model

Collins et al. (2010) proposed a second approach, based on a slightly different observation model compared to the standard PPP observation model described in Section 2.1, where different clock parameters are estimated for the code and the phase observables. By means of a network solution the so-called code and phase clocks are produced in order to be applied in a single receiver.

In this research it is reported that only small improvements in the positioning errors were gained by using the decoupled clock model, but the convergence time was reduced in a manner that with static processing with a data rate of 30 seconds after 60 minutes, 90 % of the solutions reach a horizontal error of 2 cm, compared to 10 cm for standard PPP.

According to Collins et al. (2010) the problem with the standard PPP model is, that the oscillator errors are not exactly separable from the hardware biases and the integer ambiguities. Therefore only a random constant bias, the so-called float ambiguity, is estimated instead of the 'true' ambiguity. In the standard observation model the time-constant portions of the code and phase biases are contained in the estimated phase ambiguities. To better divide these hardware-specific influences, the so-called decoupled clock model rigorously separates all hardware-specific errors belonging to different types of observables and combines them with the respective clock parameters.

Therefore, for the PPP-AR solution at the user-side one carrier phase clock is needed for each observed satellite together with one pseudorange clock and one bias correction for the WL combined observables. The user software of course must employ the decoupled clock model instead of the standard observation model.

Laurichesse et al. (2009) also employ a decoupled clock model for their investigations at CNES. A slightly different strategy is used than in Ge et al. (2008), when it comes to the determination of satellite phase bias parameters or respectively phase clocks:

Instead of SD ambiguities they directly use undifferenced ambiguity parameters for the calculation of the receiver and satellites-specific bias parameters. The WL bias determination takes place in accordance with the procedure described in Ge et al. (2008). Again the average of MW observables of e.g. one satellite pass is built to obtain estimates for the WL ambiguities. For this step no model corrections are necessary. As the receiver-specific bias parts still remain in the MW observables, these have to be estimated in the network solution. To circumvent a rank deficiency an arbitrary value is assigned to the receiver phase bias of a-specific receiver in order to determine a first set of satellite phase biases and further the receiver-specific biases of all stations involved.

The NL phase biases, however, are not determined specifically, but assimilated into the satellite clock estimates. Within a network of reference stations the NL bias corrections are calculated after estimating the propagation distance and the clock parameters precisely. The product are so-called integer clocks, that include phase bias corrections.

Both decoupled clock approaches aimed at producing clock corrections able to recover the integer nature of NL ambiguities at a single receiver.

4.2.3 Model selection in PPPserve

Within the project PPPserve one of the mentioned principles to calculate phase biases had to be chosen as a basis for own investigations. Both methods have their advantages and disadvantages, nevertheless the project consortium finally decided to calculate, transmit and implement the usage of sat-to-sat Single-difference (SD) UPDs, which of course also influenced the implementation of the user client PPPsoft. Using sat-to-sat SDs has several advantages compared to the decoupled clock model:

+ First of all in the network solution at the server-side as well as in the user client, the usage of SD phase biases enabled to completely disregard the receiver-specific bias parts, which significantly facilitates the algorithms used for the bias calculation and usage.

+ The PPP processing can be still performed by means of the standard PPP model ((2.4) and (2.5)), while by using a decoupled clock model the whole PPP processing in PPPsoft had to be changed as the clock parameters had to be divided into code clocks and phase clocks.

Along with this model decision also some inconveniences were accepted such as that

- all UPDs have to be related to a reference satellite, which can be problematic, if this satellite is not chosen properly. If the reference satellite has e.g. erroneous clock or orbit information, the whole UPD calculation and in consequence also the user's fixing routines do not work correctly.

- From the programmer's point of view, the administration of SD measures is more complicated than the use of undifferenced ones, as in case of a change of the reference satellite, all ambiguity related parameters have to be recalculated to become fully consistent with the new reference satellite.

4.3 Algorithmic approaches in PPPsoft

In the following section PPP-AR as implemented in the user client PPPsoft is described in detail with a special focus on the application of biases and the fixing algorithms.

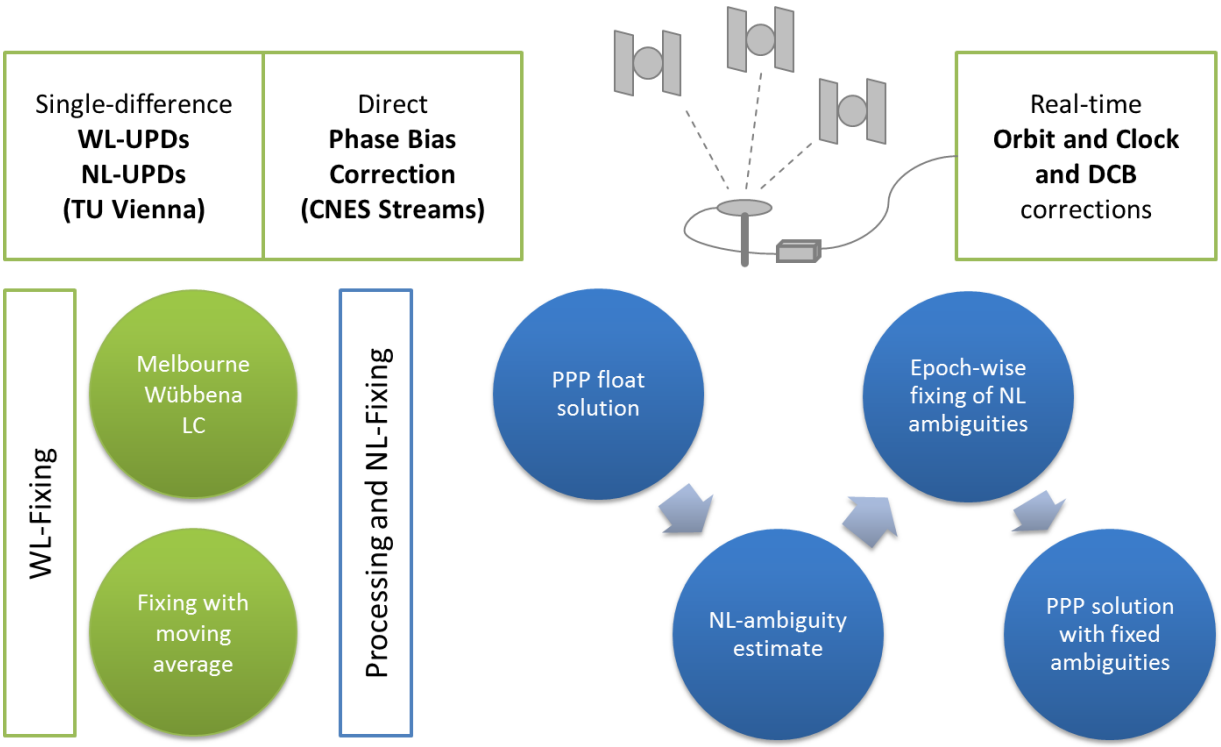

Figure 4.1: Scheme of PPP-AR in PPPsoft

4.3.1 General processing scheme

The scheme of PPP-AR as it was realised in PPPsoft is visualised in Figure 4.1. Thereby the two main components of the software are the WL-fixing routine, which is an autonomous part in the pre-processing, and the processing itself containing the NL-fixing part.

The WL-fixing procedure only needs the input of raw observations, and the WL UPDs, while no model corrections are necessary for this processing step. The possible types of UPDs implemented for the processing with PPPsoft are described later on in Section 4.4. The WL-fixing is performed by means of a moving average over the MW combinations of observables. The window size for the moving average can be chosen by the user.

The NL-fixing procedure is more complicated as it is part of the PPP processing itself. Every epoch a filtered PPP solution with float ambiguities has to be calculated using precise orbits and clock corrections such as described in Section 2.2. The estimated IF ambiguity estimates serve as an input for the fixing step itself together with the already fixed WL ambiguities and the NL UPDs. From these parameters an estimate for the NL ambiguity can be calculated to start the fixing algorithm. The strategy as recommended by Shi (2012) is, that only subsets of ambiguities are fixed to integers in every epoch, as the simultaneous fixing of all ambiguities at once is likely to be erroneous especially in the beginning of the processing, when the float solution is not fully converged. As soon as three NL integer values are found, a PPP solution with fixed ambiguities is started. Thereby the information of the fixed ambiguities is treated as known quantity, which makes the respective phase observables act as highly precise pseudoranges. This second solution

is done by means of a purely kinematic least squares adjustment. Ideally, the coordinate solution converges immediately in the case of correctly fixed WL and NL integer ambiguities of three to four satellites. The accuracy of the solution using only few fixed integer ambiguities strongly depends on the satellite geometry as shown in Section 5.6.

4.3.2 Wide-lane fixing

As mentioned earlier, the WL fixing can be performed in the preprocessing step without the use of ephemerides data or model corrections (see Laurichesse et al., 2009 and Ge et al., 2008). To obtain estimates for the WL ambiguity terms, the MW linear combinations as given in (4.8) is built for every satellite in each epoch. It eliminates the geometry and the ionospheric influence from the observables. Therefore, the resulting observable can be expressed as

$$L^s_{MW,r} = \lambda_{WL} N^s_{WL,r} + \lambda_{WL} \Delta\Phi_{WL,r} + \lambda_{WL} \Delta\Phi^s_{WL}. \tag{4.15}$$

The remaining components of the MW combination are the integer WL ambiguity $N^s_{WL,r}$ plus the remaining fractional part consisting of UPDs for the receiver $\Delta\Phi_{WL,r}$ and the satellite $\Delta\Phi^s_{WL}$ converted to units of length by the wavelength λ_{WL}. The observation noise is not mentioned explicitly in equation (4.15) but is still present in the MW observation. The noise should make up no more than 0.1 to 0.2 cycles, depending on the elevation of the satellite. Therefore, the determination of integer WL ambiguities is rather easy and can be done by averaging the MW observables of the satellites after eliminating the receiver-specific part.

Figure 4.2 shows an example of a raw Zero-difference (ZD) MW observable of a satellite, together with moving averages over the same observable. The noise of this observable is clearly below ±0.2 cycles.

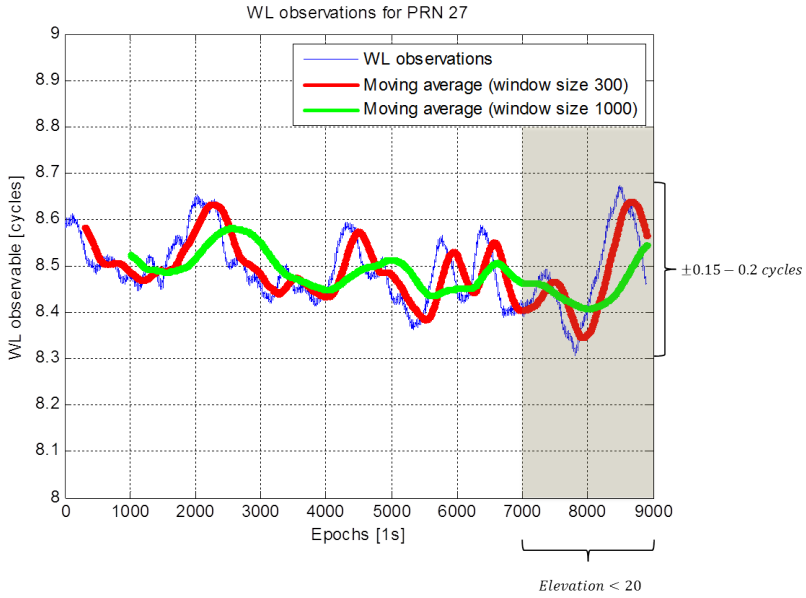

Figure 4.2: Example of ZD MW observable

The MW observables are collected for a user defined number of epochs before the fixing procedure is started. 100-200 epochs are sufficient to reliably fix most of the WL ambiguities. To get rid of the receiver dependent UPD, a sat-to-sat SD is built between a reference satellite and all other satellites in view. The reference satellite is chosen by using the satellites' elevation angle to keep the noise factor as low as possible. Rising satellites are preferred to setting satellites, as it is desirable to keep the same satellite for a long time. Of course, the availability of appropriate precise ephemerides and UPD corrections are a must for the reference satellite. If these are not available the second highest satellite is taken. A detection of erroneous ephemerides was not performed in the preprocessing, but nevertheless this case may occur and avoid the correct fixing of WL and further NL ambiguities.

The SD MW observable is built by

$$L_{MW}^{Ref-i} = L_{MW,r}^{Ref} - L_{MW,r}^{i} = \lambda_{WL} N_{WL}^{Ref-i} + \lambda_{WL} \Delta\Phi_{WL}^{Ref-i}. \tag{4.16}$$

This equation only contains the difference of the full WL cycles between the reference satellite and the current satellite N_{WL}^{Ref-i} as well as the respective SD UPD $\Delta\Phi_{WL}^{Ref-i}$. This UPD is dependent only on the satellites, not on the specific receiver equipment.

Figure 4.3 shows an example of SD MW observables of the IGS station GRAZ on DOY 087 after eliminating the satellite-specific UPDs by external phase corrections. The different colours represent different satellites. These observables were collected during two hours of observation and visualised in dependence of the satellites' elevation to show the stability of WL observables especially for highly elevated satellites. In this case all observables were in the vicinity of an integer value and could all be fixed to integers after the smoothing procedure.

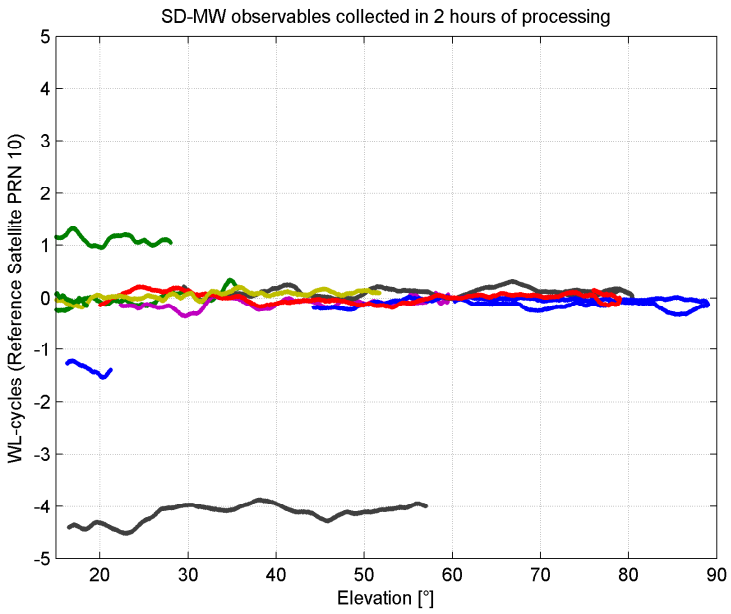

Figure 4.3: Example of SD MW observables of GRAZ DOY 087

To smooth the epoch-wise SD MW observables a moving average filter with a window size of e.g. 100 epochs is calculated, and afterwards, a simple rounding to the next integer is performed to fix the value. For an observation interval of 1 s this window size implies, that the fixing procedure can start after less than 2 minutes. Nevertheless, the window size for the moving average can be modified arbitrarily by the user. The threshold to fix the integer ambiguity is 0.25 WL cycles. Values exceeding that threshold are not fixed in the current epoch. The minimum elevation to fix WL ambiguities of rising satellites is 15°, as for lower satellites the noise may be too large for successful fixing. Whereas once a satellite is fixed, its integer value is kept until the satellite disappears, as the ambiguity value should not change during one arc anyway. Nevertheless, to avoid completely wrong WL-fixes, the WL observables are checked for changes regularly.

WL ambiguities are very stable and usually 80 to 90 % of them can be successfully fixed after 100 seconds of observation, satellites not fixed at that time do either lack appropriate UPDs or their elevation angle is below the minimum elevation for fixing in most of the cases.

4.3.3 Narrow-lane fixing

After the successful fixing of WL ambiguities, only the NL ambiguity part $b_{NL} = b_1$ remains unknown in equation (4.13). Now the more complicated part of the ambiguity fixing, namely the NL-fixing can begin. In Figure 4.4 the scheme of this NL-fixing procedure is visualised. This scheme is further explained throughout this section.

NL ambiguities are not as stable as WL ambiguities and their noise is much higher compared to their relatively short wavelength of about 10.7 cm. Further, the NL ambiguity can only be calculated from the ambiguity estimates of the float solution $\hat{B}_{IF}$ in units of length as well as the fixed integer WL ambiguity and the WL and NL UPDs $\Delta\Phi_{WL}$ and $\Delta\Phi_{NL}$ of the satellites. Generally, an estimate for b_{NL} can be calculated from

$$b_{NL} = N_{NL} + \Delta\Phi_{NL} = \frac{f_1 + f_2}{f_1}\frac{\hat{B}_{IF}}{\lambda_1} - \frac{f_1}{f_1 - f_2}(N_{WL} + \Delta\Phi_{WL}), \tag{4.17}$$

which is a reformulation of (4.13). Remember, that in PPPsoft only SD ambiguities are fixed. Therefore, the receiver-specific UPDs, which are only relevant in ZD-based fixing procedures, are not mentioned here.

Based on equation (4.17) the NL-fixing in PPPsoft is performed. The procedure of fixing NL ambiguities itself is done rather for selected subsets of satellites instead of for all satellites in view at once, since using this approach the fixed solution can be calculated much earlier. This partial ambiguity fixing procedure can be divided in four essential steps, that are described in the next paragraphs.

Partial ambiguity fixing of NL observables

As a first step, the float ambiguities estimated in the standard PPP solution of the current epoch are cut from the parameter vector together with the respective variance-covariance matrix. The ambiguities then are sorted according to their standard deviation. Depending on the use of ZD or

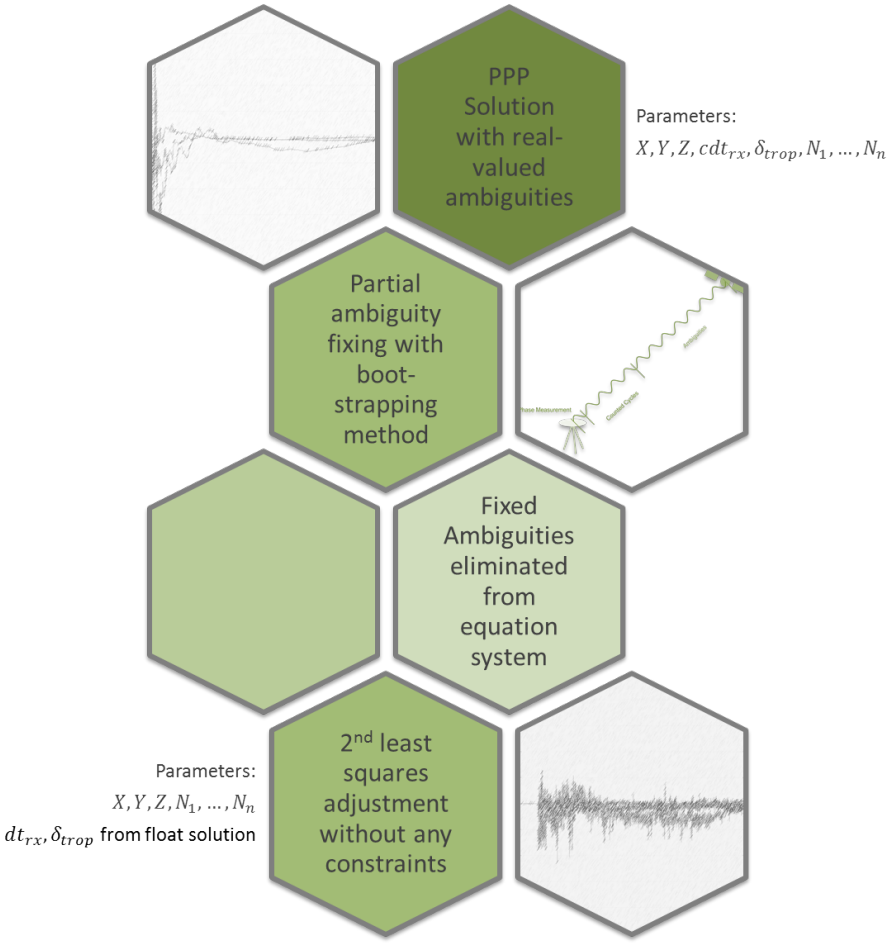

Figure 4.4: Scheme of NL ambiguity resolution and fixing

SD observations, within the float solution differences between the estimated ambiguities of the reference satellite and the other satellites may have to be built to eliminate the receiver-specific UPDs. In the ZD case the respective variance-covariance matrix has to be determined by variance propagation methods.

After sorting the ambiguities, a bootstrapping algorithm, similar to the one proposed in Shi (2012, page 101ff), to partially fix the SD NL ambiguities is started.

1. *LAMBDA method applied to ambiguity subset*

   First of all the "best" subset of ambiguities is taken. The number of ambiguities n in the first subset is 2. The NL estimates are built according to (4.17) and the most probable integer values of ambiguities are calculated by means of the Least squares AMBiguity Decorrelation Adjustment (LAMBDA) method (see Teunissen, 1995 and De Jonge and Tiberius, 1996).

   The LAMBDA method provides a technique where ambiguities are de-correlated by means

of a Z-transformation prior to the integer estimation. Its minimum principle is based on the objective to find the integer ambiguity values instead of real values that are the most likely ones and is written as

$$\chi^2(N) = (\hat{N} - N)^T Q_{\hat{N}}^{-1} (\hat{N} - N) = minimum! \tag{4.18}$$

The vector $\hat{N} - N$ is also denoted as the residual of ambiguities denoting the difference between the estimated float ambiguities $\hat{N}$ and the respective integer ambiguities N. $Q_{\hat{N}}$ is the cofactor matrix of the ambiguity estimates. Also the covariance matrix can be taken instead, as it actually only the cofactor matrix multiplied by a factor.

The source code used to calculate the LAMBDA method in PPPsoft is an open source Matlab function developed at the School of Computer Science, McGill University (see http://www.cs.mcgill.ca, 2014 and Chang et al., 2005). This function hands out not only the n best, n second best etc. integer values, but also the corresponding values for the squared norm of the residual vector r_i.

2. *Quality criteria*

Afterwards, a check for the correctness and quality of the integer subset has to be performed. Therefore, two quality criteria are calculated and tested:

a) A ratio value is calculated by means of the values for the squared norm of the residual vector r_i from the best and the second-best set of integer values r_1 and r_2. This ratio has to be compared to a threshold, the critical value, in order to see if the two solutions differ sufficiently:

$$ratio = \frac{r_2}{r_1} < THRESHOLD. \tag{4.19}$$

This critical value is defined as a fixed value as for example 3 in many software packages, like it is done in PPPsoft. Nevertheless, a more sophisticated approach of defining the critical value would certainly be more appropriate, as this value becomes larger and larger during convergence of the system and therefore should be adapted adequately.

b) The second quality criterion is the success rate of the ambiguity fixing, which denotes a probability measure for the correctness of the integer values to be the true integer values and can be calculated by

$$P(\breve{a} = a) \leq \left(2\Phi \left(\frac{1}{2\sqrt[n]{\det(Q_a)}} \right) - 1 \right)^n, \tag{4.20}$$

where $\breve{a}$ is the supposed set of n integer values, a is the set of true values and Q_a is the respective variance-covariance matrix of ambiguities. Φ denotes the normal cumulative distribution function for the mean $\mu = 0$ and the standard deviation $\sigma = 1$. The probability threshold P should optimally be a value near 1 (e.g. 0.999). It has to be mentioned that the success rate is dependent only on the satellite geometry, the stochastic model and the functional dependency – no measurements are needed to

calculate this value. Therefore, the success rate is a purely theoretical value that is based on assumptions made by means of using a least squares adjustment or Kalman filter.

3. *Ambiguities accepted*

   If both quality criteria are fulfilled, the number of ambiguities to be fixed n is increased by 1. Therefore the next best ambiguity estimate is added to the subset of ambiguities and the fixing procedure starts again with step 1. If one criterion fails, the algorithm continues with step 4.

4. *Ambiguities fixed to integers*

   This iterative procedure stops as soon as either all ambiguities are fixed, or one of the quality criteria is not fulfilled any more. In the latter case, the previous subset of integer ambiguity values, that passed the quality test is denoted as the correct subset of integer values.

The identified integer values for the NL ambiguities are fixed in the actual epoch. In the subsequent epochs the fixed integer values are always checked for changes and may be released in case of changes in the fixed ambiguity subsets. Especially in the beginning of the processing, wrong fixes may occur, as the fixing procedure relies on the estimation of float ambiguities, which underlies the same convergence procedure as the position coordinates. After convergence the fixing of integer ambiguities becomes easier. Nevertheless, the main goal is to shorten the time to convergence, which is why ambiguities are tried to be fixed early in the processing only after some minutes of observation.

The detection of wrong NL fixes is the most problematic part in PPP-AR, as there is no hint giving information about the true values, that is independent from the PPP float solution. Nevertheless, if only some correct integer values (at least 3) can be identified, the solution is expected to converge immediately. Figures and case studies showing the behaviour of PPP solutions with fixed ambiguities are presented in Chapter 5 of this thesis.

Fixed adjustment

As soon as three pairs of integer WL and NL ambiguities are known, an ambiguity fixed solution can be calculated. Therefore, the ambiguities of the IF linear combination ($\hat{B}_{IF}$ in units of length) have to be recalculated by reformulating equations (4.13) and (4.14).

$$\hat{B}_{IF} = \lambda_1 b_c = \frac{f_1}{f_1 + f_2}\lambda_1(N_{NL} + \Delta\Phi_{NL}) + \frac{f_1 f_2}{f_1^2 - f_2^2}\lambda_1(N_{WL} + \Delta\Phi_{WL}) \tag{4.21}$$

The newly gained information about the integer ambiguities can then be introduced in the equation system again as known values. This can be realised either by subtracting the ambiguity values from the respective phase observations or by introducing the SD IF ambiguity values as additional pseudo-observations with very high weights compared to the original observations. Both alternatives should in principle result in the same ambiguity fixed solutions.

The adjustment procedure for fixed ambiguities in PPPsoft is a purely kinematic least squares adjustment, meaning that the position coordinates as well as the ambiguities are treated as time-variant values without any filtering. This has the big advantage that the solution "jumps" to the correct coordinate estimates as soon as three to four correct ambiguities are fixed.

For reasons of safety the float solution is kept isolated from the fixed solution and no information is given back to the float solution of the following epoch. If the ambiguities were not fixed correctly, it would still be possible to find the erroneous integers within the following epoch on the basis of the isolated float solution. Whereas, if incorrect ambiguity information was sent back to the float solution instead, the accuracy of the float solution would also degrade and the convergence process would need to start again.

Model values, such as orbits and clock corrections, atmospheric delays or phase wind-up corrections for the individual satellites have already been calculated in the float solution as well as receiver clock and troposphere estimates. Therefore, the only parameters that must be recalculated in the fixed solution, are the position coordinates. As input observations for this second adjustment one can either use only those measurements with fixed ambiguities, or alternatively one can use all available observations and weight the ones with fixed ambiguities accordingly high. For reasons of stability the latter solution is the default setting in PPPsoft.

4.4 Types of UPDs used in PPPsoft

In the course of this thesis two different types of biases produced by different organisations were used and implemented in the user client PPPsoft.

The Centre national d'études spatiales, Toulouse, France (CNES) offers a freely available demonstrator software for their PPP-AR approach plus UPD correction data gained from their network approach using the decoupled clock model. The demonstrator software is called PPP-wizard and employs modified RTCM streams containing also UPD corrections. The use of these correction streams was implemented in PPPsoft in order to test PPP-AR when no other phase bias correction data was available.

Later on, when the research project PPPserve was in a more advanced stage, SD UPDs by TU Vienna had been available for further tests of PPP-AR in PPPsoft. These two phase bias representations are extensively described in the following.

4.4.1 PPP-wizard – real-time biases by CNES

As mentioned before, CNES offers an open source demonstrator software for PPP with ambiguity resolution (see http://www.ppp-wizard.net, 2014). This demonstrator's name is PPP-wizard which stands for 'Precise Point Positioning With Integer and Zero-difference Ambiguity Resolution Demonstrator'. It is a proof of concept of the ZD ambiguity resolution method developed by the Orbit Determination Service at CNES.

The following description of the PPP-wizard demonstrator software and bias representation is given according to the status in 2013, when the main part of the development of the PPP-AR solution in PPPsoft took place and also most of the test datasets were recorded. Meanwhile,

at the end of 2014, a completely new PPP-wizard package is offered that also uses a slightly different bias representation. Nevertheless, as mainly data from 2013 was used, only the former bias messages are treated here.

According to http://www.ppp-wizard.net (2014), the PPP-wizard project consists of three major parts:

- The *SSR computation* part computes orbits and clocks for the GPS and GLONASS satellites and transforms them to the RTCM State Space Representation (SSR), which uses a very low bandwidth for broadcast corrections. This part of the system is claimed to be the most complex one, as it has to deal with a global network of real-time GNSS stations.

- The *broadcast part*, whose main function is the transmission of the orbit and clock corrections to the users via the CNES caster, is using a predefined protocol and standard.

- The user part of the project, called *PPP Monitoring*, performs precise positioning with integer ambiguity resolution in real-time, as well as the comparison with an absolute reference position, to analyse the quality of the broadcast solutions.

The user part of PPP-wizard is based on the open-source PPP and RTCM client BNC Version 2.4 by BKG, which was originally only capable of calculating PPP with float ambiguities. CNES modified the software in a way, that it became possible to use their own phase bias corrections in order to calculate an integer-fixed PPP solution in real-time based on RTCM observation data, ephemeris streams and SSR corrections. Up to now the calculation is limited to stationary receivers.

As already mentioned the corrections produced by CNES include SSR messages for orbit and clock corrections as well as code and phase bias corrections. Phase biases are not standardised in the current realisation of RTCM (see Radio Technical Commission for Maritime Services, 2011). Therefore, CNES extended the SSR message 1059, which usually contains only code bias corrections. Additionally, the bias types 21 and 22 representing phase biases for the GPS L1 and L2 frequency are introduced. These biases are given in cycles and can be added directly to the raw phase observations to enable integer ambiguity resolution. Therefore, no additional linear combination of satellite-specific biases has to be added in the processing as it was described in equation (4.16) for the SD MW observable and equation (4.17) for the SD NL estimates. Figure 4.5 shows the modified SSR message 1059 including the phase bias messages after decoding by PPP-wizard. Figure 4.6 shows the table of possible bias numbers for CNES messages.

The representation of satellite phase biases in an extended RTCM format on the one hand does need only a low additional required bandwidth and on the other hand only slight modifications to the original format.

Originally, CNES biases are meant to be used for ZD PPP ambiguity fixing, where the treatment of receiver dependent biases is left to the user. In the case of PPPsoft this problem is circumvented by building sat-to-sat differences as mentioned earlier in this thesis.

Note, that in earlier versions of PPP-wizard the phase bias corrections were transmitted together with the clock corrections in the .sp3 format. Therefore, the user was restricted to distinguish between phase and code clocks in the observation equations as described in Section 4.2.2 and could not use biases in an arbitrary functional model. To make the corrections more consistent

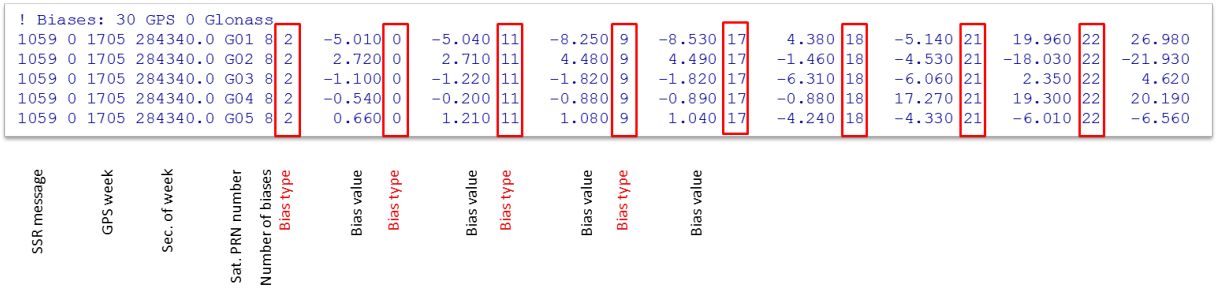

Figure 4.5: Bias SSR messages of CNES decoded by BNC

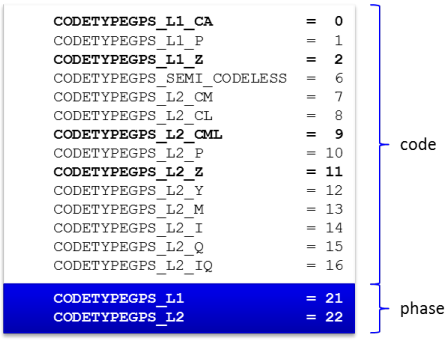

Figure 4.6: Bias types of CNES

and portable to other PPP approaches, CNES decided to extract the biases and transmit them in the aforementioned real-time format.

In the current version, in late 2014, the CNES streams containing orbits and clock corrections as well as code and phase biases are available from the IGS caster products.igs-ip.net . These employ a separate RTCM message number for the transmission of phase biases (RTCM message 1265), that, according to email exchange with Mr. Laurichesse from CNES, will be standardised in the near future.

Example calculations, where PPP was performed by means of bias corrections by CNES can be found in Chapter 5.

4.4.2 UPDs by TU Vienna

In the research project PPPserve, as already presented in Section 1.3, phase bias corrections were created, that differ from the biases by CNES in their calculation and representation. The process of calculating these so-called UPDs from a network solution is the key issue in the thesis of my colleague, Fabian Hinterberger , who is developing his dissertation at the TU Vienna, GEO simultaneously to this thesis. Therefore, for detailed information on the calculation of biases at TU Vienna the reader is referred to Hinterberger (2015).

Nevertheless, the UPDs produced there are also shortly described from the PPP user's point of view, as they represent the second type of phase bias corrections used for the user client PPPsoft in this thesis.

Analogous to the corrections offered by CNES, the UPDs by TU Vienna are calculated from a global or regional network of reference stations. The big difference is that these UPDs are not referred to single satellites but to differences between a reference satellite and all other satellites in view (sat-to-sat difference).

The WL UPDs are calculated in accordance with the scheme proposed by Laurichesse et al. (2009) and Ge et al. (2008) by building and averaging the MW observables of all satellites and stations. The NL phase biases are determined by averaging the fractional parts of all pertinent NL ambiguity estimates derived from the WL ambiguities and the IF ambiguities. Further not the raw phase delays, but the SDs of NL and WL UPDs are targeted. These are calculated similar to the approach proposed by Ge et al. (2008) (see Section 4.2) and transmitted every 30 seconds.

At the user-side the application of these biases to the respective wide- and NL combination of ambiguity estimates, described in Section 4.3.2 and 4.3.3, leads to the recovery of their integer nature and therefore enabled the fixing of these ambiguities.

Transmission of UPDs

One important task concerning both, the server- and the user-side of a PPP service, is the transmission of biases. Therefore, an ASCII text format was defined for the first tests in post-processing, that contains all necessary information to apply the WL and NL UPDs. This format contains the time represented as year, month, day, hour, minute, second as well as the second of week in the first line. The second line gives information about the reference satellite used for the UPD calculation of the current epoch. Afterwards, each line contains the UPD correction of a single satellite. The first two characters show the PRN number of the satellite followed by the UPD in cycles and its standard deviation. Separate text files are used for the transmission of WL and the NL UPDs. These both look as follows:

```
* 2013   3 28   0   0   0      345600
 6
29   -1.317    0.004
30    0.113    0.004
21   -0.772    0.004
16   -0.280    0.004
31   -1.413    0.003
18   -0.508    0.006
 3    1.144    0.010
```

For real-time transmission in a PPP service a similar approach, than the one by CNES, can be used, where already existing RTCM SSR messages are modified in order to transmit the UPDs. The simplest option is to extend the SSR message number 1059 for the transmission of code biases. Additional bias types such as wide- and narrow lane UPDs can be added. The bias type numbers currently not used by RTCM are the numbers 16 to 30, which could be used for additional corrections. The problem of using message number 1059 is that the reference satellite information must be transmitted somehow to the user. This could be managed by adding an extra line for the reference satellite with a fake bias value that is completely out of range of

the correction values. Such a fake number could be e.g. 99.99. In the user software PPPsoft, the proposed bias representation works without modification thanks to the similarity with the CNES-format. Nevertheless, commercial receivers and RTCM decoders will not understand this format for sure as long as phase bias corrections are not standardised in an RTCM format. Nevertheless, phase bias messages are proposed to be standardised in the next RTCM release. Until then, only customised RTCM clients can be used for PPP-AR.

Results and analysis of PPP solutions using the UPDs by TU Vienna are visualised in the subsequent Chapter 5.

Stability of UPDs

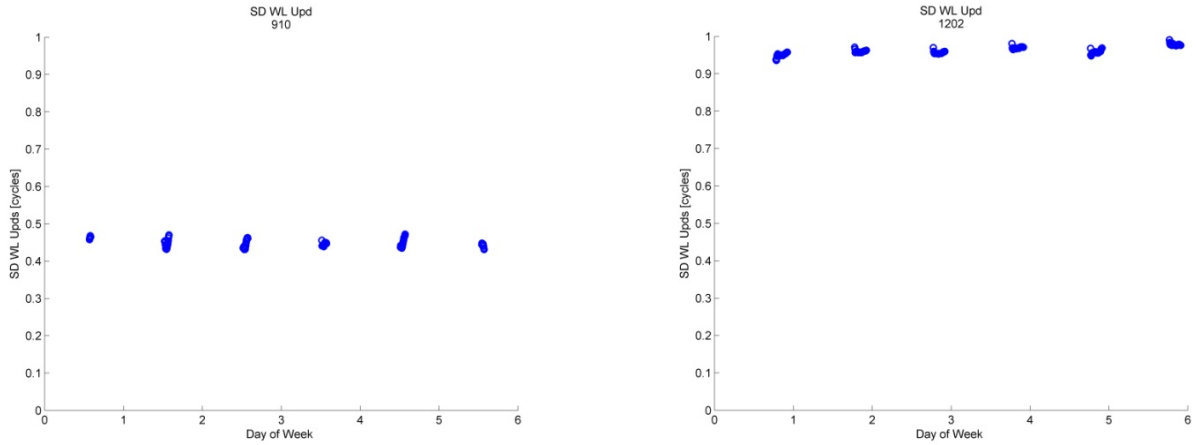

Figure 4.7: The stability of two WL bias pairs over a whole week, source Weber et al. (2013)

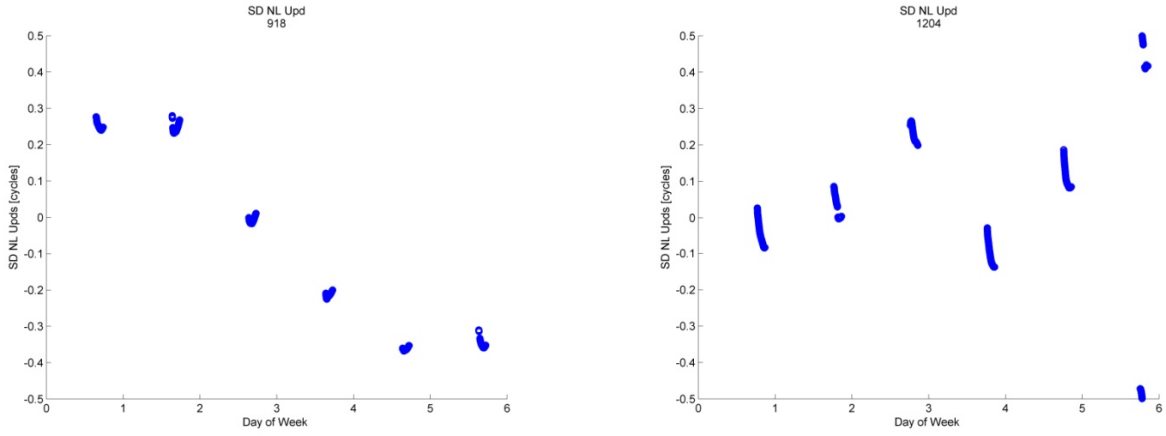

Figure 4.8: The stability of two NL bias pairs over a whole week, source Weber et al. (2013)

The stability of WL and NL biases is an important issue concerning the bandwidth or memory

size needed for PPP corrections. Generally, satellite-specific WL biases do not change very fast. According to Hinterberger (2015) they are not only valid for the duration of observation, but also for much longer periods such as several days, which becomes clear when looking at Figure 4.7. Therefore, the transmission of WL UPDs does not need a broad bandwidth. Nevertheless, they should be transmitted as often as the NL UPDs, since the user does not want to wait for minutes to get the first WL correction data set.

The more interesting part concerning stability are the NL UPDs. Several tests in project PPPserve showed that NL biases are more stable than expected, usually for the whole time a satellite is visible, but not for longer periods (see Huber et al., 2014). Figure 4.8 shows the behaviour of NL UPDs over one week. From one day to another instability and offsets arise that may result from inaccuracies of orbits and clock corrections or the used mapping function. Sometimes unmodelled satellite-specific errors can also result in a drift behaviour of the NL UPDs.

Nevertheless, as a NL cycle has only a short wavelength of about 10 cm, even a large variation in the NL UPDs would be only a few centimetres in range. The NL UPDs, like the WL UPDs, are calculated every 30 s and transmitted to the user in the same interval.

5 Results and problems

In the following chapter selected results of PPP solutions calculated in the course of this thesis using the Matlab-based PPP client PPPsoft are shown by means of different test data sets in order to proof the concept of PPP with Ambiguity Resolution and Fixing (PPP-AR) as implemented in this thesis. Further, problems occurring with integer ambiguity fixing in PPPsoft and in general are shown and discussed on the basis of processing examples. The coordinate output of solutions with and without ambiguity fixing is compared in order to identify advantages and disadvantages of both concepts.

5.1 Data used for the test scenarios

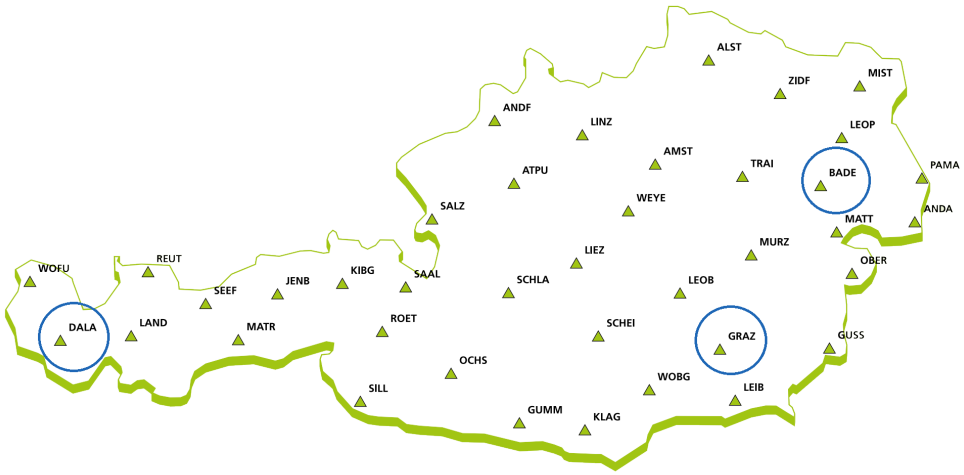

Figure 5.1: EPOSA station network – source: EPOSA Info folder (2011)

The data used for the calculations presented in this chapter consists of several sets of observations from GNSS stations in Austria from Day Of Year (DOY) 335 in 2012 and DOY 087 and DOY 088 in 2013. All observation data was recorded with a data rate of 1 Hz.

Observation files from the IGS station Graz Lustbühel as well as EPOSA stations in Graz (GRAZ), Dalaas (DALA) and Baden (BADE), as visualised in Figure 5.1, were used for the production of the results. The observation data from station Graz Lustbühel was collected by using the RTCM decoder BNC, which is an open source software offered by the BKG as already described in Section 3.1. The observation data of all EPOSA stations was freely provided by the company

operating the EPOSA network, the Wiener Netze GmbH. An overview on the EPOSA station network in Austria is given in Figure 5.1.

Additional to the observation data also real-time orbit and clock corrections were collected together with code and phase bias data produced by CNES and provided as RTCM-like correction stream CLK9B via the PPP-wizard Ntrip-caster. These streams were decoded by a modified version of BNC also offered by CNES in the course of their PPP-wizard project (see Section 4.4.1). After decoding, these files can either be processed immediately in near real-time or archived for a later use in post-processing. Alternatively, these decoded streams can also be transmitted/accessed via TCP-IP port for real-time use only. But, for the sake of repeatability, this option was not used for the tests in this thesis.

For the observed days the TU Vienna also produced Wide-Lane (WL) and Narrow-Lane (NL) Uncalibrated Phase Delays (UPD) for all satellites in view in order to compare the PPP-AR solutions calculated with CNES and TU Vienna UPDs. The latter are up to now transmitted as proprietary ASCII files, but a transmission via a modified RTCM stream is foreseen for the future. The phase bias products calculated by TU Vienna were already described in Section 4.4.2.

Beside the real-time orbit and clock products also IGS final orbits and clocks (see Section 2.2) were downloaded and used in combination with the bias products by TU Vienna.

In the following, several PPP solutions based on the aforementioned data and calculated with different settings are shown. Ambiguity-fixed solutions are compared with float solutions in order to show the advantages of PPP-AR. Further, problems and difficulties still occurring with this technique are analysed by means of several example calculations in the course of the following sections.

5.2 The effect of phase bias corrections on WL observables

Corrections for UPDs in general shall have the characteristics to re-establish the integer nature of ambiguities when applied to the respective phase observables. In the algorithms presented in this thesis and also in the software PPPsoft the dual-frequency Ionosphere-free (IF) linear combination of ambiguities is reformulated as described in Section 4.1.2 in order to address the WL and NL ambiguity parts, instead of the L1 and L2 ambiguities themselves. This has the advantage, that the WL ambiguity can be calculated and fixed to an integer value already in the preprocessing step. Therefore, the presence of hardware delays on phase observables can be demonstrated easily by means of this WL phase observable, since it can be build completely independently from the actual PPP processing and no models have to be applied.

In the following, a comparison of WL observables before and after the application of the respective satellites-specific UPD corrections is given. In Figure 5.2 the single-differenced Melbourne-Wübbena (MW) linear combinations (described in equations (4.15) and (4.16)) of all visible satellites at the station Graz Lustbühel on Day Of Year (DOY) 335 in 2012 are plotted with respect to the satellites' elevation angle. Different colours represent the different satellites. The combined MW observables contain only the integer values of the WL ambiguity, the satellite specific UPDs and noise. Without the presence of UPDs and noise, the observables would be integer numbers.

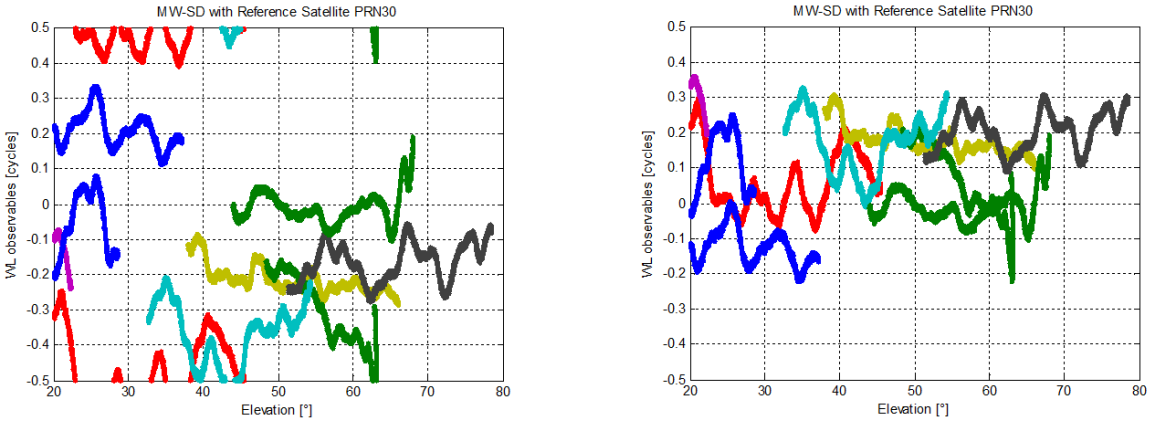

(a): MW without phase bias correction

(b): MW with phase bias correction by CNES

Figure 5.2: Single-difference MW observables of GRAZ DOY 335 2012

In Figure 5.2 (a) no phase corrections were applied. The receiver specific part of the UPDs has already been eliminated by producing satellite-to-satellite differences. As expected, the observables of the single satellites in (a), represented as coloured lines, do not approach integer values at all, because they still contain the satellite specific UPDs. Note, that for a better visualisation integer values were subtracted from the observables to produce values in the range of -0.5 to 0.5 cycles.

In Figure 5.2 (b) the phase biases are strongly reduced by using bias corrections from the CNES data stream CLK9B. As a result of applying these corrections, the observables clearly do approach integer values within the range of approximately 0.25 WL cycles. The noise is strongly depending on the satellites' elevation, which is why a cut-off angle should be defined for the satellites used for the WL ambiguity fixing.

As expected, this test shows that without using external products, the WL ambiguity observations do not approach integer values (here represented by zero) at all. This happens only after the compensation for satellite-specific phase hardware biases. Therefore, it can be concluded that the integer fixing of WL observables is possible by using external products for the correction of hardware delays, as they are produced for example by CNES.

5.3 CNES and TU Vienna bias data

In the following, it is shown that the use of both different bias types, the UPDs by CNES and the UPDs computed at the TU Vienna lead to the successful fixing of ambiguities in PPPsoft. The example data used for the calculations is shortly summarised in Table 5.1.

At first, a PPP float solution was processed by means of orbit and clock corrections calculated by CNES and visualised in Figure 5.3 in order to give the reader the opportunity to compare the float and the fixed solutions. The north, east and up (NEU) coordinate differences with respect to the known station coordinates over the processing time are visualised in Figure 5.3 (a), while the estimated float ambiguities with respect to the processing epochs are shown in Figure 5.3 (b).

Type	Format	File	Information
Observations	RINEX 2.11	GRAZ0870.13O	interval of 1s
Epochs	1 Epoch is 1s	1801 – 16200	–
Obs. Time	GPS time	10:36:56 – 14:36:56	–
ORBIT/CLOCK	SSR correction by CNES	CLK9B0870.13C	recorded by PPP-wizard
	Final products by IGS	igs17334.sp3	–
		igs17334.clk_30	–
DCBs	SSR correction by CNES	CLK9B0870.13C	recorded by PPP-wizard

Table 5.1: Example data used for tests with CNES and TU Vienna UPDs

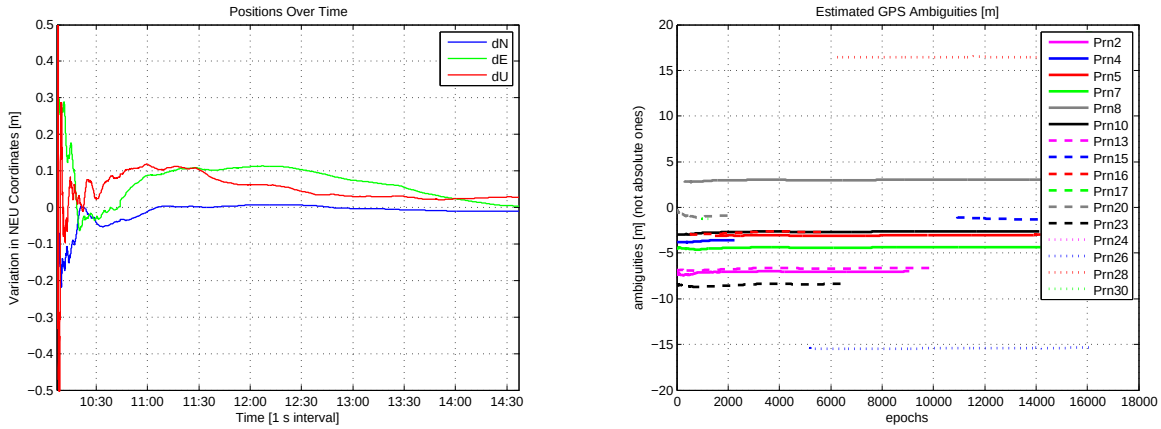

(a): NEU solution w.r.t. reference coordinates

(b): Float ambiguity estimates

Figure 5.3: PPP float solution of Graz Lustbühel DOY 087 2013 using broadcast corrections + SSR messages by CNES

Both, the coordinates in (a) and the ambiguity estimates in (b) show the typical behaviour of converging slowly to their optimum accuracy. Especially the convergence of the estimated ionosphere-free ambiguities is important for the later ambiguity resolution, since the estimates for the NL ambiguities are based on the ambiguity estimates from the float solution (c.f. Section 4.3.3).

5.3.1 Solution with CNES phase biases

One ambiguity-fixed solution was calculated using the same dataset as for the float solution before, but with the phase bias corrections by CNES applied to the observations. WL and NL ambiguities were determined and fixed to integer values. The resulting fixed PPP solution is shown in Figure 5.4 on the left side.

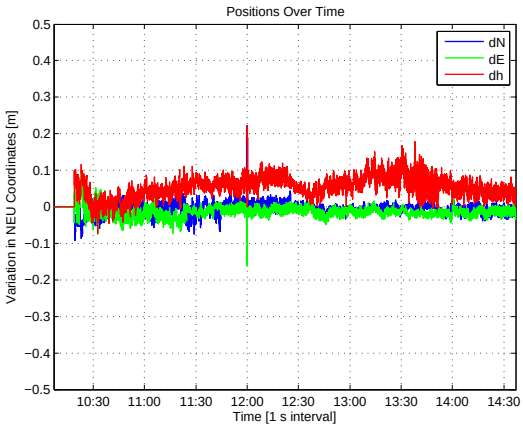

(a): NEU solution with CNES biases

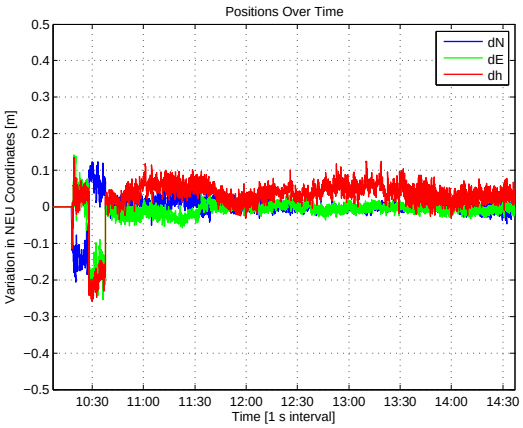

(b): NEU solution with TU Vienna biases

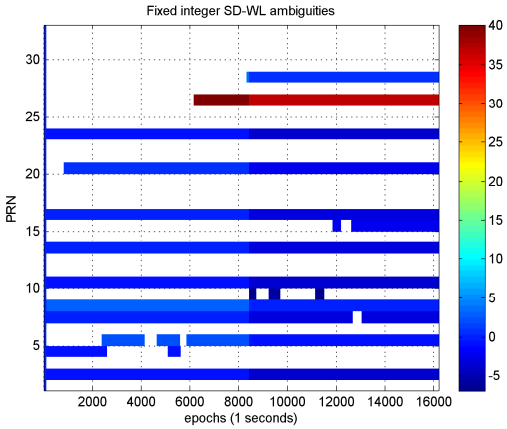

(c): Fixed WL ambiguities with CNES biases

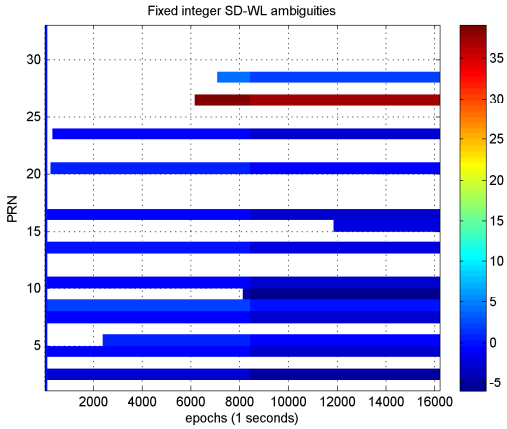

(d): Fixed WL ambiguities with TU Vienna biases

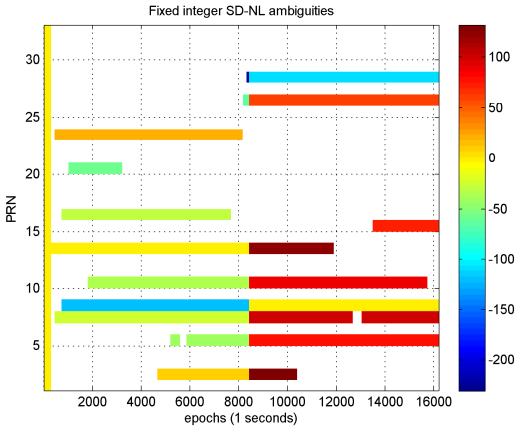

(e): Fixed NL ambiguities with CNES biases

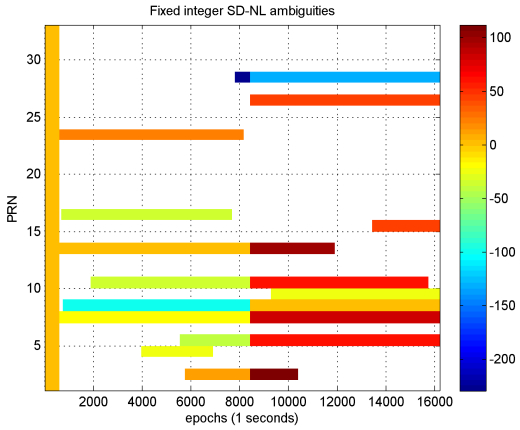

(f): Fixed NL ambiguities with TU Vienna biases

Figure 5.4: PPP fixed solution of Graz Lustbühel DOY 087 2013 using broadcast corrections + SSR messages by CNES (left) or final IGS orbits and clocks + UPDs by TU Vienna (right)

Figure 5.4 (a) shows the NEU coordinate differences with respect to the station's reference coordinates of the ambiguity fixed solution. Here, the noise is rather high compared to the float solution. This is, because the fixed solution is calculated in pure kinematic mode, which means that the coordinates were not filtered or constrained at all. The kinematic mode is chosen, because for the investigations in this thesis it is desirable to see changes in fixed ambiguities immediately as jumps in the coordinate solution. In this example the first position using fixed ambiguities can be calculated after about 12 minutes of processing. After that initialisation time the horizontal coordinates always stay at the sub-decimetre level. The height component has a slight offset, that may have its origin in remaining systematic modelling errors. Nevertheless, the height component also stays around an accuracy of one decimetre.

Figure 5.4 (c) shows the fixed WL integer ambiguities and (e) the fixed NL integer ambiguities as a function of the processing epochs. In these ambiguity plots, the PRN numbers of the satellites are visualised in the Y-axis, while the current integer values of the fixed ambiguities are represented by the colours in the colourbar on the right hand side of each plot. It should be mentioned here, that the figures showing the fixed ambiguity values do still contain the ambiguity of the current reference satellite with a value of zero.

The third and fourth NL ambiguity can be fixed after about 700 epochs corresponding to approximately 12 minutes of observation time. This is exactly the same time, when the first set of parameters can be calculated in PPP-AR mode. Before that time only the float adjustment is performed.

Note, that the abrupt changes in color in the NL solution in Figure 5.4 (e) between the epochs 8000 and 9000 indicate a change of the reference satellite. After a new reference satellite is chosen all ambiguity related values have to be recalculated to be consistent with the new satellite. This process of changing the reference satellite and its consequences have already been described in Section 3.2.1.

In summary, it has been shown, that the PPP-AR solution with CNES' phase biases does work and WL as well as NL ambiguities can be fixed to obviously correct values, which leads to a precise and accurate estimation of the station's position.

5.3.2 Solution with UPDs by TU Vienna

Again, the same observation data as in the previous test was used to proof that fixing with PPPsoft does also work in combination with the WL and NL UPDs calculated at the TU Vienna. Instead of the CNES orbit and clock correction stream, here, the final orbits and clocks by the IGS were used, as these were also used for the bias calculation.

In Figure 5.4 (b) the ambiguity fixed solution of NEU coordinates is shown, again referenced to the known station coordinates. This fixed solution is rather equivalent to the one shown in Figure 5.4 (a), except for that the two NL ambiguities belonging to the satellites PRN 7 and PRN 8 were fixed incorrectly in the beginning of the processing. These fixed values are corrected for only one cycle between the epochs 1277 and 1847, which is clearly visible as coordinate jumps in the beginning of the solution. The problem and effect of wrong integer NL-fixes is further illuminated in the subsequent Section 5.4.

Nevertheless, the test shows, that within PPPsoft it is possible to successfully use the UPD corrections for the WL and NL linear combinations as produced by the TU Vienna, as well as the CNES bias corrections, to calculate a PPP-AR solution of high quality.

5.4 Effect of wrong fixes on the coordinates

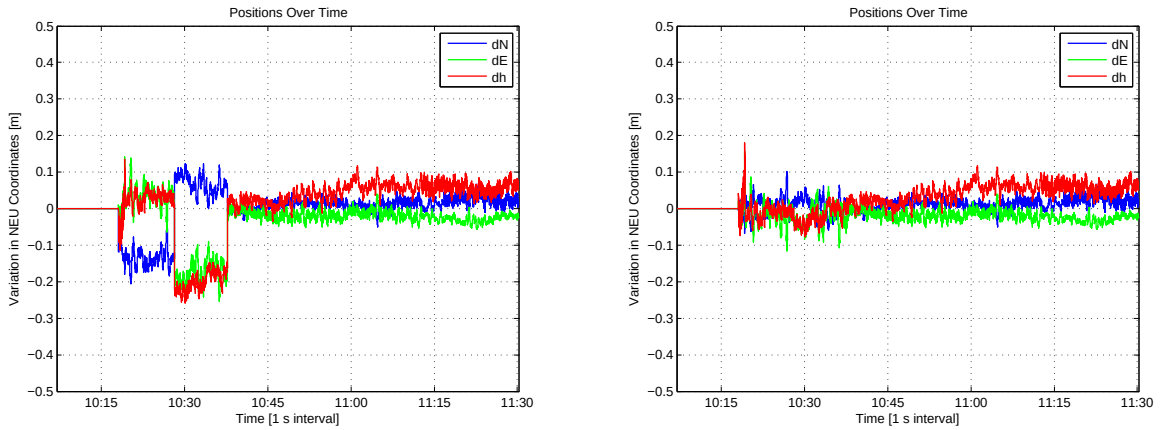

(a): Original coordinate solution

(b): Coordinate solution with corrected ambiguity fixes

Figure 5.5: Comparison of original (left) and artificially manipulated (right) PPP fixed solution of Graz Lustbühel DOY 087 2013 using final IGS orbits and clocks + UPDs by TU Vienna

To illustrate, what small errors in the integer ambiguity fixes mean to the coordinate solution, the example shown in Figure 5.4 (b) was calculated again. Now the two wrongly fixed NL ambiguity values of PRN 7 and PRN 8 were corrected manually to the "true" values, in the same epoch they were fixed. These "true" values were found by processing the scenario for some hours in advance.

Figure 5.5 shows a comparison of the original coordinate solution in (a) and the coordinate solution calculated with corrected ambiguity values in (b). The result of the immediate correction of ambiguity fixes is a smooth position solution from the beginning, where the jumps from the original coordinate solution are gone. This shows, that even small errors in fixes can dramatically worsen the result. Therefore, it is essential to avoid or at least detect wrongly fixed NL and also WL ambiguities as soon as possible.

Unfortunately, the detection of a incorrectly fixed integer ambiguity value is not an easy task, since the only comparison measure is the noisy float ambiguity. Therefore, without the effort of investigations on enhanced algorithms solving that task, the NL ambiguities can only be detected within a range of $\pm$1-2 cycles in the early processing phase. This means that coordinate jumps are likely to occur in the first minutes of the fixing procedure.

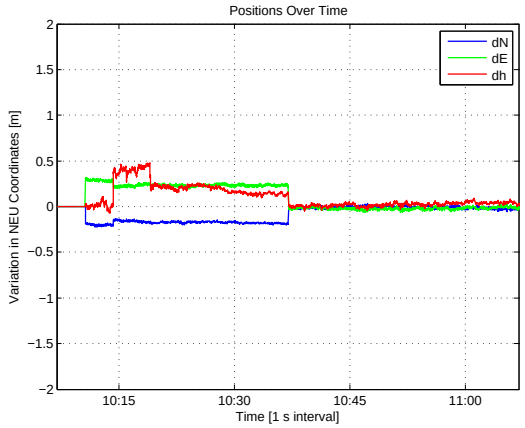

(a): NEU-differences – cut-off angle 10 °

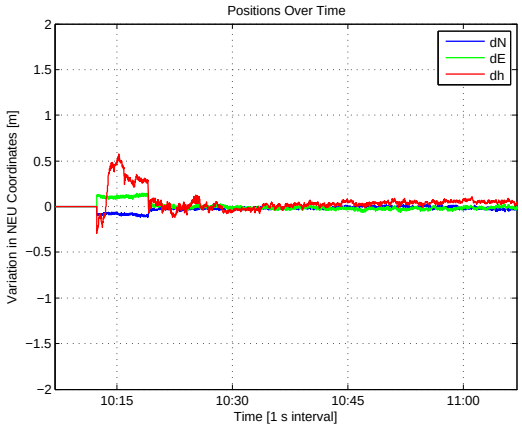

(b): NEU-differences – cut-off angle 30 ° till 500 s, 15 ° till 1000 s and 10 ° after that time

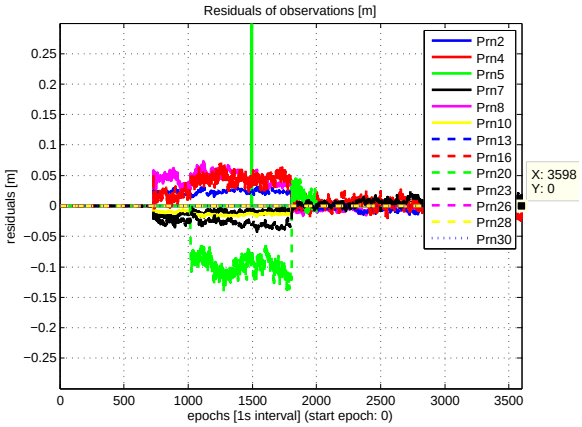

(c): Phase residuals – cut-off angle 10 °

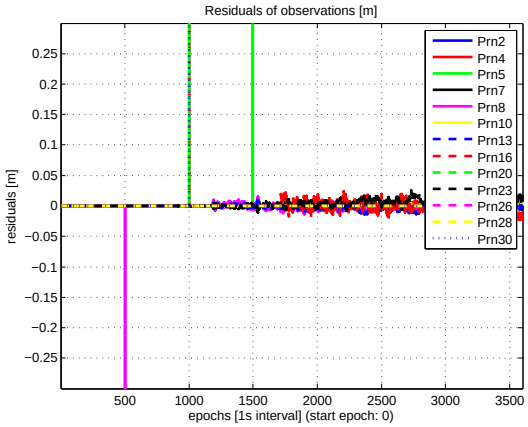

(d): Phase residuals – cut-off angle 30 ° till 500 s, 15 ° till 1000 s and 10 ° after that time

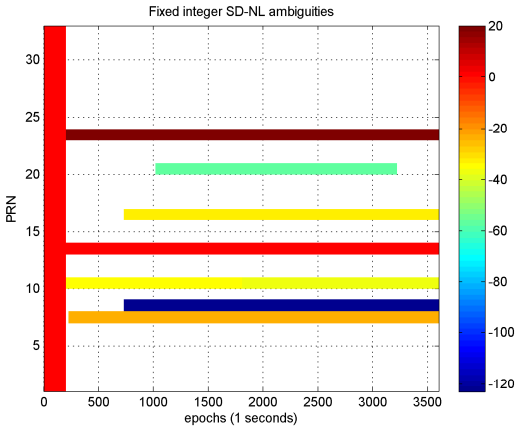

(e): Fixed NL ambiguities – cut-off angle 10 °

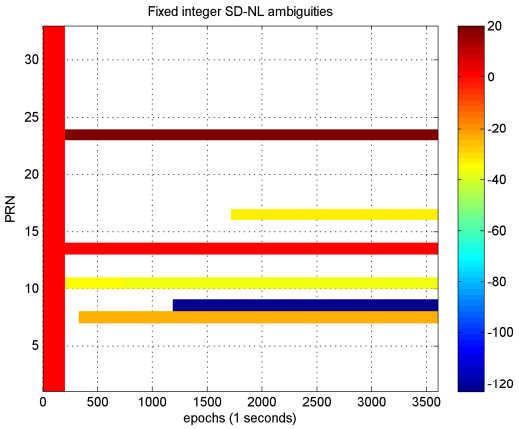

(f): Fixed NL ambiguities – cut-off angle 30 ° till 500 s, 15 ° till 1000 s and 10 ° after that time

Figure 5.6: Test with adapted cut-off angle for ambiguity fixing of Graz Lustbühel DOY 087 2013 using CNES data

5.4.1 Adapt cut-off angle

The first investigation on options to decrease the fixing time and limit the number of wrong NL-fixes was the limitation of the cut-off angle for satellites to be fixed in the beginning of the processing. The underlying assumption was that signals of lower satellites experience a larger noise and larger errors originating from residual atmospheric effects. Therefore, in this test, the elevation angle in the first epochs is limited to 30 °, while lower satellites are added later on in the processing. For the used data set in combination with the actual processing settings this investigation shows promising results:

Figure 5.6 (a) shows the NEU offsets from the reference coordinates over the processing time calculated with a cut-off angle of 10 ° over the whole observation period. Figure 5.6 (c) illustrates the post-fit phase residuals, where the observed satellites are plotted with different colours over the processing epochs. Figure 5.6 (e) contains the integer values of the fixed NL ambiguities of the different satellites, where the values themselves are represented by the colours as defined by the colourbar on the right hand side of the figures. The Y-axis contains the satellites' PRN number and the X-axis represents the epoch number.

In the beginning of the processing many NL ambiguities can be fixed to integers, as it can be seen in Figure 5.6 (e), but the phase residuals in Figure 5.6 (c) show inconsistencies in the phase measurements, which result from incorrectly fixed NL ambiguities.

Figures 5.6 (b), (d) and (f) show the same data, but now processed with an initial cut-off angle of 30 °. In the second solution the NEU coordinates as well as the phase residuals indicate, that the ambiguity fixes fit together better than in the solution with the 10 ° cut-off angle. Fewer satellites are fixed, but more of them seem to be correct from the beginning.

Nevertheless, one should be careful, when increasing the cut-off angle, since the geometry automatically gets worsened by doing so. The fact, that fewer satellites can be fixed when using a larger cut-off angle, may also result in fewer correct fixes. Therefore, two series of tests followed this single investigation in order to give a more profound recommendation on the adaptation of the cut-off angle for the fixing procedure. For this investigation data from the station Graz Lustbühel from DOY 087 2013 was calculated with various start epochs in an interval of 30 minutes, while the processing length was limited to 100 minutes, as only the convergence time was interesting in this test. For the first test-series the general cut-off angle and the angle for the ambiguity fixing were set to 10 °, while for the second test series the general cut-off angle was adapted starting with 30 ° for a processing time <500 s. For a processing time <1000 s a cut-off angle of 15 ° and after that time 10 ° were used.

The solutions of all tests were compared concerning the dependence of the coordinate convergence from the cut-off angle. The comparison of both test series showed, that the limitation of the cut-off angle is rather dangerous. As the number of satellites is reduced, also the geometry in the beginning of the solution worsens, which in turn is important for the estimation of ambiguities. There are in fact only few cases, where the convergence of the fixed solution becomes better or faster after increasing the initial cut-off angle. Nevertheless, it is not recommendable to use satellites with an elevation angle below 10 °, as for very low satellite signals the model values for the atmosphere are inaccurate and the observation noise becomes too large.

5.4.2 Post-fit residuals of phase observations

By comparing Figure 5.6 (c) and (d) it becomes obvious, that the post-fit phase residuals can give information about the correctness of fixed ambiguity values. If single phase residuals do have a significant offset from zero (see Figure 5.6 (c) between epoch 1000 and 1750), one can conclude, that one or more ambiguities are incorrectly fixed. Unfortunately, this does only work, after at least four NL ambiguities have been fixed to integers, as before the 4^{th} ambiguity is fixed, there is hardly any redundancy in the phase measurements and therefore the residuals approach zero. Further, the residuals do not directly indicate, which NL value is incorrect, especially when there is not only one but two or more wrong fixes. They rather show general inconsistencies in the equation system, that disperse in all observations.

Nevertheless, it seems to be possible to make use of the information of the post-fit phase residuals for detecting incorrect NL ambiguity fixes. Generally, ambiguity fixes should be questioned in the case that the phase residuals of the PPP-AR solution contain outliers. Correcting only one incorrectly fixed ambiguity value increases the quality of the whole PPP solution. For example, if the residuals' standard deviation does exceed a certain threshold (e.g. 0.5 cycles), an iterative procedure can be started, where fixed integer NL ambiguities are released or shifted by ± 1 cycle, until the residuals' standard deviation becomes a minimum.

In the following, this approach is verified in further experiments using a series of PPP runs. Note, that in these tests, the outlier is only detected when a minimum of five NL ambiguities is fixed. This originates in the fact, that a minimum of three fixed ambiguities only allows a fixed PPP solution, but the phase residuals are more or less meaningless, as long as the solution is not redundant. Using four fixed ambiguities produces residuals that are clearly different from zero and five fixed ambiguities even allow to detect which ambiguity fix is incorrect. Therefore, five satellites with fixed ambiguities are mandatory to localise one wrong fix.

In the following tests several datasets of DOY 087 in 2013 are calculated with different start epochs for different times of the day. As soon as an outlier is detected in the phase residuals, the adjustment is repeated, but now one of the fixed ambiguities is chosen to be excluded. One adjustment is calculated for every satellite and afterwards the residuals are checked again. The one observation set producing the lowest residuals is taken for the final processing of this epoch and the NL ambiguity of the excluded satellite is released for the following epochs. As already mentioned, five fixed satellites are necessary in order to get representative residuals, after excluding one satellite. Further, this procedure does only work, if only one ambiguity is incorrectly fixed. As soon as two or more wrong fixes occur, they cannot be detected by using the proposed method. In this case more sophisticated methods have to be found.

Figure 5.7 shows the north, east and up (NEU) coordinate offsets from all solutions of the station Graz Lustbühel on DOY 087 GRAZ as a function of the processing time in hours. The red color indicates, that no residual checking was applied, while the blue solutions were processed by using the residual checking procedure. It can be shown that some severe outliers can be avoided or corrected by using the residual checking method.

Figure 5.8 shows one example of the PPP-AR test series, where a huge profit has been gained by applying the residual checking technique. In Figure 5.8 (a) and (c) the NEU coordinate differences from the reference are visualised, while Figure 5.8 (b) and (d) shows the post-fit phase residuals of the visible satellites.

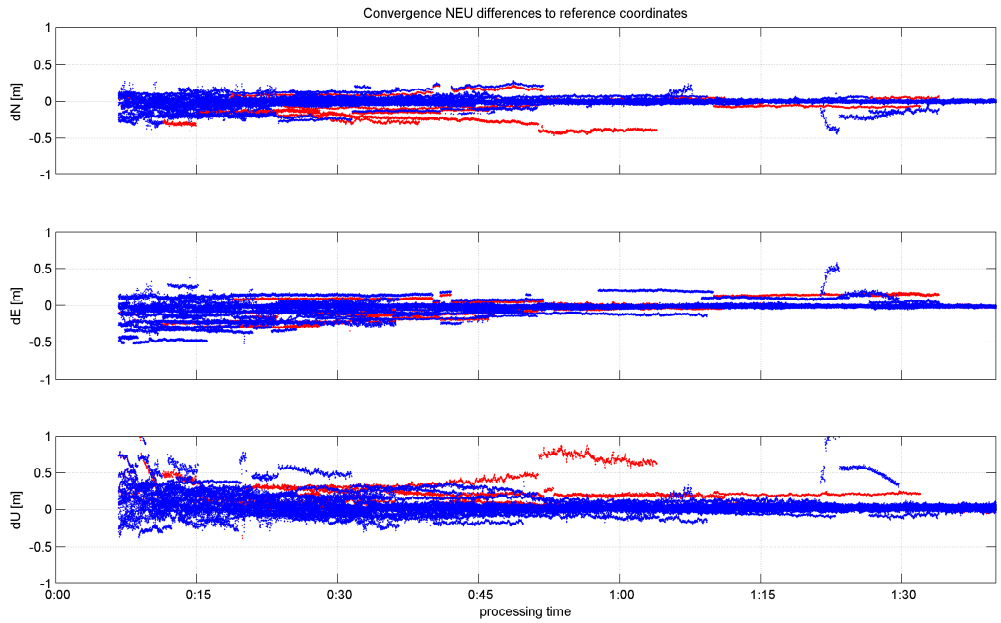

Figure 5.7: Test series of Graz Lustbühel DOY 087 2013 using CNES data with (blue) and without (red) checking the post-fit phase residuals

In Figure 5.8 (a) wrong NL ambiguity fixes heavily distort the PPP-AR solution, which is also visible in the corresponding phase residuals in (c). In Figure 5.8 (b) and (d) the incorrect fixes were detected by means of the phase residuals in the early processing phase. After 15 minutes of processing the corrected solution is significantly better and the residuals do not show any severe outliers any more. Therefore, in this case the residual checking is successful and clearly increases the accuracy of the PPP processing.

Nevertheless, there are still a lot of cases, especially in the early processing phase, where the proposed residual checking procedure cannot help to eliminate errors in the fixed ambiguities, which can also be seen in Figure 5.7. This mainly has the following reasons:

Commonly, in the first 15 minutes only few NL ambiguities can be fixed at all, while for the detection and localisation of wrong fixes by means of the phase residuals at least five satellites with fixed ambiguities are necessary. This requirement is fulfilled only later on in the processing for most PPP-AR runs. Further, if two or more incorrect fixes occur, the algorithm implemented in PPPsoft cannot localise them any more. For these cases PPPsoft offers only a primitive solution: At the moment the ambiguity fixing routine in PPPsoft is repeated every epoch for all satellites in view to enable the correction of single ambiguities, based on the currently fixed values proposed by the LAMBDA method (cf. Section 4.3.3). Unfortunately, the success of this procedure only depends on the quality of the float estimates of the current epoch, while it would be desirable to find also other quality measures to verify the fixed solution.

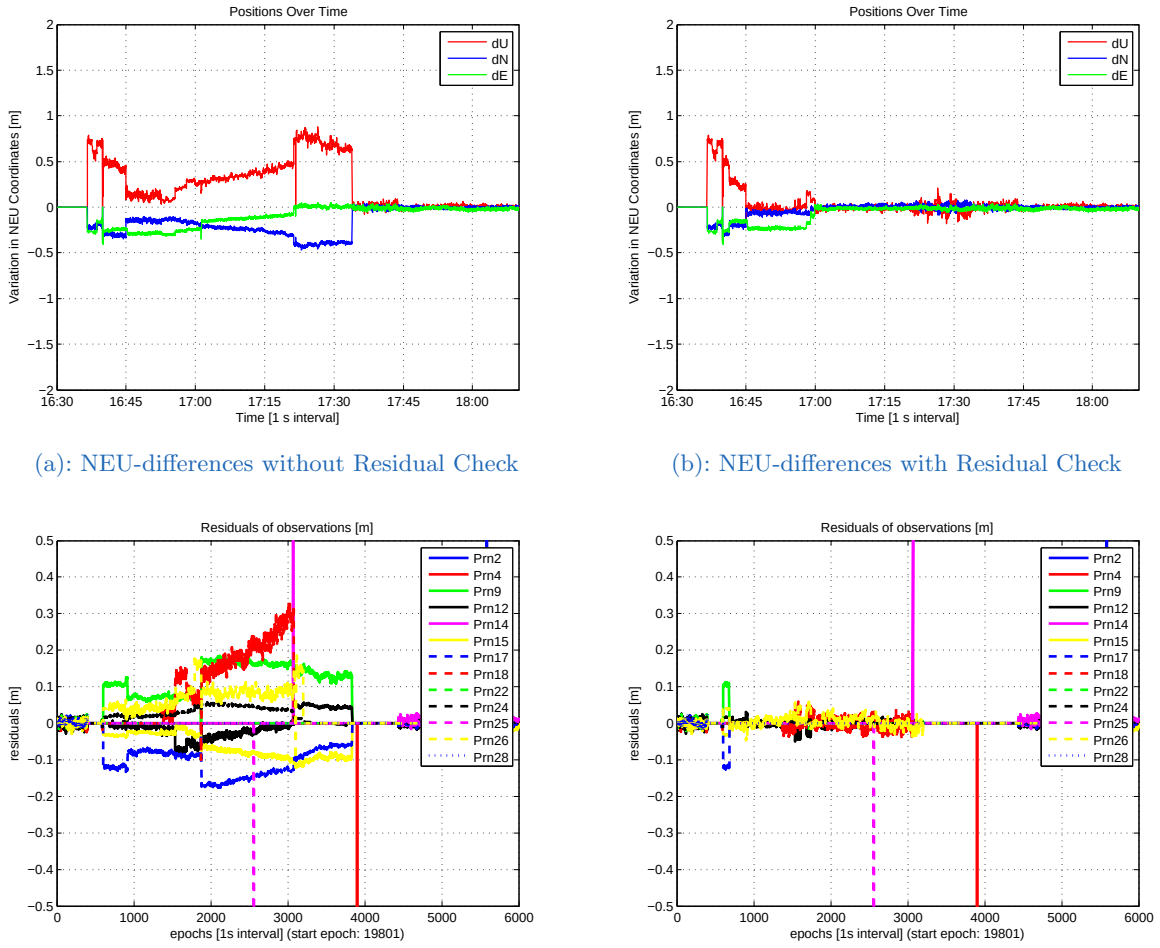

(a): NEU-differences without Residual Check

(b): NEU-differences with Residual Check

(c): Phase residuals without Residual Check

(d): Phase Residuals with Residual Check

Figure 5.8: Test example of Graz Lustbühel DOY 087 2013 using CNES data with and without checking the post-fit phase residuals

5.5 Ways to shorten the general convergence

5.5.1 Accurate start values for rover coordinates

A shorter convergence time in the PPP float solution would also shorten the elapsed time to the first fix in the ambiguity-fixed solution. One option to accelerate the convergence is to introduce better initial coordinates, which is not an easy task for roving receivers. Nevertheless, when using reference station data, the receiver position is accurately known and therefore the effect of good initial coordinates on the convergence can be tested easily.

Therefore, observation data from station GRAZ Lustbühel on DOY 087 and DOY 088 was processed several times by putting different constraints on the initial position coordinates, which are known with an accuracy of only millimetres. The different solutions were calculated with constraints on the initial coordinates with a standard deviation of 1 m, 5 cm and 1 cm. The

Type	Format	File	Information
Observations	RINEX 2.11	GRAZ0870.13O	interval of 1s
Epochs	1 Epoch is 1s	10801 – 18000	–
Obs. Time	GPS time	13:06:56 – 15:06:56	–
ORBIT/CLOCK/DCBs	SSR correction by CNES	CLK9B0870.13C	recorded by PPP-wizard

Table 5.2: Example data used for single test using initial XYZ constraints

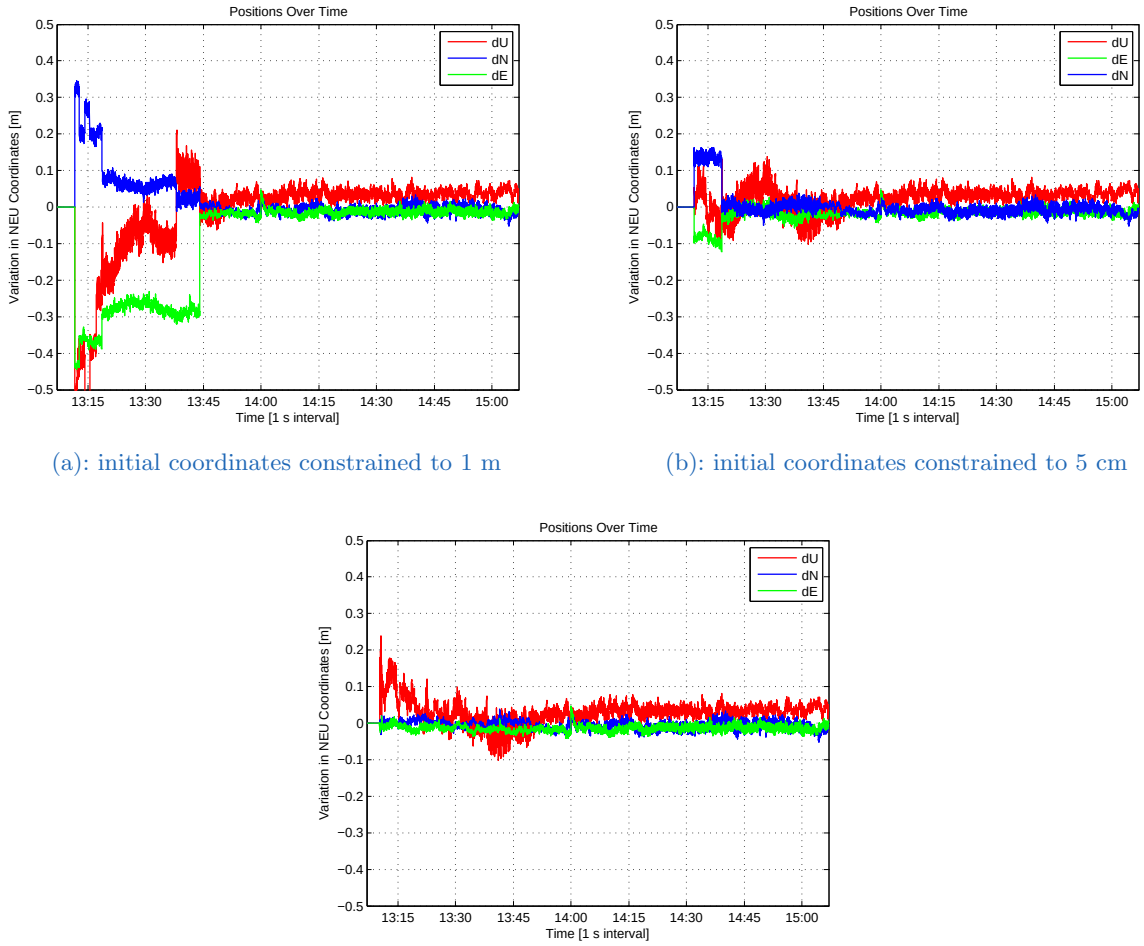

(a): initial coordinates constrained to 1 m

(b): initial coordinates constrained to 5 cm

(c): initial coordinates constrained to 1 cm

Figure 5.9: NEU differences of PPP-AR solution of Graz Lustbühel DOY 087 2013 using CNES data with different standard deviations for initial coordinates

reference coordinates themselves were not changed, only their assumed accuracy was adapted. In all examples the routines for the ambiguity fixing were started in epoch 200 (after 200 seconds), which is long before the solution usually converges.

The Figures 5.9 (a), (b) and (c) show example coordinate results of solutions calculated from the same observation data, but with different constraints on the approximate coordinates. The data and the products used for these tests are summarised in Table 5.2.

In this example in Figure 5.9 the solution with the initial coordinate constraint of 1 m (a) needs 37 minutes to produce valid fixed coordinates, the solution with the 5 cm initial coordinate constraint (b) needs 12 minutes and the solution with the 1 cm constraint (c) only needs 4 minutes for a fixed solution with optimum accuracies.

To get a better overview on the convergence behaviour of the coordinate solutions in dependency of the initial coordinate constraints, the Tables 5.4 and 5.5 show the convergence times of several PPP-AR solutions calculated from the data in Table 5.3, where only the start epoch was shifted by 1800 s for the solutions 1-7.

Type	Format	File	Information
Observations	RINEX 2.11	GRAZ0880.13O	interval of 1s
Epochs	1 Epoch is 1s	10801 – 18000	solutions shifted by 1800 s
Obs. Time	GPS time	13:06:56 – 15:06:56	solutions shifted by 1800 s
ORBIT/CLOCK	SSR correction by CNES	CLK9B0870.13C	recorded by PPP-wizard
	Final products by IGS	igs17334.sp3	–
		igs17334.clk_30	–

Table 5.3: Example data used for test series using initial XYZ constraints

Table 5.4 shows the time to convergence from the beginning of the calculations in minutes. These samples were processed using UPDs by CNES, while for the solutions in Table 5.5 UPDs produced by the TU Vienna were used. The time of convergence is defined by the time, when a minimum of three satellites are fixed and the coordinate errors are smaller than 5 cm in the horizontal plane and 10 cm in height.

init std	1	2	3	4	5	6	7	mean	median
1 cm	3,35	3,35	5,98	52,67	16,67	–	18,32	16,72	11,33
5 cm	46,72	52,60	32,67	25,22	70,43	19,65	30,00	39,61	32,67
1 m	44,43	53,03	32,50	29,25	69,68	19,28	30,00	39,74	32,50

Table 5.4: Convergence behaviour of fixed coordinate solutions at different start epochs of station Graz Lustbühel DOY 088 2013 dependent on initial coordinates and their standard deviations, convergence time is given in minutes, UPDs by CNES

The solutions in Table 5.4 and Table 5.5 are comparable, even though both have their outliers originating from either imprecise ephemeris products or phase bias corrections. The convergence with coordinate constraints of 1 m is equivalent to completely unknown initial coordinates and converges between 20 and 40 minutes. Introducing better initial coordinates slightly accelerates

init std	1	2	3	4	5	6	7	mean	median
1 cm	7,53	3,35	16,67	4,38	10,58	20,00	31,67	13,45	10,58
5 cm	46,53	18,33	26,67	12,27	15,00	17,67	32,13	24,09	18,33
1 m	47,35	27,60	28,33	9,93	29,17	14,15	32,25	26,97	28,33

Table 5.5: Convergence behaviour of fixed coordinate solutions at different start epochs of station Graz Lustbühel DOY 088 2013 dependent on initial coordinates and their standard deviations, convergence time is given in minutes, UPDs by TU Vienna

the convergence, even though a significant improvement is only possible with initial rover positions known better than 5 cm. Unfortunately, it is rather unrealistic for real scenarios to have initial coordinates better than 10 cm.

5.5.2 Accurate start values for troposphere delay

Another possibility to accelerate the convergence may be the use of external troposphere data, so that the remaining wet tropospheric delay does not have to be estimated in the adjustment procedure. As reported in Shi et al. (2014), from introducing external troposphere data especially the height component of the coordinate solution can be expected to converge faster.

Constraints on initial height component

In order to verify, if introducing accurate start values for the tropospheric delay influences the coordinate convergence and simultaneously also the convergence of the ambiguity estimates, a new test scenario was defined. Therefore, accurate start values for the height component are introduced to the solution and the initial standard deviation of the height component std_{h0} is constrained to 1 mm, while the horizontal components stay unconstrained. Constraining the height component should have a similar effect on the solution, as if accurate initial values for the Zenith Wet Delay (ZWD) of the troposphere was known. However, introducing highly accurate initial values for the height component and constraining it is easier to realise, as the station coordinates are accurately known by the network provider.

To visualise the results an example calculation was chosen; Figure 5.10 shows an extract of the float (first row) and fixed (second row) solution of DOY 087 of station Graz Lustbühel between 11:00 and 12:40. In detail, the figures show the NEU coordinate variation from the reference coordinates over the processing time.

In Figure 5.10 (a) and (c) the height component of the initial coordinate values is constrained to 1 mm, while the initial height in Figure 5.10 (b) and (d) is unconstrained. The horizontal coordinate convergence of the float solution in (a) is significantly improved, and the height component, as expected, is nearly error-free. Nevertheless, the convergence of the fixed solution in (c) shows only a weak improvement compared to the fixed solution in (d).

Therefore, a closer look on the float ambiguity estimates of the two solutions is taken in Figure 5.11. Here, again (a) shows the ambiguities of the constrained solution, while (b) shows the ambiguity

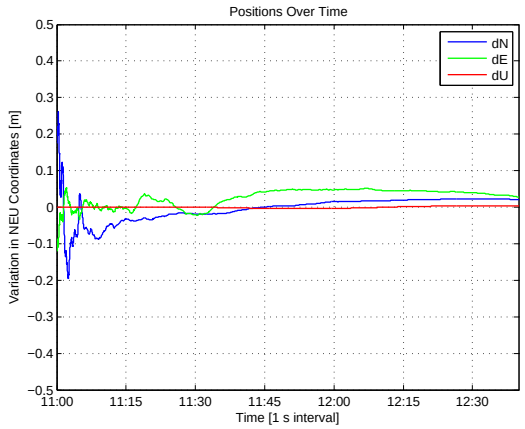

(a): Float solution with std_{h0}=1 mm

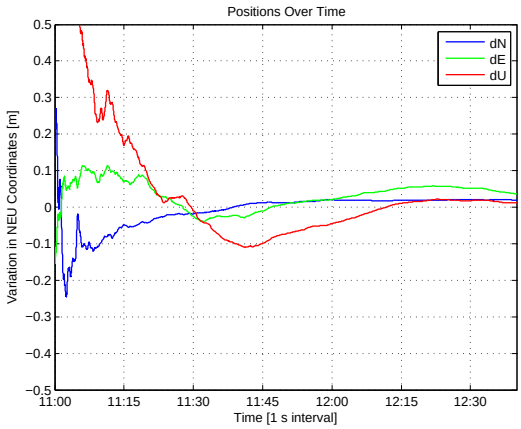

(b): Float solution with unconstrained height

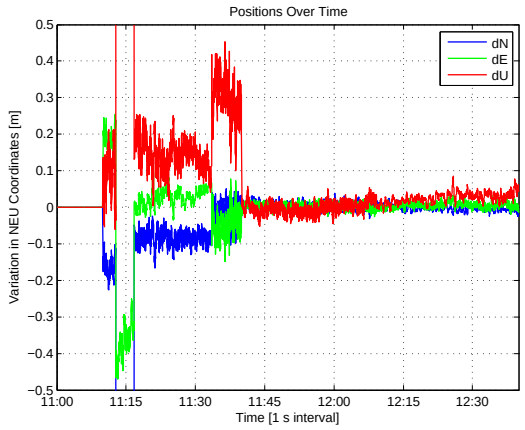

(c): Fixed solution with std_{h0}=1 mm

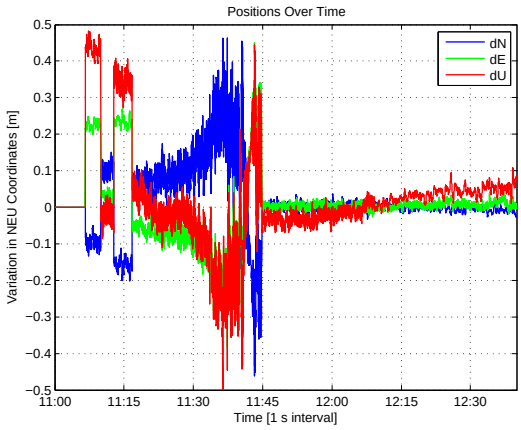

(d): Fixed solution with unconstrained height

Figure 5.10: Test with constrained height component – NEU solution of Graz Lustbühel DOY 087 2013

estimates of the unconstrained solution. Note, that for a better visualisation the ambiguity plots show only a limited range in the Y-axis. Figure 5.12 (a) and (b) contain the respective plots for the satellites' elevation in degrees visualised by the colours in the colourbar and a skyplot in order to get an overview on the satellite constellation.

Obviously, the float ambiguity estimates visualised in Figure 5.11 (a) do not significantly converge faster after constraining the height component as in Figure 5.11 (b), where they height is unconstrained. Therefore, it can be assumed, that only small improvements can be gained for ambiguity fixing from introducing only accurate approximate values for the receiver height. A similar behaviour can be expected from introducing external values for the ZWD.

In order to get a better overview on the behaviour of PPP-AR solutions, when on the one hand only the height component (std_0 = 1 mm), and on the other hand the height (std_0 = 1 mm) in combination with the horizontal position (std_0 = 1 dm) is constrained, a series of fixed PPP solutions is calculated. For this investigation observation data of the Austrian GNSS stations EPOSA GRAZ, EPOSA BADE, and EPOSA DALA were chosen at DOY 087 in 2013. Different

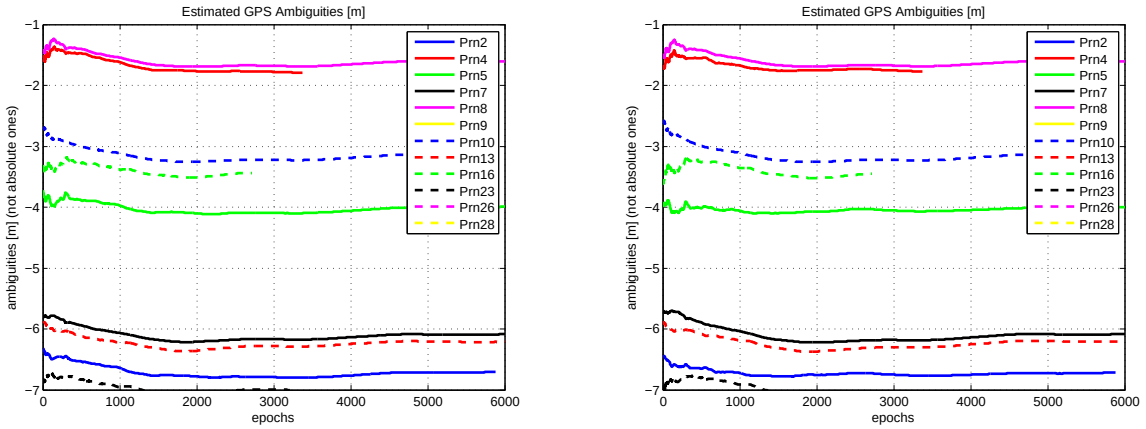

(a): Detail of ambiguty solution with std_{h0}=1 mm

(b): Detail of ambiguity solution with unconstrained height

Figure 5.11: Test with constrained height component – Ambiguity float solution detail of Graz Lustbühel DOY 087 2013

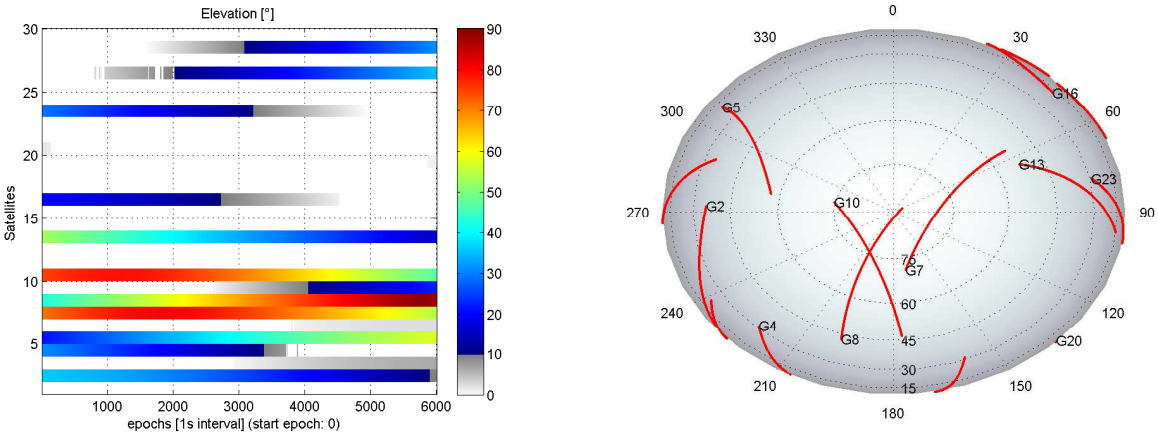

(a): Elevation

(b): Skyplot

Figure 5.12: Test with constrained height component – Satellite constellation of Graz Lustbühel DOY 087 2013

solutions of one station on the same day were calculated by time shifting the start epoch by 30 minutes. The processing length for all solutions is 100 minutes corresponding to 6000 epochs for each solution.

Figures 5.13 and 5.14 show diagrams of the accuracy of PPP-AR coordinate solutions of the EPOSA stations BADE and GRAZ at 15, 30, 45, and 60 minutes of processing. The median of the NEU coordinate differences with respect to the reference coordinates is visualised. The median was preferred to the mean value in order to ignore outliers. The figures in (a) show the coordinate offsets of the fixed solution with unconstrained initial height values, the figures in (b) show the solutions where the standard deviation of the initial height component is set to 1 mm and the figures in (c) show the fixed solutions, where the height and the horizontal initial position components were constrained in the beginning of the processing.

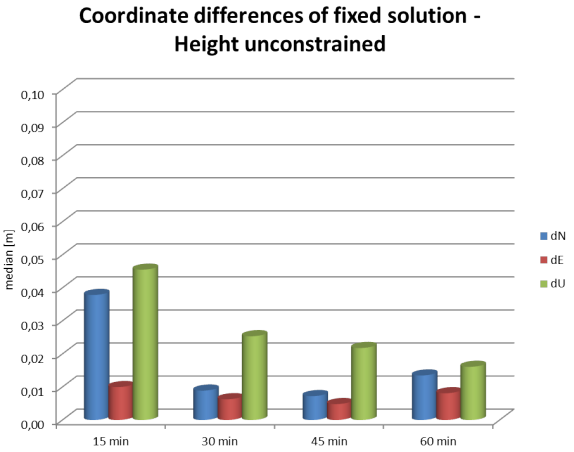

(a): Unconstrained height

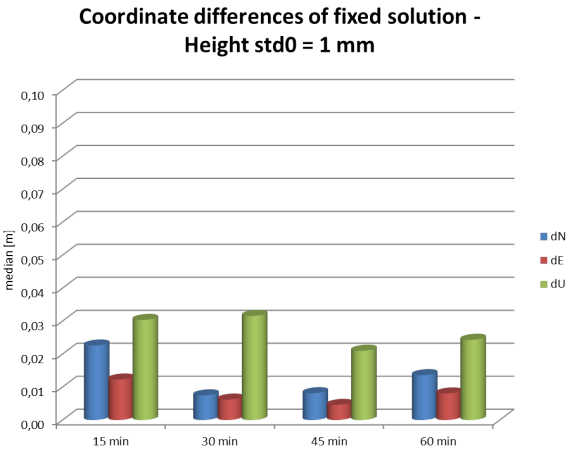

(b): $std_{h0} = 1$ mm

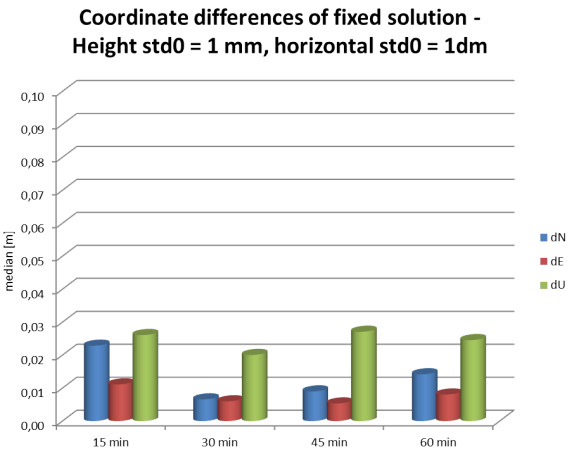

(c): $std_{h0} = 1$ mm and $std_{hor} = 1$ dm

Figure 5.13: Median of NEU differences with constrained and unconstrained height – station BADE DOY 087 2013

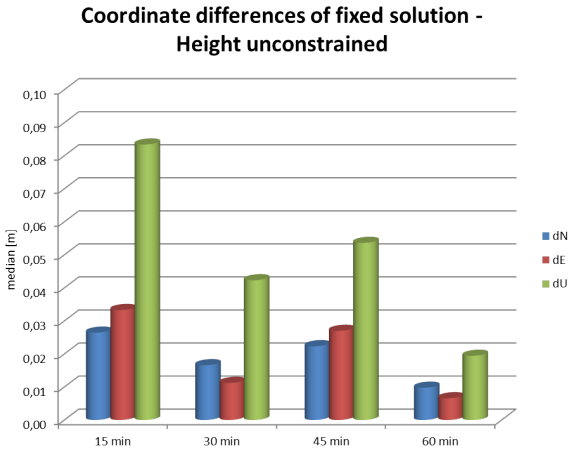

(a): Unconstrained height

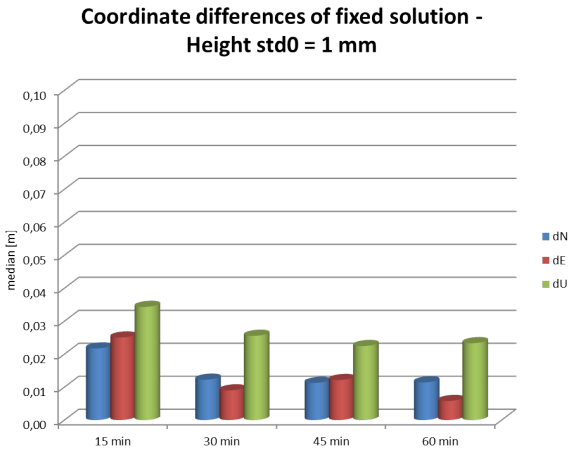

(b): $std_{h0} = 1$ mm

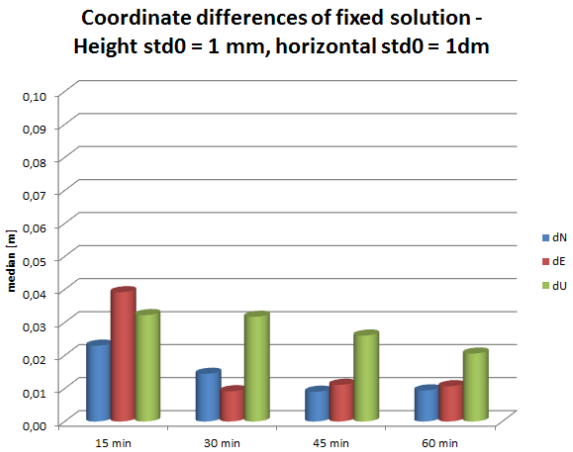

(c): $std_{h0} = 1$ mm and $std_{hor} = 1$ dm

Figure 5.14: Median of NEU differences with constrained and unconstrained height – station GRAZ DOY 087 2013

These figures manifest the same behaviour as expected from looking at Figure 5.10 and Figure 5.11 before: Even though the convergence of the float solution is clearly improved by the accurate initial height values, the fixed solution experiences only a slight improvement in the convergence of the horizontal position, as the height constraints hardly influence the ambiguity estimation. The height component of the fixed solution, however, can get improved by introducing height constraints.

The knowledge of better horizontal approximate coordinates with an accuracy of 1 dm or worse in combination with a very accurate a priori height does not influence the convergence significantly either. The standard deviation of 1 dm was chosen, because at the moment it is unrealistic to get better horizontal a priori positions for an arbitrarily located rover. But, maybe in the near future code measurements will become more precise and therefore, better initial positions may be obtained from them.

Using accurate values for the troposphere delay from an external source

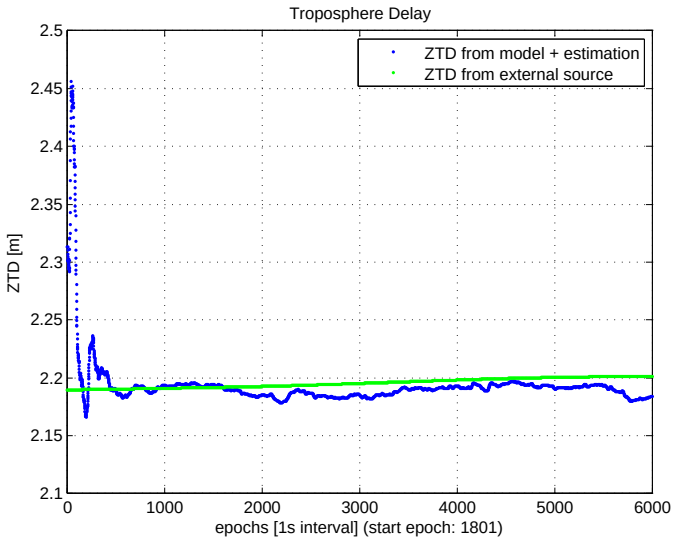

Figure 5.15: Comparison of estimated and external troposphere – station GRAZ (IGS)

In a further test scenario, the Zenith Total Delay (ZTD) of the troposphere was taken from an external source, instead of modelling and estimating it within the user client. Estimates for the station Graz Lustbühel on DOY 087 in 2013 were calculated at the network side at TU Vienna and introduced in the PPP solution in order to see the influence of accurate troposphere data on the coordinate convergence and the ambiguity fixing.

In the following, two types of solutions are compared: On the one hand the ZWD of the troposphere was estimated in a PPP solution by PPPsoft, while on the other hand the troposphere estimates were taken from a daily solution calculated at the TU Vienna. The troposphere solution by the TU Vienna is given every hour of DOY 087, and has to be interpolated in between.

Figure 5.15 shows a comparison of the troposphere solution estimated by means of the user client PPPsoft and the external troposphere data. Therefore, their ZTD in meters is visualised for a

timespan of 6000 epochs or 100 minutes. In PPPsoft the ZTD was calculated from the modelled Zenith Hydrostatic Delay (ZHD) plus the estimated ZWD from one GNSS station on the fly. The troposphere estimates by TU Vienna were also obtained by means of a PPP solution, but processed over the whole day, while the calculations using PPPsoft started at 11:00 am. One can see, that the solutions strongly resemble each other, whereas the estimated solution by PPPsoft naturally is still a bit unstable in the first 1000 epochs of processing.

Figure 5.16 shows the NEU coordinate differences to the reference coordinates of a series of PPP float solutions from the station Graz Lustbühel, started at different times of the day (DOY 087). The X-axis shows the processing time, whereby only an extract of one hour is visualised in order to check the convergence time. For the solutions in green the troposphere was modelled/estimated within the processing, while for the solutions in red the external troposphere values were used instead. All float solutions were calculated with the aid of final orbits and clock corrections obtained from the IGS in post-processing.

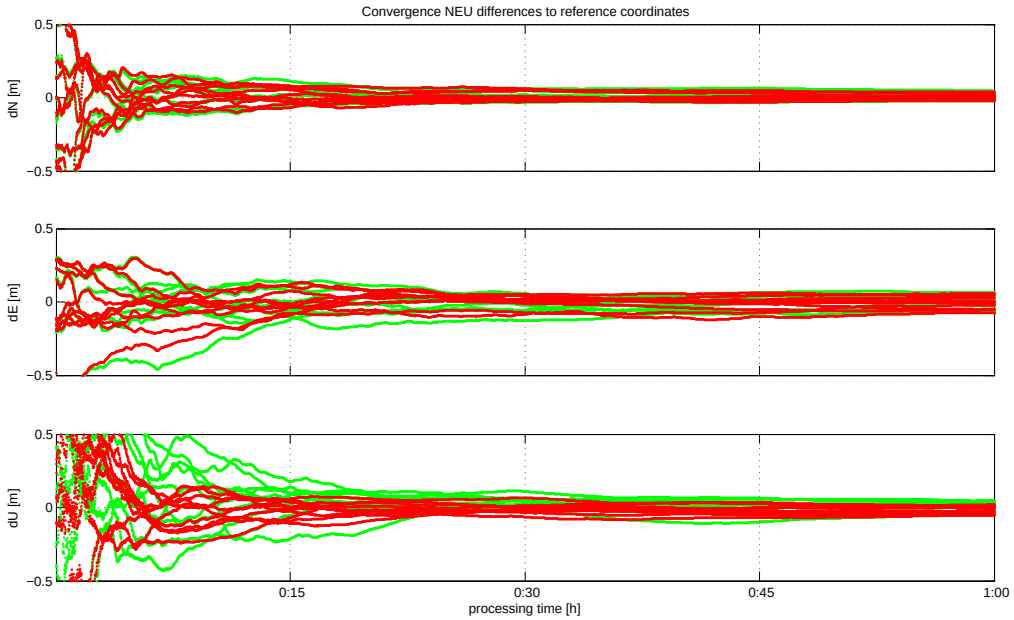

Figure 5.16: NEU differences of solutions with estimated (green) or external (red) troposphere – station GRAZ (IGS)

As expected, the coordinate solutions calculated with the external troposphere data show a clearly better convergence behaviour in the height component. The accuracy level approaches the decimetre after only 10-15 minutes in all processed solutions, while half of the solutions with estimated ZWD at that time have an accuracy level of only 2-3 decimetres.

The horizontal components are less influenced by the introduction of external troposphere values, than the height component; especially the north direction shows absolutely no improvement in the float solution. Nevertheless, the convergence here could be supported by introducing not only external troposphere values but also more accurate approximate coordinates as shown in Section 5.5.1.

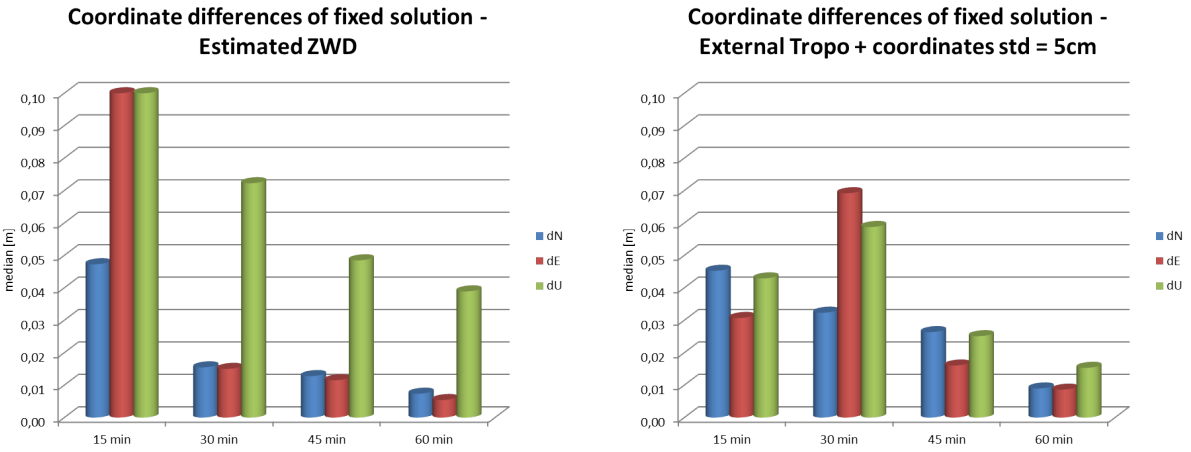

(a): Tropo ZHD modelled + ZWD estimated

(b): External Tropo by TU Vienna used + constraint on approx. coordinates (std_0 = 5 cm)

Figure 5.17: Median of NEU differences with estimated troposphere and external troposphere data – station Graz Lustbühel DOY 087 2013

Figure 5.17 visualises the influence on the NEU coordinate accuracies of the PPP-AR solution, when introducing external troposphere data (see Figure 5.17 (b)) instead of modelling and estimating it during the processing (see Figure 5.17 (a)). Additional to introducing the external troposphere data in (b) also the initial standard deviation of the coordinates was set to 5 cm, which is already an optimistic accuracy for approximate coordinates. Both figures show the median of the coordinate differences at 15, 30, 45 and 60 minutes of the processing.

Concluding from these figures, the convergence of the horizontal coordinate solution gets only slightly better due to the use of external troposphere data. But, as expected, the height component is better at any time of the processing. Unfortunately, most land-based applications prefer a good horizontal accuracy to an accurate height component, which is why the transmission of external troposphere corrections provides only minor improvements for the user when it comes to ambiguity fixing. Nevertheless, further tests with different data sources have to be performed in order to give a more profound conclusion on this topic.

5.6 Influence of geometry and correlations on ambiguity fixing

5.6.1 Geometry of fixed satellites

In order to get an impression of good and unfavourable conditions for PPP with ambiguity fixing, a sample of solutions at different times and with different satellite geometry was calculated. The EPOSA station BADE 087 was chosen for this test to show the dependence of fixing results from the satellite geometry.

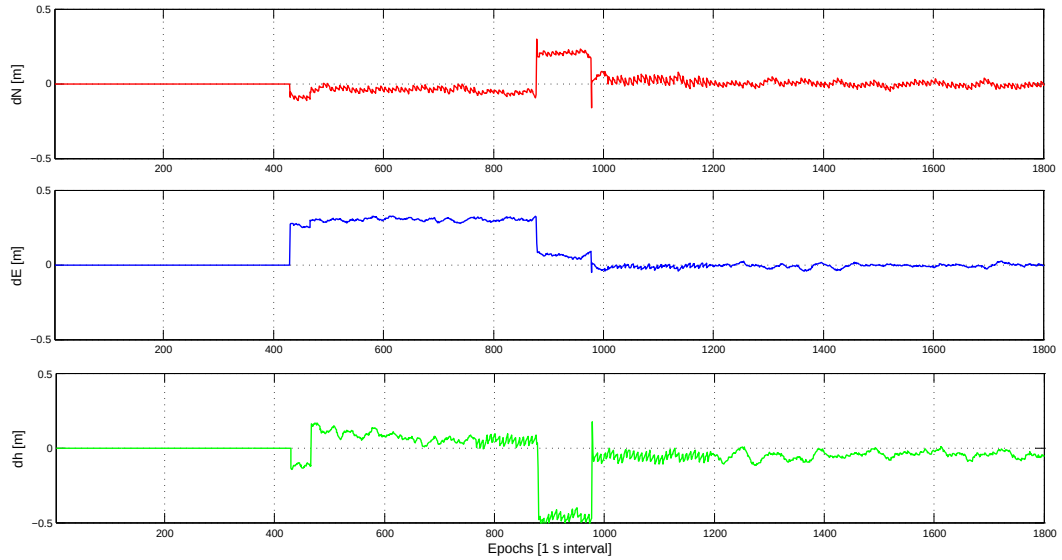

(a): NEU coordinate differences vs. epochs

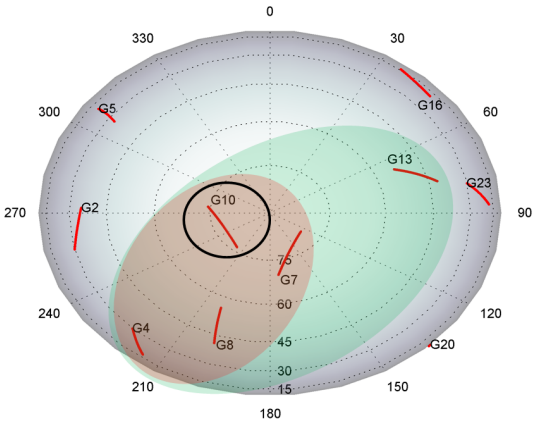

(b): Satellite Skyplot

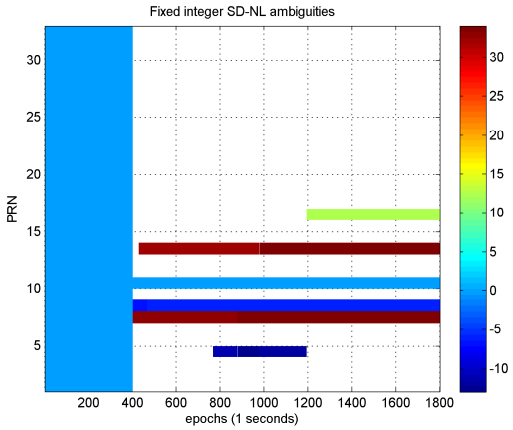

(c): NL ambiguity fixes

Figure 5.18: Dependence of coordinate results from the satellite geometry – EPOSA BADE 087 at 11:00

BADE 087 11:00

Figure 5.18 (a) shows the first 30 minutes of a PPP-AR coordinate solution. Only the coordinate differences with respect to the reference coordinates of station BADE are given. The full convergence of the north, east and height components is reached after 978 Epochs or approximately 16 minutes. This is the time when the fourth NL integer fix is corrected to the true value. An overview on the whole NL-fixing process for this calculation is given in Figure 5.18 (c) showing the values of NL-fixes of all satellites over the processing epochs. The fixed integer values are represented by the colours as defined in the colourbar on the right hand side of the figure. The reference satellite has the fixed value zero. The important steps of the fixing procedure are further summarised in in Table 5.6. In this table four different states for the NL ambiguity occur; no entry means that the ambiguity is not fixed at all yet, x means that the ambiguity is incorrectly

EPOCH	401	429	466	766	878	879	977	978	1193
PRN 7	x	x	x	x	F	F	F	F	F
PRN 8	x	x	F	F	F	F	F	F	F
PRN 13		x	x	x	x	x	R	F	F
PRN 4				x	R	x	F	F	R
PRN 16									F

Table 5.6: Fixing procedure of station BADE at DOY 087 11:00 – Reference satellite PRN 10

fixed, F means that it is correctly fixed and R means that it is released for some reason.

The first correct NL integer value can be obtained for PRN 8 in epoch 466, the second fix is obtained for PRN 7 in epoch 878 and the third fix is obtained in epoch 977 for PRN 4. After this third correct integer ambiguity fix one can see a short jump in the coordinate solution, which occurs due to the very poor geometry of the fixed satellites in this epoch. In Figure 5.18 (b) the geometric distribution of fixed satellites is visualised by means of a reddish ellipse. The black circle marks the actual reference satellite. Already in the following epoch the fourth satellite PRN 13 can be fixed. This event enhances the geometry of the fixed satellites drastically, which can be seen in the green ellipse in Figure 5.18 (b). In the coordinate solution in Figure 5.18 (a) this mirrors in accurate and precise coordinate components from that epoch on.

BADE 087 12:30

EPOCH	401	526	691
PRN 7	F	F	F
PRN 5	F	F	F
PRN 28		F	F
PRN 10			F

Table 5.7: Fixing procedure of station BADE at DOY 087 12:30 – Reference satellite PRN 8

Figure 5.19 again shows the coordinate differences in (a), the satellite skyplot in (b) and the NL-fixes in (c), but this time of an example, where the first three fixed satellites have a very good geometric distribution. Within 526 epochs corresponding to less than 9 minutes a fully converged PPP-AR solution can be reached (see Figure 5.19 (a)). At this time only three correct NL-fixes could be obtained, but the respective satellites show a very good satellite geometry, which is also visualised as red ellipse in Figure 5.19 (b). Here, the fourth fixed satellite cannot enhance the coordinate precision any more. Further, it is noticeable, that in this solution no NL ambiguities are incorrectly fixed, which happens rarely especially when the fixing starts so soon. In this case the NL-fixing process is started after 400 epochs or less than 7 minutes. An overview on the whole

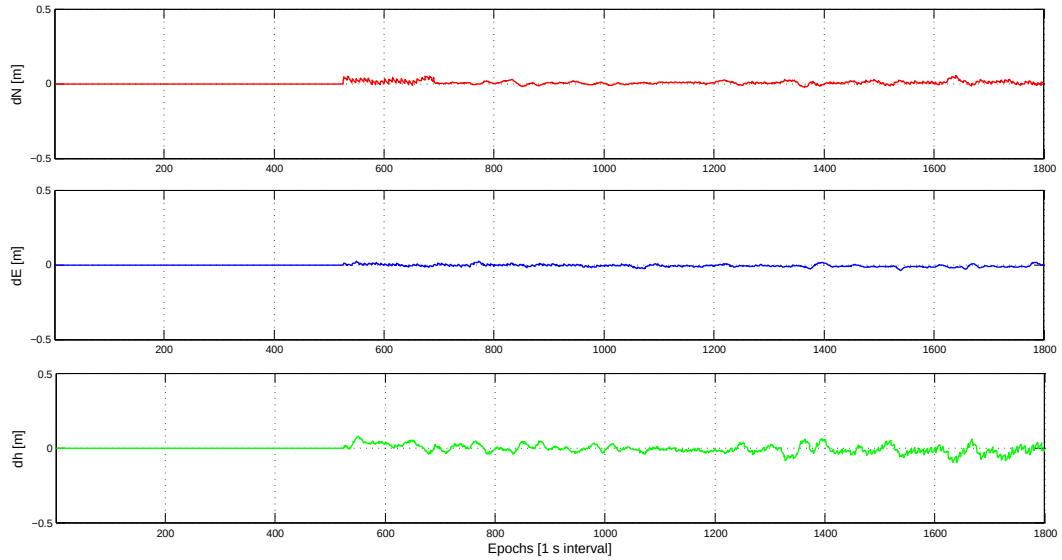

(a): NEU coordinate differences vs. epochs

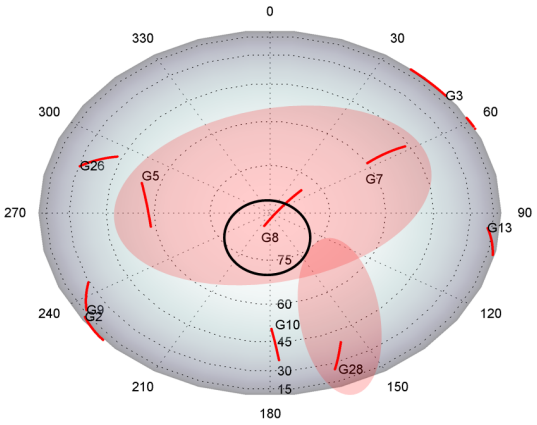

(b): Satellite Skyplot

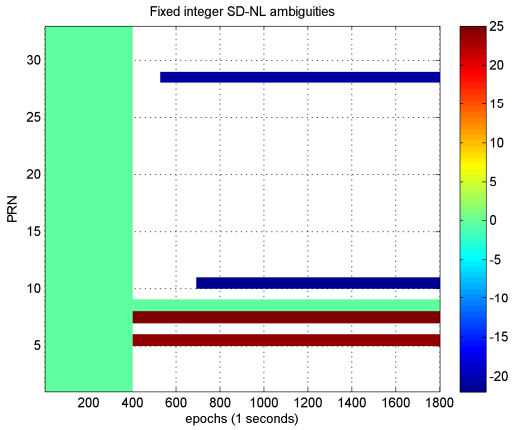

(c): NL ambiguity fixes

Figure 5.19: Dependence of coordinate results from the satellite geometry – EPOSA BADE 087 at 12:30

NL-fixing process for this calculation is given in Figure 5.19 (c) showing the values of NL-fixes over the processing epochs, as well as in Table 5.7 in a summarised version.

To sum it up, the geometry of the satellites with fixed ambiguities is important for the solutions' accuracy and precision. Under good geometric conditions only three satellites with correctly fixed WL and NL ambiguities are enough for the convergence of the PPP-AR solution.

5.6.2 Correlations influencing the fixing procedure

Sometimes it may happen that the high correlations occurring with the filtering, as already described in Section 3.2.2, prohibit the correct fixing of ambiguities. Figure 5.20 shows an example of a PPP-AR position solution of station Graz Lustbühel at DOY 088 (processing started at hour

EPOCH	422	508	509	624	1232	1336	3124	4473	4536
PRN 6	-16	**-15**	**-15**	**-15**	**-15**	**-15**	**-15**	**-15**	**-15**
PRN 21	8	R	6	6	6	6	6	**5**	**5**
PRN 3				**-20**	**-20**	**-20**	**-20**	**-20**	**-20**
PRN 18					-5	-5	-5	R	**-6**
PRN 22						11	11	**10**	**10**
PRN 19							**28**	**28**	**28**

Table 5.8: Fixing procedure of station GRAZ at DOY 088 2013 00:00 – Reference satellite PRN 16

00:00), where this phenomenon occurs. The corresponding satellite constellation is visualised in Figure 5.21. The skyplot in (a) shows the satellite distribution from the receiver position and contains azimuth and elevation angles in degrees, while (b) contains the elevation angles of all satellites over the processing time. The different values in degrees are represented by the colours in the colourbar on the right hand side.

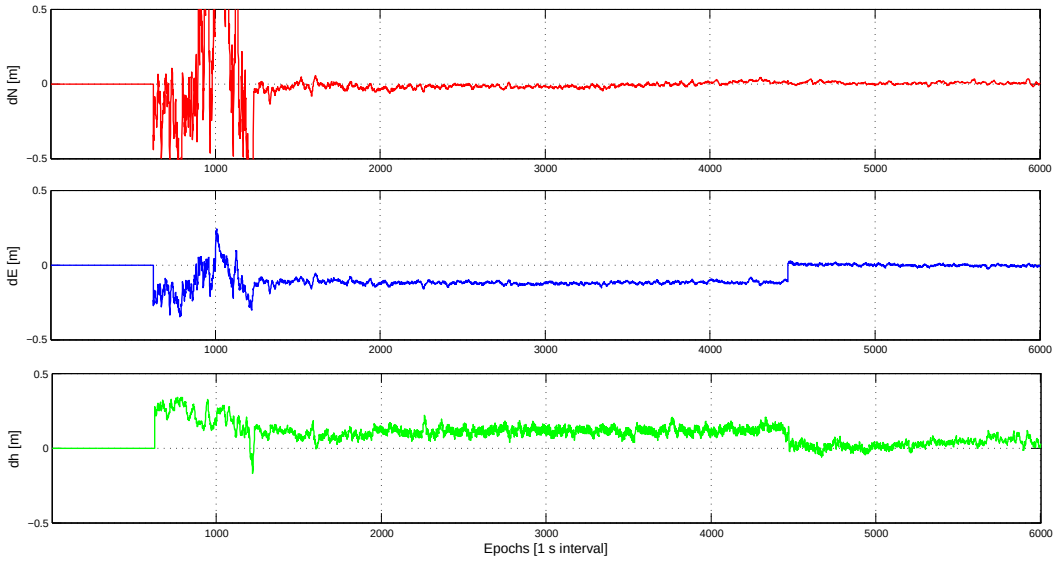

Figure 5.20: NEU coordinate differences of correlation experiment – IGS GRAZ DOY 088 2013 at 0:00

The observable of the satellite with the highest elevation, PRN 21 (see Figure 5.21 (a)) has some problem, leading to the incorrect fixing of its NL ambiguity. Unfortunately, the correlation between the satellites PRN 21 and PRN 18 is that high, that also the estimated float ambiguity of this satellite is slightly adulterated, which as a result, leads to the incorrect fixing of the NL ambiguity of PRN 18 too. The corresponding correlation matrices are visualised in Figure 5.22, where high positive correlations are represented by a dark red colour, while negative correlations are dark blue. Paler colours indicate weaker correlations between the estimated parameters, which are the three-dimensional coordinates, the receiver clock offset, the ZWD of the troposphere and

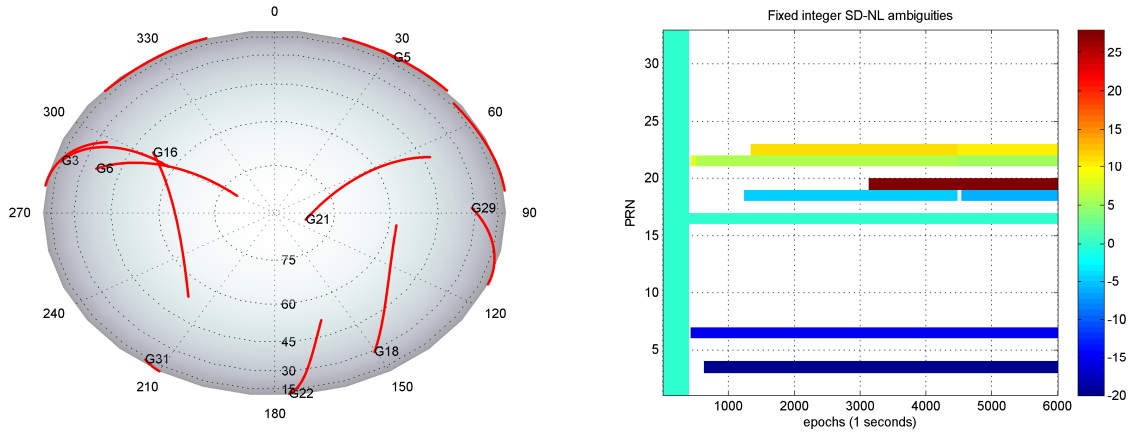

(a): Satellite Skyplot

(b): NL ambiguity fixes

Figure 5.21: Correlation experiment – IGS GRAZ DOY 088 2013 at 0:00

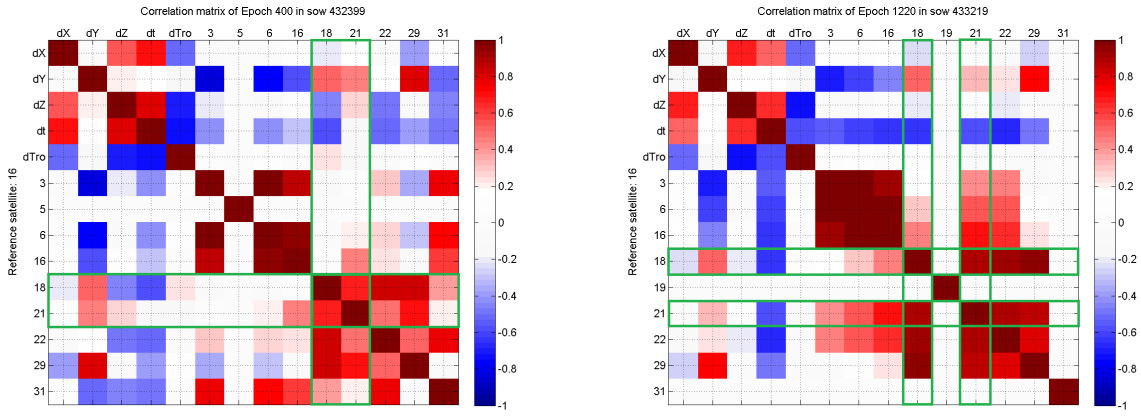

(a): Epoch 400: shortly before NL-fixing starts

(b): Epoch 1220: PRN 21 already fixed to an incorrect value, PRN 18 gets fixed in the subsequent epochs

Figure 5.22: Correlation matrix – IGS GRAZ DOY 088 2013 at 0:00

the ambiguities of the satellites in view.

The whole NL-fixing procedure until the epoch of convergence is summarised in Table 5.8 (the bold style indicates the final values for the NL ambiguities), while the NL-fixes gained during the processing until epoch 6000 (corresponding to minute 100) are visualised in 5.21 (b). The solution does not converge until epoch 4473, in other words, the solution needs more than one hour of processing time to reach the full accuracy. The corresponding NEU coordinate differences with respect to the station's reference coordinates are shown in Figure 5.20.

In a further experiment several different satellites were excluded from the solution. Thereby, it turned out that the problem lies within the observations of PRN 21. As a result, the satellite PRN 21 was excluded during the whole processing. Even though the position accuracy of the float solution got worse, the fixed solution shows a different behaviour. Figure 5.23 now visualises

the NEU differences of the same solution than before, but now, without using PRN 21. Usually, excluding the satellite with the highest elevation angle in a PPP-AR solution decreases the solutions' accuracy and convergence, but in this case, the coordinates converge much faster than before with satellite PRN 21.

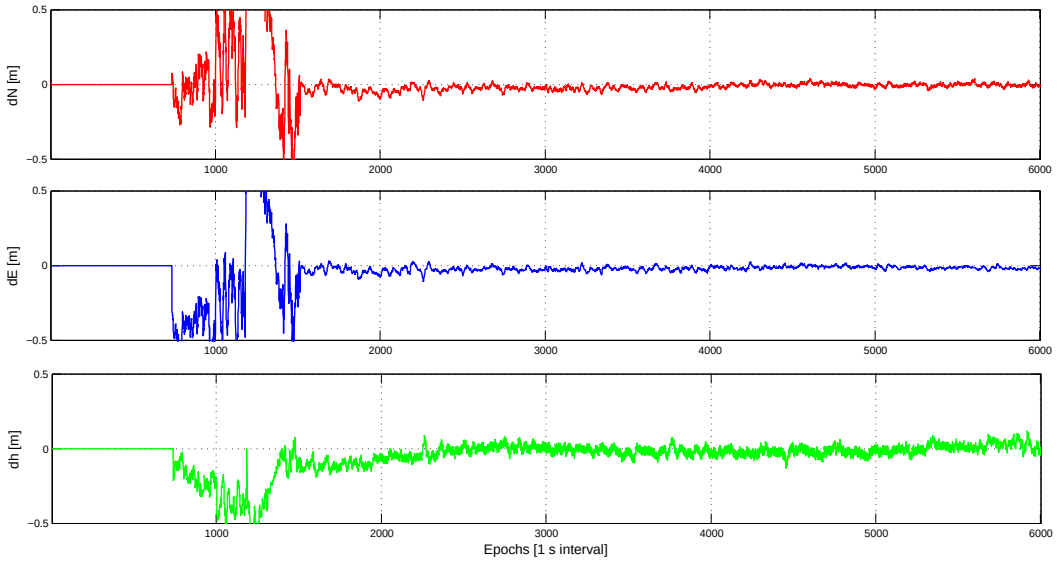

Figure 5.23: NEU coordinate differences of correlation experiment without PRN 21 – IGS GRAZ DOY 088 2013 at 0:00

Table 5.9 shows the summary of the fixing procedure of this second calculation: In epoch 1184 (or minute 20) the third NL ambiguity of a satellite can be fixed to the correct integer. Due the suboptimal satellite geometry of the fixed satellites PRN 6, PRN 3 and PRN 18 also visualised in the skyplot in Figure 5.21 (a) the position solution is still imprecise until the fourth satellite PRN 22 is fixed in epoch 1513 corresponding to the 26$^{\text{th}}$ minute of the processing. This is a much faster convergence than before, where PRN 21 was used for the solution.

EPOCH	**624**	**738**	**1183**	**1184**	**1513**	**3124**
PRN 6	-16	-16	**-15**	**-15**	**-15**	**-15**
PRN 3	-22	-22	R	**-20**	**-20**	**-20**
PRN 18		-4	R	**-6**	**-6**	**-6**
PRN 22					**10**	**10**
PRN 19						**28**

Table 5.9: Fixing procedure of station GRAZ at DOY 088 2013 00:00 without PRN 21 – Reference satellite PRN 16

Summing up, it should not be the general rule, that the high correlations between satellite ambiguities occurring during the Filter procedure disturb the PPP-AR solutions, but it may happen that observations of highly weighted satellites, that additionally are highly correlated with others, show problems at individual stations/rovers. Such problems may be multipath reception or

a bad signal-to-noise ratio but can also occur from bad satellite specific orbit or clock corrections, especially in the real-time case. Therefore, in further investigations better preprocessing routines have to be investigated, in order to avoid such problems in the solutions. This also is very important, when it comes to the choice of the reference satellite, as this severely influences the whole PPP-AR solution.

Another method to detect outliers in the solution, that unfortunately needs a higher computing capacity, would be the simultaneous calculation of not only one, but various PPP-AR solutions in every epoch, where different subsets of satellites are used already for the float solution. This kind of processing could avoid outages or long convergence times in the PPP solution more effectively, and should be contemplated in future investigations.

5.7 Example results of PPP-AR solution calculated with PPPsoft

In the following examples of PPP-AR solutions from the EPOSA stations GRAZ (Figures 5.24 to 5.25 (a) and (b)), BADE (Figures 5.24 to 5.25 (c) and (d)) and DALA (Figures 5.24 to 5.25 (e) and (f)) are shown. An overview on the EPOSA network can be found in Figure 5.1. All observation data was recorded on DOY 88 in 2013 and calculated by using the UPD corrections by TU Vienna in combination with final IGS orbits and clock corrections.

All visualisations are snapshots of two hours of observation between 1:00 and 3:00 (GPS time) and consist of the NEU differences compared to the reference coordinates of the fixed solution and the respective satellites' elevation angles in Figure 5.24, as well as the corresponding fixed WL and NL ambiguities in Figure 5.25. The values of the fixed ambiguities for the satellites correspond to the colours as defined in the colourbar and are given in cycles. Only two hours of the processing are shown, as the solution's accuracy usually does not change after the ambiguities are fixed. The fixing procedure itself was started in epoch 600 corresponding to 10 min of observations.

In each of the three solutions 3 to 4 NL ambiguities can be successfully fixed to integer values immediately after the fixing procedure has started. At that time the horizontal solution accuracy is better than 1 dm and becomes optimal when the 4^{th} to 5^{th} satellite can be fixed depending on the satellite geometry. As expected, the height component of the solution is a bit worse, which arises from the GNSS geometry in general together with remaining unmodelled error effects. The integer values of the remaining ambiguities can be fixed after 2000 to 3000 seconds of observation, exceptions are only those satellites without UPD corrections.

To show that the position solution after the correct fixing of WL and NL ambiguities remains stable, Figure 5.26 shows the NEU coordinate differences of the EPOSA station GRAZ over a period of 14 hours. The solution remains stable over the whole period once the ambiguities are fixed to integer values. Unfortunately, for that day the UPD corrections end at approximately 16:00 which is why the calculation also is stopped at that time.

The solutions presented here, show on the one hand, that the UPDs produced at the TU Vienna are applicable to the observation data of arbitrary reference stations, and on the other hand, that the fixing routines of PPPsoft are able to detect the correct integer values for WL and NL ambiguities after the correction of the phase measurements or rather linear combinations of measurements by the UPD products, which enables the calculation of a stable PPP-AR solution.

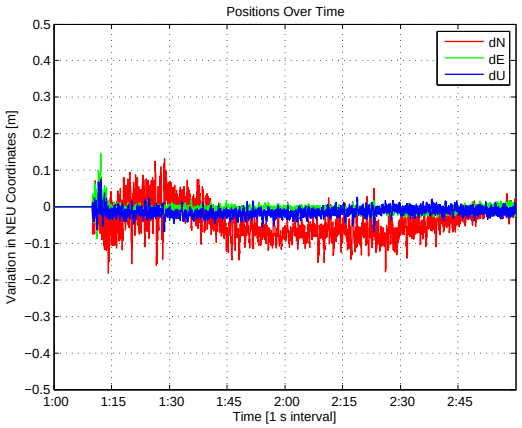

(a): NEU differences station GRAZ

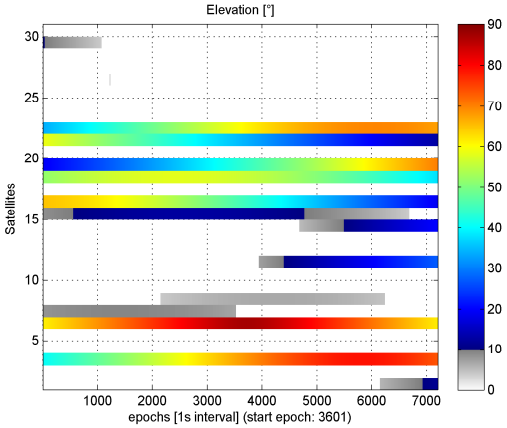

(b): Elevation of satellites station GRAZ

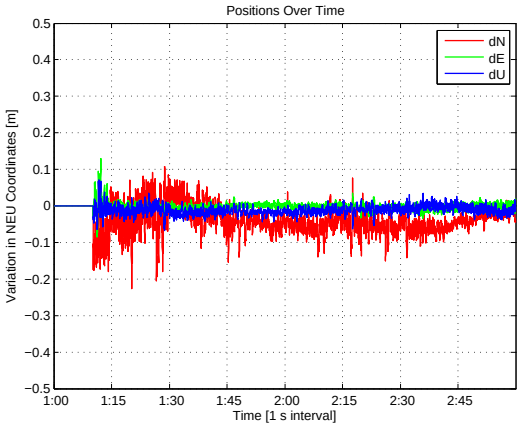

(c): NEU differences station BADE

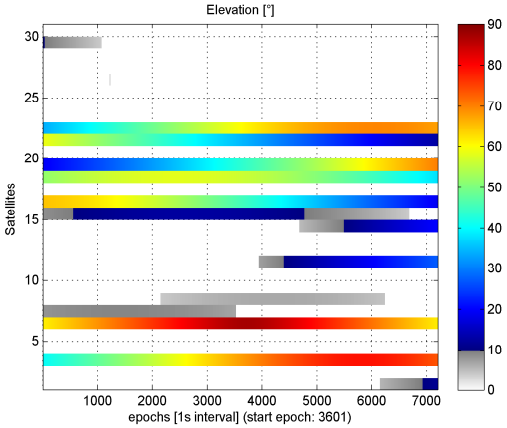

(d): Elevation of satellites station BADE

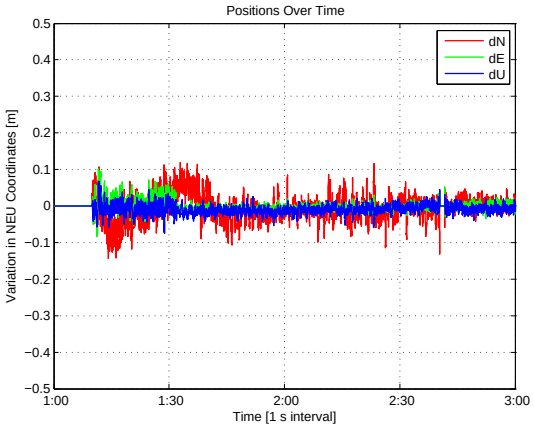

(e): NEU differences station DALA

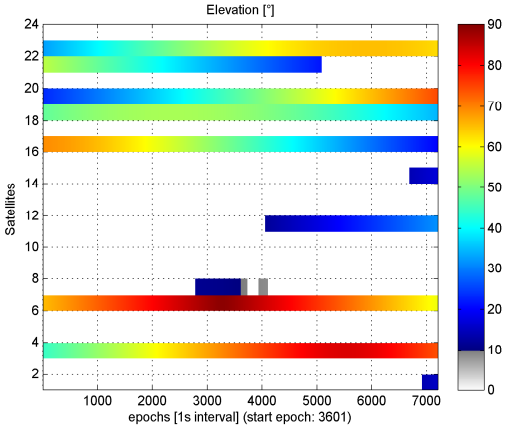

(f): Elevation of satellites station DALA

Figure 5.24: Solutions of EPOSA stations on DOY 088 in 2013 using TU Vienna UPDs – NEU coordinates and elevation

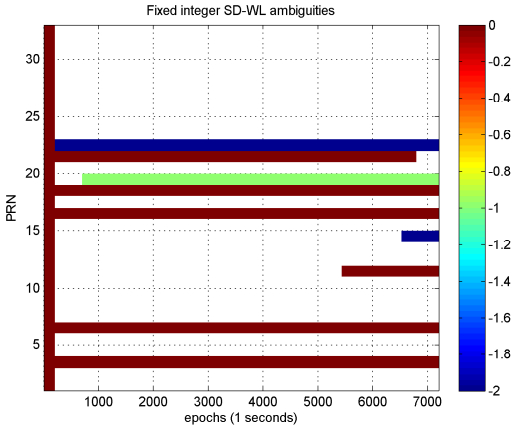

(a): WL ambiguities station GRAZ

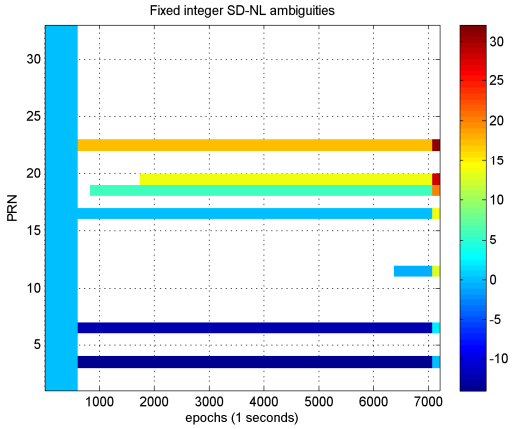

(b): NL ambiguities station GRAZ

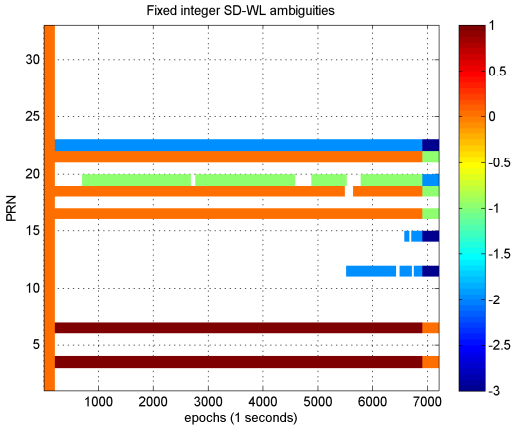

(c): WL ambiguities station BADE

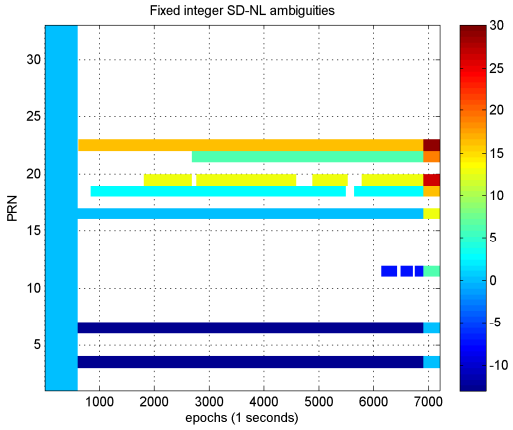

(d): NL ambiguities station BADE

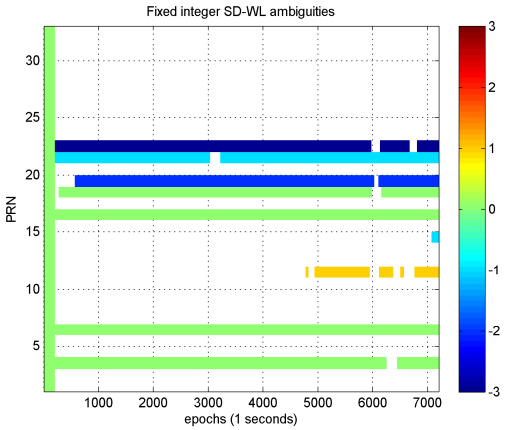

(e): WL ambiguities station DALA

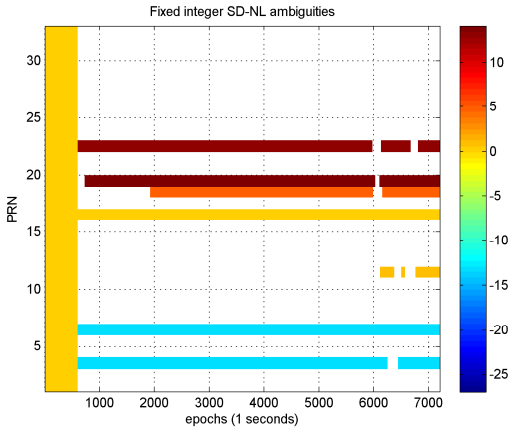

(f): NL ambiguities station DALA

Figure 5.25: Solutions of EPOSA stations on DOY 088 in 2013 using TU Vienna UPDs – WL- and NL-fixes

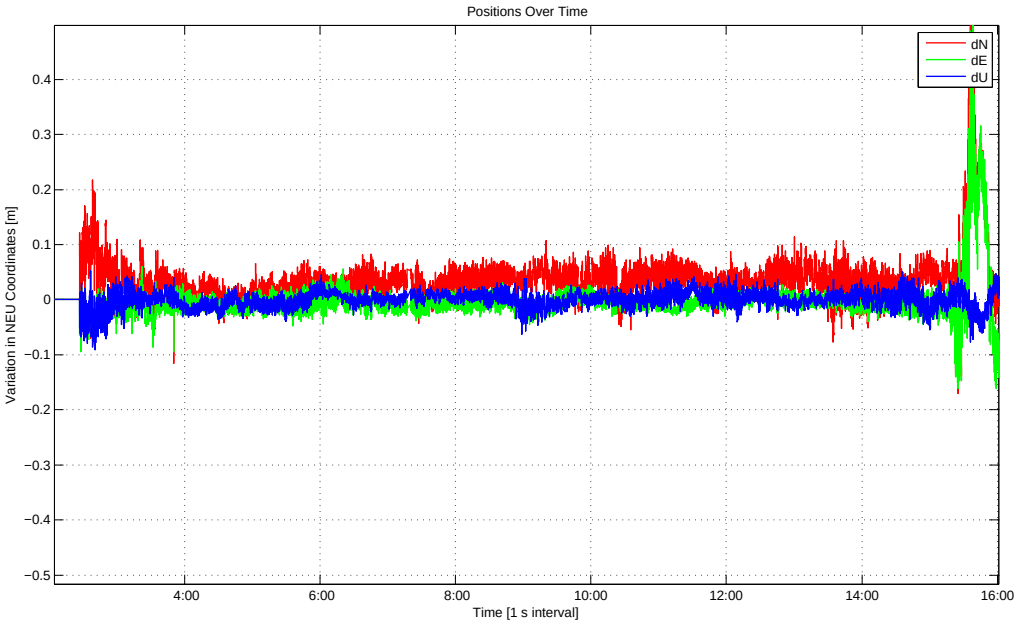

Figure 5.26: Solution over 14 hours of EPOSA station GRAZ on DOY 088 in 2013 using TU Vienna UPDs

5.8 Comparison of float and fixed solutions

In order to get a comparison between the behaviour of float and fixed PPP solutions a series of 10 calculations was produced with CNES as well as with TU Vienna biases of DOY 087 2013. Observations of 6000 epochs (corresponding to 100 minutes) were calculated in intervals of 30 minutes for all available stations. The outcome of the position results of EPOSA station BADE calculated with CNES orbits, clocks and UPDs is visualised showing the direct comparison of float NEU differences in Figure 5.27 (a) and NEU differences of the fixed solution in Figure 5.27 (b), both as a function of the processing time in hours. The float solution becomes better with time slowly, especially in the first 15 to 30 minutes of observation. The north component is rather accurate, while the east component is significantly worse in most of the solutions. Due to the Kalman filter used in the float solution, the coordinates seem smooth and show no outliers, as it is the case with the fixed solution.

In comparison to the float solution, the fixed solution shows a completely different behaviour. As soon as the fixed solution can be calculated, which is possible with three or more fixed ambiguities, the coordinate result is rather comparable in north and in the east component. Some solutions show a large noise in the beginning of the processing. This occurs, when only few (3-4) ambiguities of satellites with a bad geometry are fixed to integers (see Section 5.6). As soon as the correct integer values are fixed, the solution jumps to the true coordinates with a noise of only few centimetres. Wrong fixes mirror in the coordinate solution in the form of a clear offset in the coordinates with respect to the true values. Especially in the first 15 to 30 minutes this is likely to occur. As soon as the majority of ambiguities is fixed correctly the solution is stable and invariably accurate. The outliers, that can be seen in the fixed solution after 45 minutes of observation are

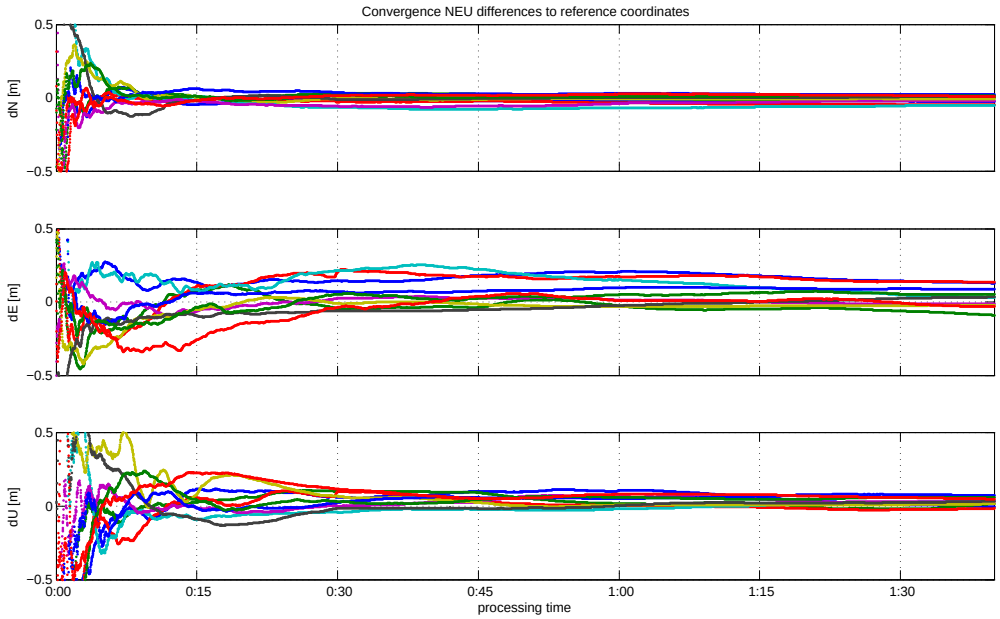

(a): Float solutions EPOSA station BADE

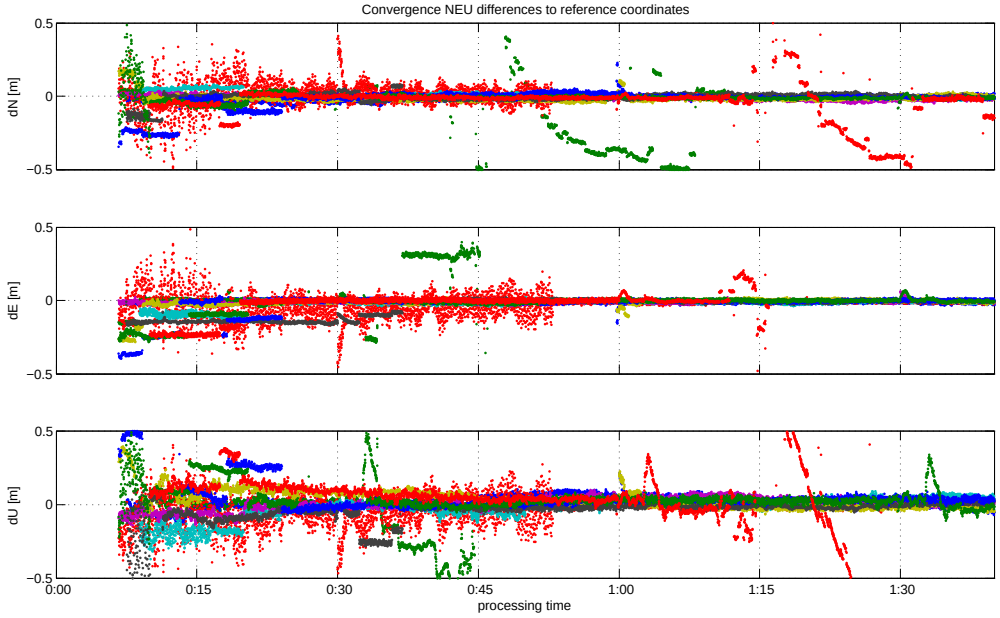

(b): Fixed solutions EPOSA station BADE

Figure 5.27: Fixed solutions of DOY 087 – EPOSA station BADE NEU differences of solutions shifted for 30 minutes

caused by problems or outages of correction products such as ephemerides or UPD corrections of some or all satellites. The major strength of the fixed solution after some time of processing is the accurate estimation of the east component compared to the float solution.

The statistics of the solutions using EPOSA stations and CNES orbit and clock data plus their phase bias corrections are summarised in the diagrams in Figure 5.28 to Figure 5.30. There, the median of absolute differences in north, east and up coordinates of the solutions after 15 minutes, 30 minutes, 45 minutes and 60 minutes of observation are visualised in order to get an overview on the convergence behaviour. The median was chosen as a quality measure in order to deal with the outliers occurring in the fixed solution and though show representative values for the performance.

For the station BADE the diagram for the float solutions in Figure 5.28 (left) shows the improvement of the east and up component over time, while the north component is rather accurate from 15 minutes observation time on and does not increase with time. The east component is significantly worse than the north component as already seen in Figure 5.27 (a). The fixed solution in Figure 5.28 (right) shows one major improvement in the coordinate solution between 15 and 30 minutes of observation. This arises from the fact, that most fixes to the correct integer values of the solution are not found yet after 15 minutes. However, after 30 minutes the correct integer values for the WL and NL ambiguities seem to be fixed, as the solutions show a clear jump in the accuracy of all components. North, east and up coordinates now are clearly more accurate than in the float solution and stay at the level of only few centimetres after that time.

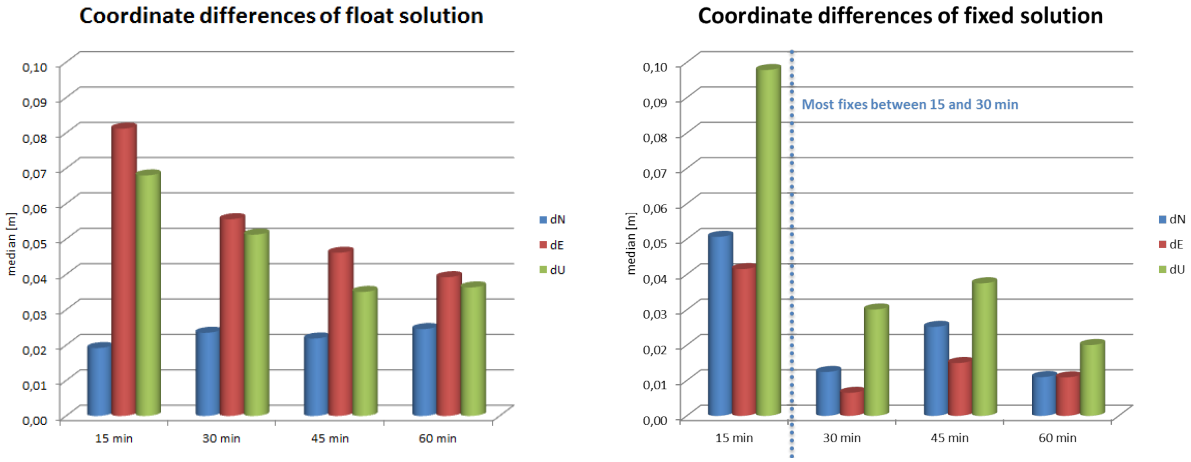

Figure 5.28: Median of NEU differences of float and fixed solutions of DOY 087 – EPOSA station BADE

Station DALA (Figure 5.29) shows a similar behaviour in the float solution on the left side, even though the east and up components seem to be even worse than for station BADE. For this station the significant improvement in the horizontal solution already occurs after 15 minutes of processing with ambiguity fixing as it is shown in Figure 5.29 on the right side. Regarding the fixed solutions of this station, the up-component cannot compete with the up components calculated in the float solutions. This already occurred for many calculations of that station and most likely originates in the used of bad reference coordinates in the vertical component. Nevertheless, the horizontal results especially in the east component are accurate already in the early processing, which cannot be reached when estimating float ambiguities.

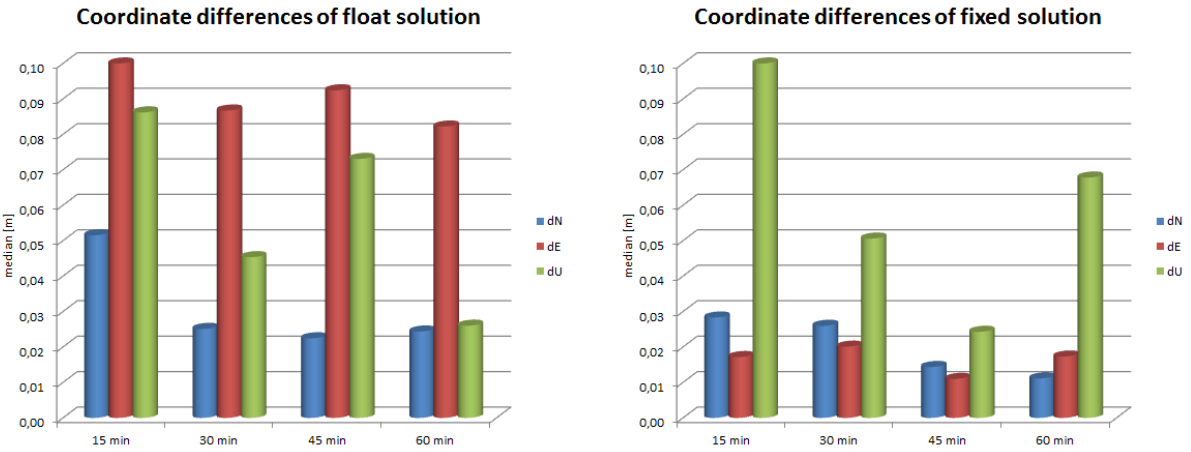

Figure 5.29: Median of NEU differences of float and fixed solutions of DOY 087 – EPOSA station DALA

The last station shown from this experiment is the EPOSA station GRAZ in Figure 5.30. The results of station GRAZ also show, that the fixed solution is clearly better than the float solution after theWL and NL ambiguities can be fixed correctly which seems to be on average after 15 to 30 minutes of processing time. After that point the solutions stay stable and show again a clearly more accurate east coordinate than the float solution.

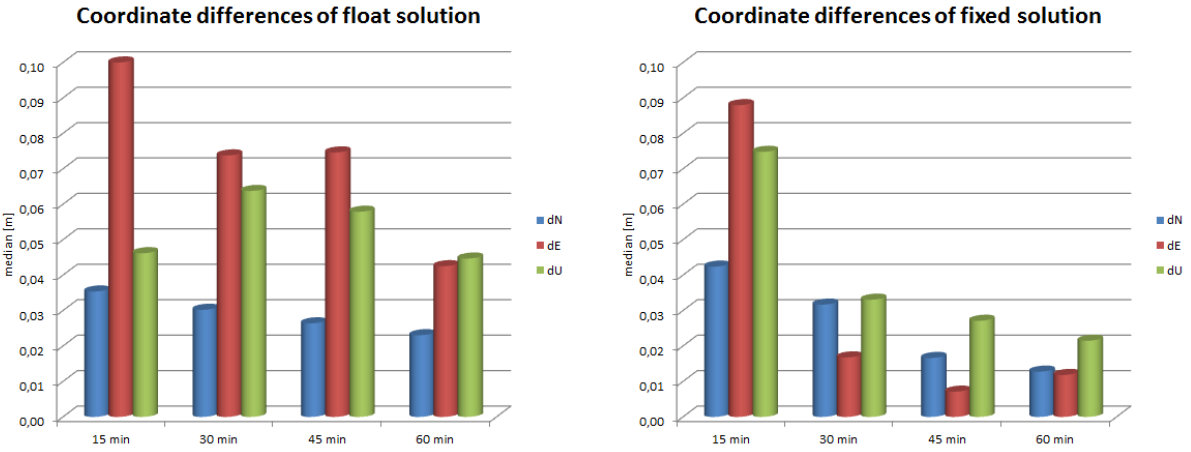

Figure 5.30: Median of NEU differences of float and fixed solutions of DOY 087 – EPOSA station GRAZ

It can be concluded, that PPP-AR has clear advantages over standard PPP methods, that are estimating the ambiguities as float values. The two main advantages are the accurate east components and the early coordinate convergence. Nevertheless, the performance of fixed solutions is strongly dependent on a good satellite geometry in the beginning of the processing and on the phase bias corrections provided by external sources. Only short outages of corrections can cause severe problems in the coordinate solution especially when no filtering is applied to the coordinate estimates.

6 Conclusions and potential future developments

Precise Point Positioning (PPP) is an emerging positioning technique, that allows a precise position determination with the aid of precise ephemeris data from the observations of a single GNSS receiver. Concerning the accuracy it can compete with relative positioning techniques, such as RTK, but the convergence of the solution is rather slow. Nevertheless, the level of independence of PPP is much higher as of RTK, since no regional data from a nearby reference station or a dense station network is necessary. As no baselines and, therefore, no observation differences between receivers are built, there is no spatial limitation for PPP. Further, the precise products necessary for PPP are freely available and when it comes to real-time processing, these can be transmitted also if only a low bandwidth is available. Ephemerides are usually referenced to the current ITRF realisation at the epoch of the observation date, which implies that also the estimated PPP parameters are referred to that epoch. PPP is already a common technique for many post-processing applications, but when it comes to the application of PPP in real-time, there is still room for improvement, as for example the reduction of the long convergence times. For this reason the research in the field of PPP concerning real-time applications, attracted the authors attention in order to start a Ph.D. thesis on this topic.

The goal of this thesis was the development of adequate algorithms for PPP in post-processing and also real-time, that enable the calculation of positions with high accuracies on the basis of dual-frequency GPS observation data. Further research goals were the investigation and application of phase specific corrections enabling integer ambiguity fixing for PPP. The calculation of such phase bias corrections, also called Uncalibrated Phase Delays (UPD), has been the focus of many recent studies in the field of PPP. Together with the application of UPDs also the algorithms for ambiguity fixing, applicable to the PPP technique, had to be investigated and implemented. As a result from all the investigations on the topic of PPP the experimental user client PPPsoft was developed, that finally was able to perform any kinds of PPP processing, but especially was designed for highly accurate real-time PPP using dual-frequency observations with an option for PPP with Ambiguity Resolution and Fixing (PPP-AR). PPPsoft initially served as a playground for testing different models and algorithms concerning zero-difference GNSS processing, but today is a rather powerful tool able to perform PPP-AR with two different types of phase bias corrections.

In the following, the contents of this thesis, coinciding also with the progress of this research, are shortly summarised:

After a short introduction to GNSS techniques in Chapter 1, the main principles of PPP processing including all necessary model corrections were discussed. These principles include the used observation equations, the treatment of the influence of the ionosphere and troposphere on the GNSS signal, as well as the content and the application of several products for precise satellite

orbits and clock corrections in post-processing and real-time. Additionally, smaller error influences such as tidal effects, antenna phase centre corrections and also the carrier phase wind-up effect is treated in Chapter 2. Finally, the principles of the adjustment and filtering used in PPPsoft as well as in many other PPP clients are described.

The user client itself is presented in Chapter 3, together with the options and settings that can be chosen by the user and including a variety of input files. The real-time functionality of PPPsoft is described based on the new SSR messages contained in the current RTCM standard. The orbit, clock and code bias corrections contained in these messages are explained in detail. In order to decode the binary RTCM format, the open source RTCM client software BNC by the BKG was used in combination with PPPsoft. In the end of this chapter, results of PPP with float ambiguity estimates using post-processing as well as real-time ephemerides are shown. The PPP calculations employing the RTCM SSR corrections deliver comparable results concerning accuracy and convergence compared to introducing the precise ephemerides for post-processing solutions. Nevertheless, the real-time corrections are not always that reliable, as they are calculated by only one analysis centre in real-time, while e.g. the final precise ephemerides by the IGS are results of the combination of different solutions by several analysis centres. Even though, PPP in real-time can yield similar accuracies (cm-level) as relative positioning techniques like RTK, the convergence of PPP solutions estimating float ambiguities is rather long. At least 10 to 15 minutes are required for the solution to approach at least the dm-level, while an accuracy level of a few centimetres is reached only after observation times of 30 to 90 minutes. This is still too long to compete with RTK techniques.

An early fixing of integer ambiguities in PPP would be the solution to the convergence problem: If integer ambiguities could be successfully fixed, the PPP solution would immediately converge to its optimum accuracy of 1 to 3 centimetres depending on the quality of the used ephemeris products. Unfortunately, the estimated ambiguities in a zero-difference processing are contaminated by receiver and satellite specific hardware delays that are called UPDs or phase biases in this thesis. These phase biases have to be calculated and applied prior to the ambiguity fixing routines. The research project PPPserve, that ended in 2013, had the goal to investigate and calculate such phase biases and test their applicability by means of a PPP user client, that was developed on the basis of the client software PPPsoft. Therefore, this thesis is strongly connected to PPPserve as well as to a parallel thesis on the topic of the creation of phase biases written by Fabian Hinterberger at the TU Vienna.

In PPPserve satellite specific Wide-Lane (WL) and Narrow-Lane (NL) UPDs were calculated in a network solution while receiver-specific UPDs were meant to be eliminated by building satellite-to-satellite differences as it was done in the presented research. Knowing these biases, the ionosphere-free ambiguity term can be reformulated and WL and NL ambiguities can be fixed to integer values. The WL-fixing is done independently from the PPP solution, while the NL ambiguities are calculated on the basis of the estimated ionosphere-free ambiguities. Partial ambiguity fixing routines are employed, as the fixing of NL ambiguities would be rather unreliable when done all in one. This is due to the fact that the estimated ionosphere-free ambiguities need some time to converge, meaning that they vary for some decimetres in the beginning of the PPP processing until they stay constant in the magnitude of one NL cycle. Therefore, it is especially tricky to fix NL ambiguities before the float solution converges and to exploit the full potential of an ambiguity fixed PPP solution in order to comply with the demands of (near) real-time applications. False fixes are likely to occur in the first 30 minutes of the solution. That

still is a rather long time for initialisation, which has to become shorter to compete with other GNSS techniques such as RTK. Nevertheless, as soon as the ambiguities are correctly fixed, the PPP-AR solution is extremely precise and stable. The application of UPDs and the theoretical fundamentals of PPP-AR are treated in Chapter 4, whereby the thesis especially focuses on the algorithms employed by the user client.

Experimental results, using on the one hand UPDs produced at the TU Vienna, and on the other hand phase bias correction products by CNES, are shown and analysed in Chapter 5. Different settings for the PPP solutions and their effects on the coordinate results are provided by means of several case studies. Among others it is shown, that CNES and TU Vienna UPDs both are suitable to re-establish the integer nature of WL and NL ambiguities. Under good geometric conditions, and assuming a high quality float solution, a PPP-AR solution with a horizontal accuracy of only few centimetres can be obtained after some minutes, and after only three to four satellites possess correctly fixed WL and NL ambiguities. Incorrectly fixed ambiguities, especially in the beginning of the processing, can degrade the solution dramatically, which also mirrors in the phase residuals. Exploiting this knowledge can help to find those incorrect ambiguity fixes under certain circumstances. Also introducing more accurate approximate coordinates and external troposphere data does slightly help to fasten the solutions' convergence. Unfortunately, for roving receivers it is not that easy to reach accuracies better than 10 cm for the initial coordinates. Though, for certain applications it would be thinkable to start the positioning at a known reference point. One problematic issue for PPP-AR, as it is implemented in PPPsoft, is the detection of outliers within the measurements, as a reference satellite for the fixing procedure has to be chosen. If the measurements of this satellite still contain unmodelled systematic or severe errors, the whole success of the fixing procedure is endangered. But also measurements of other satellites can distort the PPP-AR solution, as there can be high correlations between the ambiguity estimates of the satellites that become even tighter during processing. These high correlations originally are caused by the satellite geometry, and sometimes stay present for a long time as a result of the processing filter. Nevertheless, the PPP-AR results show several advantages over the standard PPP solutions, such as an increased performance in the east component of the coordinates and a faster convergence.

Eventually, this thesis shows that ambiguity fixing using the software produced in this research is possible, if external products containing UPD corrections (in this research from CNES and TU Vienna) are available. Fixing times can be reduced by means of integer ambiguity resolution, but 8 to 10 minutes of initialisation time are still needed in the best case. Even though the fixed solutions are more precise (especially in the east-component) than float solutions commonly are, the actual convergence time is still too long for many real-time applications. Therefore, future investigations may focus on better and more stable algorithms to, on the one hand, fix ambiguities earlier and, on the other hand, detect wrong fixes earlier, knowing that the correctness of the solution is mirrored in the phase ambiguities of the ambiguity-fixed solution.

One further topic for a continuative research could be the application and success of the ambiguity fixing routines to kinematic data after a static initialisation time. Therefore, the fixing has to become more reliable and better preprocessing routines have to be found. Nevertheless, this would be a major step for PPP-AR to become a marketable technique for many applications.

Due to the continuous modernisation of the GNSS, it may be possible to use triple- or multiple-frequency combinations in PPP-AR systems soon, which for example offer a better noise behaviour than the currently used ionosphere-free linear combination of GPS L1 and L2. Further, in the

future code observables may be that accurate that an estimation of a priori coordinates below the dm-level may be possible. This would also be a big step forward to accelerate the convergence of PPP-AR solutions.

Bibliography

Printed Sources

Abdallah, A. and V. Schwieger (2014). "Accuracy Assessment Study of GNSS Precise Point Positioning for Kinematic Positioning". In: *Proceedings on 4th International Conference on Machine Control and Guidance. TU Braunschweig, Braunschweig.* (Cit. on p. 5).

Anderle, R. J. (1977). "Point positioning concept using precise ephemeris". In: *Satellite Doppler positioning.* Ed. by G. Veis and O. W. Williams, pp. 47–75 (cit. on p. 6).

Anquela, A., A. Martín, J. Berné, and J. Padín (2013). "GPS and GLONASS Static and Kinematic PPP Results". In: *Journal of Surveying Engineering* 139.1, pp. 47–58 (cit. on p. 5).

Borre, K., D. M. Akos, N. Bertelsen, P. Rinder, and S. H. Jensen (2007). *A Software-Defined GPS and Galileo Receiver.* Birkhäuser Boston (cit. on p. 35).

Borre, K. (2009). "The GPS EASY Suite II: A Matlab Companion". In: *Inside GNSS* (March-April 2009) (cit. on p. 35).

Chang, X.-W., X. Yang, and T. Zhou (2005). "MLAMBDA: a modified LAMBDA method for integer least-squares estimation". In: *Journal of Geodesy* 79.9, pp. 552–565 (cit. on p. 64).

Collins, P., S. Bisnath, F. Lahaye, and P. Heroux (2010). "Undifferenced GPS Ambiguity Resolution Using the Decoupled Clock Model and Ambiguity Datum Fixing. Journal of The Institute of Navigation". In: *Journal of the Institute of Navigation* Vol. 57, No. 2, pages (cit. on p. 57).

Dach, R., U. Hugentobler, P. Fridez, and M. Meindl (2007). *Bernese GPS Software Version 5.0.* Astronomical Institute, University of Bern (cit. on pp. 25, 26).

De Jonge, P. and C. Tiberius (1996). "The LAMBDA method for integer ambiguity estimation: implementation aspects". In: *Delft Geodetic Computing Centre LGR Series* 12 (cit. on p. 63).

Ge, M., G. Gendt, M. Rothacher, C. Shi, and J. Liu (2008). "Resolution of GPS carrier-phase ambiguities in Precise Point Positioning (PPP) with daily observations". In: *Journal of Geodesy* 82.7, pp. 389–399 (cit. on pp. 56, 57, 60, 69).

Geng, J., X. Meng, A. H. Dodson, and F. N. Teferle (2010). "Integer ambiguity resolution in precise point positioning: method comparison". In: *Journal of Geodesy* 84.9, pp. 569–581 (cit. on p. 56).

Hinterberger, F. (2015). *Ph.D. Thesis. GNSS based single point positioning at cm level (PPP) assisted by regional network information.* (in print). TU Vienna (cit. on pp. 10, 57, 68, 71).

Hofmann-Wellenhof, B. and K. Legat (2003). *Navigation*. Springer Vienna (cit. on pp. 20, 31, 32).

Hofmann-Wellenhof, B., H. Lichtenegger, and E. Wasle (2007). *GNSS – Global Navigation Satellite Systems: GPS, GLONASS, Galileo, and more*. Springer (cit. on pp. 2–4, 12–14, 22, 23, 31).

Hopfield, H. S. (1969). "Two-quartic tropospheric refractivity profile for correcting satellite data". In: *Journal of Geophysical Research* 74.18, pp. 4487–4499 (cit. on p. 21).

Huber, K., P. Berglez, B. Hofmann-Wellenhof, R. Weber, and M. Troger (2011). "The development of enhanced algorithms for rapid precise point positioning". In: *Österreichische Zeitschrift für Vermessung und Geoinformation (VGI)* Austrian Contributions to the XXV General Assembly of the International Union of Geodesy and Geophysics (IUGG).2, pp. 114–121.

Huber, K., F. Hinterberger, R. Lesjak, and R. Weber (2014). "Real-time PPP with Ambiguity Resolution – Determination and Application of Uncalibrated Phase Delays". In: *Proceedings of the 27th International Technical Meeting of The Satellite Division of the Institute of Navigation (ION GNSS+ 2014), Tampa, Florida, September 2014*, pp. 976–985 (cit. on p. 71).

Huber, K., F. Hinterberger, R. Lesjak, R. Weber, C. Klug, and G. Thaler (2013). "PPPserve - Network based GNSS phase biases to enhance PPP applications". In: *The European Navigation Conference 2013, Vienna, Austria*.

Kalman, R. E. (1960). "A New Approach to Linear Filtering and Prediction Problems". In: *Transactions of the ASME – Journal of Basic Engineering* 82 (Series D), pp. 35–45 (cit. on pp. 30, 32).

Klobuchar, J. A. (1987). "Ionospheric Time-Delay Algorithm for Single-Frequency GPS Users". In: *Aerospace and Electronic Systems, IEEE Transactions on* AES-23.3, pp. 325–331. ISSN: 0018-9251 (cit. on p. 24).

Kouba, J. (2009). *A guide to using International GNSS Products (IGS) Products*. Geodetic Survey Division, Natural Resources Canada (cit. on pp. 14, 16, 28, 30, 33).

Kouba, J. and P. Héroux (2001). "Precise Point Positioning Using IGS Orbit and Clock Products". In: *GPS Solutions* 5.2, pp. 12–28 (cit. on p. 6).

Landau, H. (1988). *Zur Nutzung des Global Positioning Systems in Geodäsie und Geodynamik: Modellbildung, Software-Entwicklung und Analyse*. Schriftenreihe (Universität der Bundeswehr München. Studiengang Vermessungswesen). Studiengang Vermessungswesen, Universität der Bundeswehr München (cit. on p. 32).

Landau, H., X. Chen, S. Klose, R. Leandro, and U. Vollath (2009). "Trimble's RTK And DGPS Solutions In Comparison With Precise Point Positioning". In: *Observing our Changing Earth*. Ed. by M. G. Sideris. Vol. 133. International Association of Geodesy Symposia. Springer Berlin Heidelberg, pp. 709–718 (cit. on p. 4).

Laurichesse, D., F. Mercier, J. P. Berthias, P. Broca, and L. Cerri (2009). "Integer Ambiguity Resolution on Undifferenced GPS Phase Measurements and its Application to PPP and Satellite Precise Orbit Determination". English. In: *Journal of the Institute of Navigation* Vol. 56, No. 2, pages (cit. on pp. 57, 60, 69).

Melbourne, W. G. (1985). "The case for ranging in GPS-based geodetic systems". In: *Proc. 1st Int. Symp. on Precise Positioning with GPS, Rockville, Maryland (1985)*, pp. 373–386 (cit. on p. 54).

Montenbruck, O., P. Steigenberger, R. Khachikyan, G. Weber, R. B. Langley, L. Mervart, and U. Hugentobler (2014). "IGS-MGEX – Preparing the Ground for Multi-Constellation GNSS Science". In: *Inside GNSS* (January/February 2014) (cit. on p. 36).

Petovello, M. (2011). "GNSS solutions: The differences in differencing". In: *Inside GNSS*, 28ff (cit. on p. 44).

Radio Technical Commission for Maritime Services (2011). *Differential GNSS (Global Navigation Satellite Systems) Services – Version 3. RTCM 10403.1 RTCM Paper 142.* 2011/SC104-STD with Amendment 5. Version 3. (Cit. on pp. 5, 8, 17, 19, 36, 67).

Saastamoinen, J. (1972). "Contributions to the theory of atmospheric refraction". English. In: *Bulletin Géodésique* 105.1, pp. 279–298. ISSN: 0007-4632. DOI: 10.1007/BF02521844. URL: http://dx.doi.org/10.1007/BF02521844 (cit. on p. 21).

Shi, J. (2012). *Ph.D. thesis. Precise Point Positioning Integer Ambiguity Resolution with Decoupled Clocks* (cit. on pp. 56, 59, 63).

Shi, J., C. Xu, J. Guo, and Y. Gao (2014). "Local troposphere augmentation for real-time precise point positioning". In: *Earth, Planets and Space* 66.1 (cit. on p. 86).

Teunissen, P. (1995). "The least-squares ambiguity decorrelation adjustment: a method for fast GPS integer ambiguity estimation". English. In: *Journal of Geodesy* 70.1-2, pp. 65–82. ISSN: 0949-7714. DOI: 10.1007/BF00863419. URL: http://dx.doi.org/10.1007/BF00863419 (cit. on p. 63).

Weber, R. and F. Hinterberger (2013). "Precise Point Positioning (PPP) - Berechnungsmodell, Einsatzbereiche, Grenzen". In: *GNSS 2013 - Schneller. Genauer. Effizienter. Schriftenreihe Band 70/2013.* DVW e. V. - Gesellschaft für Geodäsie, Geoinformation und Landmanagement, pp. 63–82. ISBN: 978-3-89639-902-1 (cit. on p. 7).

Weber, R., F. Hinterberger, K. Huber, R. Lesjak, C. Klug, and G. Thaler (2013). *Final Report of project PPPserve* (cit. on pp. 9, 70).

Wu, J. T., G. Hajj, S. C. Wu, W. I. Bertiger, and S. M. Lichten (1993). *Effects of Antenna Orientation on GPS Carrier Phase.* Manuscripta Geodaetica. Springer-Verlag (cit. on p. 27).

Wübbena, G. (1985). "Software developments for geodetic positioning with GPS using TI-4100 code and carrier measurements". In: *Proceedings of the First International Symposium on Precise Positioning with the Global Positioning System.* Vol. 19 (cit. on p. 54).

Wübbena, G., A. Bagge, and M. Schmitz (2001). "Network-Based Techniques for RTK Applications". In: *Presented at the GPS Symposium, GPS JIN 2001, GPS Society, Japan Institute of Navigation, Tokyo, Japan, November 14.-16.* (Cit. on p. 4).

Zhang, W., R. Langley, A. Komjathy, and S. Banville (2013). "Eliminating Potential Errors Caused by the Thin Shell Assumption: An Extended 3D UNB Ionospheric Modelling Technique". In: *Proceedings of the 26th International Technical Meeting of The Satellite Division of the Institute of Navigation (ION GNSS+ 2013), Nashville, TN, September 2013*, pages (cit. on p. 24).

Zumberge, J. F., M. B. Heflin, D. C. Jefferson, M. M. Watkins, and F. H. Webb (1997). "Precise point positioning for the efficient and robust analysis of GPS data from large networks". In: *Journal of Geophysical Research: Solid Earth* 102.B3, pp. 5005–5017 (cit. on p. 6).

Online Sources

http://igs.bkg.bund.de/ntrip (2014). *Ntrip Homepage by GNSS Data Center*. Ed. by BKG. URL: http://igs.bkg.bund.de/ntrip (cit. on pp. 17, 36, 38).

http://igscb.jpl.nasa.gov (2014). *Homepage of the Jet Propulsion Laboratory (JPL)*. URL: http://igscb.jpl.nasa.gov (cit. on pp. 14, 29, 38).

http://itrf.ensg.ign.fr/ITRF_solutions/2008 (2015). *ITRF website*. URL: http://itrf.ensg.ign.fr/ITRF_solutions/2008 (cit. on p. 15).

http://kom.aau.dk/borre/easy (2014). *Easy – Matlab GPS tools*. URL: http://kom.aau.dk/~borre/easy (cit. on p. 35).

http://software.rtcm-ntrip.org/svn/trunk/BNC/src/bnchelp.html (2015). *SVN server on Ntrip homepage*. URL: http://software.rtcm-ntrip.org/svn/trunk/BNC/src/bnchelp.html (cit. on p. 17).

http://www.aiub.unibe.ch/content/research/satellitengeodaesie (2014). *Homepage of the Center for Orbit Determination in Europe by the Astronomical Institute of the University of Bern*. URL: http://www.aiub.unibe.ch/content/research/satellitengeodaesie (cit. on p. 7).

http://www.cs.mcgill.ca (2014). *Homepage of the School of Computer Science, McGill University*. URL: http://www.cs.mcgill.ca (cit. on p. 64).

http://www.eposa.at (2014). *EPOSA homepage*. URL: http://www.eposa.at (cit. on p. 3).

http://www.iers.org (2014). *Homepage of the International Earth Rotation and Reference Systems Service*. URL: http://www.iers.org (cit. on p. 39).

http://www.igs.org (2014). *Homepage of the International GNSS Service*. URL: http://www.igs.org (cit. on pp. 14, 15).

http://www.mathworks.de/products/matlab (2014). *Matlab homepage*. URL: http://www.mathworks.de/products/matlab (cit. on p. 37).

http://www.navipedia.net (2014). *Navipedia – The reference for Global Navigation Satellite Systems*. Ed. by E. S. Agency. URL: http://www.navipedia.net (cit. on pp. 12, 26).

http://www.ppp-wizard.net (2014). *Homepage of the PPP-wizard demonstrator by CNES*. URL: http://www.ppp-wizard.net (cit. on pp. 10, 66, 67).

http://www.rtcm.org (2015). *Homepage of the Radio Technical Commission for Maritime Services (RTCM)*. URL: http://www.rtcm.org (cit. on p. 36).

http://www.rtigs.net (2014). *Homepage of the IGS Real Time Pilot Project*. URL: http://www.rtigs.net (cit. on pp. 6, 20).

http://www.trimble.com/positioning-services (2014). *Homepage of Trimble's Positioning Services*. URL: http://www.trimble.com/positioning-services (cit. on p. 7).